

JOHNS HOPKINS APL

TECHNICAL DIGEST

2025, Volume 37, Number 4

Countering Chemical, Biological,
Radiological, Nuclear, and Explosives
(CBRNE) Threats



CHEMICAL

BIOLOGICAL

RADIOLOGICAL

NUCLEAR

EXPLOSIVES

CBRNE

The *Johns Hopkins APL Technical Digest* is an unclassified technical journal published twice a year by the Johns Hopkins Applied Physics Laboratory. Its purpose is to communicate recent Laboratory advances in science, technology, engineering, and mathematics, along with expository articles by APL staff members that accelerate education and understanding of new capabilities, results, and discoveries.

EDITORIAL BOARD

James R. Schatz, *Chair and Editor in Chief*
Miquel D. Antoine
Ra'id S. Awadallah
Benjamin H. Barnum
Joshua B. Broadwater
Michael R. Buckley
Betsy A. Congdon
Constantine K. "Dean" Demetropoulos
Ariel M. Greenberg
David O. Harper
James P. "Jamie" Howard
Dana M. Hurley
Kevin M. Ligozio
Zaruhi R. Mnatsakanyan
Peter P. Pandolfi
Julia B. Patrone
Valoris R. "Reid" Smith
James C. Spall
Robin M. Vaughan

Elena C. Wicker
Gary L. Wood
Scott E. Wunsch

Ex Officio

Erin M. Richardson

STAFF

Managing Editor: Erin M. Richardson
Editorial Support: Anne E. King, Kelly K. Livieratos, and
Peggy M. Moore
Illustration Support: Gloria J. Crites and
Robin A. Walker
Front Cover Art: Karim R. Whalen
Inside Back Cover Art: Karim R. Whalen
Web Publisher: Alex Van Horn
Photographers: Craig S. Weiman and
Edward G. Whitman
Clearance Coordinators: Rachel N. Brown, Ashley M.
Moore-Greco, and Chad Sillery
Production Assistant: SiRod A. Foster

The *Johns Hopkins APL Technical Digest* (ISSN 1930-0530) is published quarterly under the auspices of the Johns Hopkins University Applied Physics Laboratory (APL), 11100 Johns Hopkins Road, Laurel, MD 20723-6099.

Requests to be added to the email distribution list announcing each issue should be submitted to TechnicalDigest@jhuapl.edu. Permission to reprint text and/or figures should be requested at <http://bit.ly/apl-3sxU2bS>.

The following abstracting services currently cover the *Johns Hopkins APL Technical Digest*: Chemical Abstracts; Current Contents; Science Citation Index; Engineering Village; and the following CSA abstracts: Aerospace and High Technology Database; Aquatic Sciences and Fisheries Abstracts; Computer and Information Systems Abstracts; Electronics and Communications Abstracts; Mechanical and Transportation Engineering Abstracts; Meteorological and Geostrophical Abstracts; and Oceanic Abstracts.

Distribution Statement A: Approved for public release; distribution is unlimited.

© 2025 The Johns Hopkins University Applied Physics Laboratory LLC. All Rights Reserved.



JOHNS HOPKINS APL

TECHNICAL DIGEST

Volume 37, Number 4

Countering Chemical, Biological, Radiological, Nuclear, and Explosive (CBRNE) Threats

Guest Editors' Introduction: Countering Chemical, Biological, Radiological, Nuclear, and Explosive (CBRNE) Threats

Kelly A. Van Houten, Christopher C. Carter, and Joshua B. Broadwater

Simulants for Chemical and Explosive Threats

David S. Lawrence and Kelly A. Van Houten

Large-Scale Production of Radiopure ^{135}Xe from Bremsstrahlung γ -Irradiation of Solid Xenon Difluoride

Evan P. Lloyd, Ciara B. Sivels, Alan W. Hunt, and Yenuel S. Jones-Alberty

APL's Contributions to the Odor Detection Canine Community

Shirley M. Klimkiewicz and David M. Deglau

Using Knowledge Graphs to Counter Weapons of Mass Destruction

Ray H. Mariner, Timothy P. Lipka, Phillip T. Koshute, David W. Boyce, Josef C. Behling, and Michael J. Peters

MLM: Machine Learning for Threat Characterization of Unidentified Metagenomic Reads

Benjamin D. Baugher, Phillip T. Koshute, N. Jordan Jameson, Kennan C. Lejeune, Joseph D. Baugher, and Christopher M. Gifford

Assessment of Sequencing for Pathogen-Agnostic Biothreat Diagnostics, Detection, and Actionability for Military Applications

Christopher E. Bradburne, Robert A. Player, Sarah L. Grady, Ellen R. Forsyth, Kathleen J. Verratti, and Jeffrey B. Bacon

Wearables-Based Disease Surveillance: SIGMA+ Human Sentinel Networks Concept of Operations

Ivan Stanish, Jane E. Valentine, Damon C. Duquaine, Robert A. Stoll, Ray H. Mariner, and Dorsey R. Woodson

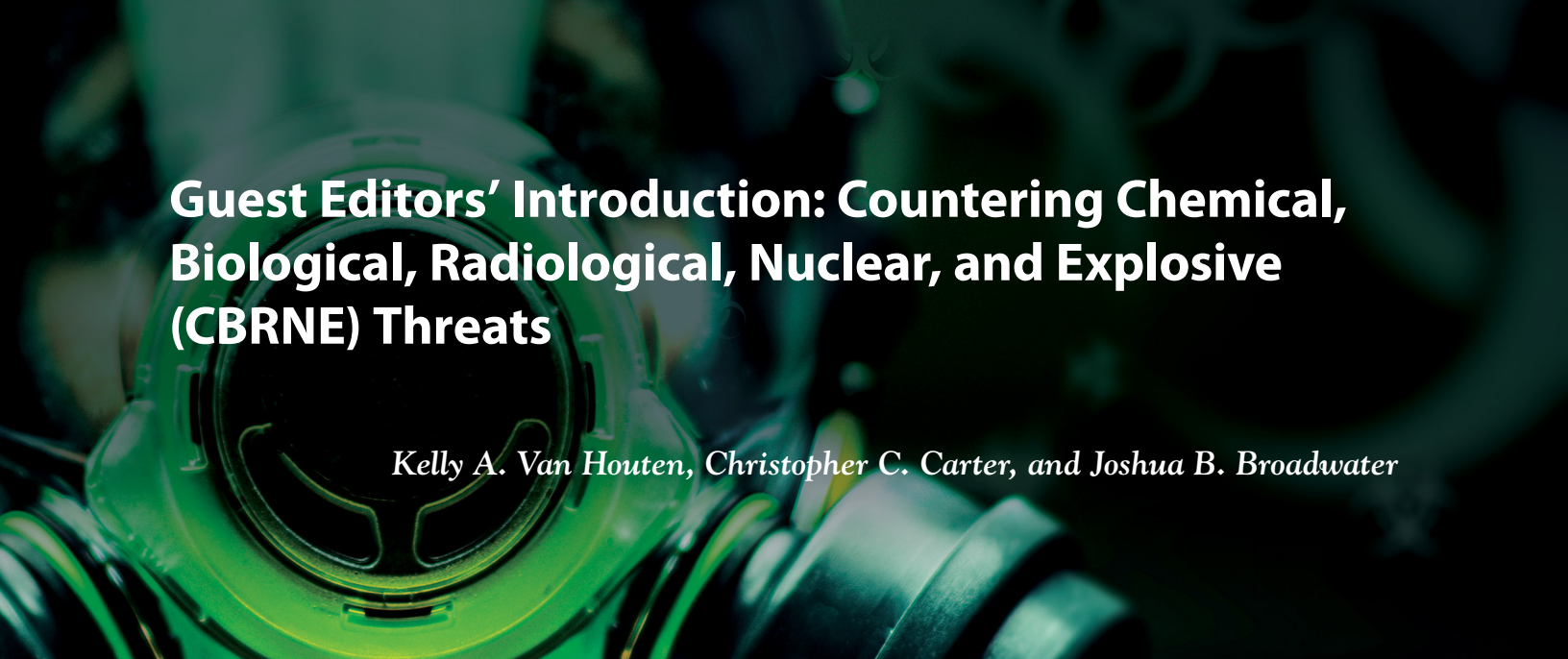
SPECIAL FEATURE

APL Achievement Awards and Prizes: The Lab's Top Inventions, Technical Breakthroughs, and Staff Achievements for 2023 and 2024

APL Staff Writers

IN MEMORIAM

Harry K. Charles Jr. (1944–2025)



Guest Editors' Introduction: Countering Chemical, Biological, Radiological, Nuclear, and Explosive (CBRNE) Threats

Kelly A. Van Houten, Christopher C. Carter, and Joshua B. Broadwater

ABSTRACT

The Johns Hopkins University Applied Physics Laboratory (APL) plays a crucial role in helping the United States anticipate, counter, and prevail against chemical, biological, radiological, nuclear, and explosive (CBRNE) threats. APL researchers create innovative technologies and methodologies that enhance national security and provide decision-makers with actionable intelligence in the face of evolving threats. The counterterrorism and homeland security landscape has dramatically changed since the Johns Hopkins APL Technical Digest last published a comprehensive review on these topics in 2003. In the years since, APL's expertise has expanded significantly, integrating advancements in artificial intelligence, data analytics, autonomous systems, and sensor technologies to address increasingly sophisticated CBRNE challenges. This issue highlights APL's latest contributions to detecting, identifying, and mitigating CBRNE threats to strengthen national and global security.

INTRODUCTION

Although asymmetric threats are a focus of international security efforts, the risk of a chemical, biological, radiological, nuclear, and explosive (CBRNE) attack remains ever-present, and capabilities are constantly evolving. These threats can be anthropogenic (e.g., chemical warfare agents or explosions) or naturally occurring (e.g., disease outbreaks) and are among the most insidious challenges facing our nation. Their impact, evidenced in the terrorist attacks on 9/11 or the COVID-19 pandemic, can be catastrophic in both the immediate and long terms. APL is dedicated to developing game-changing capabilities to enhance resilience, detect and neutralize threats before they materialize, and create asymmetric advantages for national security.

APL leverages a broad range of expertise to counter CBRNE threats, employing advanced competencies in molecular and cell biology, omics characterization, public health and epidemiology, aerosol science, chemical synthesis, chemical and nuclear engineering, nuclear physics, advanced analytics, and sensor design and development. Additionally, we integrate artificial intelligence, data science, complex systems, and autonomy to develop innovative technologies and systems that transform vast amounts of data into actionable intelligence and strategic advantages.

This issue highlights APL's latest contributions to detecting, identifying, and mitigating CBRNE threats to strengthen national and global security.

THE ARTICLES

This issue begins with “Simulants for Chemical and Explosive Threats” in which Lawrence and Van Houten describe the development of a systematic process to design and select effective simulants. Because working with real chemical warfare agents and explosives is dangerous and highly regulated, simulants (nontoxic substances that mimic the key properties of chemical warfare agents and explosives) are used to facilitate research, training, and technology development. The systems-engineering-based approach ensures that selected simulants closely match the properties of real threats but are safe to handle. The article also describes how these simulants help improve detection technologies, decontamination methods, and training exercises for security and defense personnel.

Next, in “Large-Scale Production of Radiopure ^{135}Xe from Bremsstrahlung γ -Irradiation of Solid Xenon Difluoride,” Lloyd et al. present a novel method for producing the radioactive xenon isotope ^{135}Xe , which plays a critical role in monitoring nuclear tests worldwide. This research was conducted in APL’s linear accelerator facility, which was established in 2022 to support experiments requiring extremely high radiation fields. The team successfully generated ^{135}Xe from solid xenon difluoride (XeF_2) using an innovative approach that significantly increases yield while ensuring the isotope remains pure and free of contaminants. This breakthrough enhances the calibration of nuclear test monitoring equipment, improving the ability to detect illicit underground nuclear explosions. Additionally, the study outlines strategies for refining the process to enable more efficient large-scale production.

In “APL’s Contributions to the Odor Detection Canine Community,” Klimkiewicz and Deglau highlight 15 years of advancements in odor detection canine research. These canines play a crucial role in security, law enforcement, and disaster response, assisting in detection of explosives, narcotics, and other hazardous materials. APL has contributed to multiple aspects of advancing canine detection capabilities, including breeding high-performance detection dogs, developing advanced training methodologies, and designing safer training aids that mimic real threats without using dangerous substances. Additionally, APL researchers have explored methods to enhance communication between dogs and handlers and have optimized deployment conditions through airflow monitoring and other tools. These innovations significantly improve the effectiveness and reliability of odor detection canines in real-world operations. Through ongoing research and collaboration, APL continues to advance the role of detection dogs in national security and public safety.

The next few articles highlight advancements in artificial intelligence and machine learning. First, in

“Using Knowledge Graphs to Counter Weapons of Mass Destruction,” Mariner et al. describe the development of a knowledge graph system designed to help US government agencies combat weapons of mass destruction. Many government databases contain critical yet fragmented information about CBRNE threats, making it challenging to track emerging risks. To address this, APL developed the CBRNE Semantic Framework, a structured data model that organizes and connects disparate sources of information, enabling more effective pattern recognition and threat detection. This framework powers a tool that allows analysts to rapidly retrieve relevant data, assess potential risks, and anticipate how adversaries might develop weapons of mass destruction. By leveraging this technology, agencies can enhance their ability to detect, prevent, and respond to evolving threats.

Next, in “MLM: Machine Learning for Threat Characterization of Unidentified Metagenomic Reads,” Baugher et al. describe their development of a machine learning system to analyze unidentified genetic material in biological samples. The Machine Learning for Metagenomics (MLM) pipeline is designed to detect potential biological threats by analyzing DNA sequences that do not match known organisms. Using advanced classification models, the system assigns threat levels to these unidentified sequences, providing forensic and military investigators with real-time hazard assessments. Tests of the system have demonstrated its high accuracy in identifying threats, highlighting its value for monitoring emerging or engineered biological dangers. The technology is being refined for deployment in field-ready devices, enhancing rapid threat detection and response capabilities.

In “Assessment of Sequencing for Pathogen-Agnostic Biothreat Diagnostics, Detection, and Actionability for Military Applications,” Bradburne et al. explore the use of genomic sequencing as a tool for detecting biological threats in military and field settings. While traditional methods, such as polymerase chain reaction (PCR), remain the fastest, most cost-effective, and most reliable option for identifying known pathogens, sequencing can be valuable when dealing with unknown threats. The researchers tested different sequencing methods and found that a hybrid enrichment approach was the most effective for detecting biothreats in simulated patient samples. However, sequencing remains slower and more expensive than PCR, making it most useful in cases where the infectious agent is unknown or emerging. As sequencing technology advances and costs decline, it may become a more viable tool for military and field applications, improving biothreat detection and response capabilities.

In “Wearables-Based Disease Surveillance: SIGMA+ Human Sentinel Networks Concept of Operations,” Stanish et al. describe how wearable technology, such

as smartwatches, could be used to detect and monitor disease outbreaks in real time. A network of volunteers wearing sensors could provide early warning of infectious disease outbreaks, ranging from seasonal flu to biothreats such as anthrax. By analyzing changes in heart rate, temperature, and other physiological markers, the system can alert individuals to seek medical testing, enabling public health officials to rapidly respond. Modeling showed that tracking just 5% of a population with these sensors could detect outbreaks days earlier than traditional surveillance methods. This innovative approach has the potential to enhance early disease detection, improve emergency response efforts, and strengthen public health preparedness.

CONCLUSION

The articles in this issue reflect the breadth and depth of APL's sustained commitment to countering CBRNE threats through innovation, scientific rigor, and cross-disciplinary collaboration. From advancing threat-based training tools and pioneering new methods for nuclear test detection to enhancing real-time bio-surveillance through wearable technology and applying cutting-edge machine learning to genomic data, APL continues to push the boundaries of what is possible in national and global security. These capabilities are not only advancing threat detection and response, but they are also reshaping the landscape of preparedness and resilience in an era of increasingly complex and asymmetric threats. As adversaries evolve and technologies advance, APL remains at the forefront of developing the tools, systems, and strategies necessary to protect our nation and its allies.



Kelly A. Van Houten, Asymmetric Operations Sector, Johns Hopkins University Applied Physics Laboratory, Laurel, MD

Kelly A. Van Houten is the supervisor of APL's Applied Chemistry and Physics Group, which is responsible for developing solutions to detect, defeat, and deny chemical and nuclear threats. She has a BA in

chemistry from Johns Hopkins University, a PhD in chemistry from the University of Maryland, College Park, and an MBA from Johns Hopkins University. She has over 20 years of experience developing novel detection methodologies for organophosphates, designing and synthesizing chemical simulants, and developing chemistry-based warfighter tools. Her email address is kelly.van.houten@jhuapl.edu.



Christopher C. Carter, Asymmetric Operations Sector, Johns Hopkins University Applied Physics Laboratory, Laurel, MD

Christopher C. Carter is the acting manager of APL's Counter Chemical, Biological, Radiological, Nuclear, and Explosive (CBRNE) Threats program area. He has a BS in physics from Washington & Jefferson College and an MS and a PhD in chemical physics from Ohio State University. He has a broad technical background in physics, chemistry, CBRNE defense systems, and optical/laser-based techniques, with experience in research and development of systems for the detection, identification, and defeat of CBRNE species. His email address is christopher.carter@jhuapl.edu.



Joshua B. Broadwater, Asymmetric Operations Sector, Johns Hopkins University Applied Physics Laboratory, Laurel, MD

Joshua B. Broadwater is the manager of APL's Health Protection and Assurance program area. He has a BEng in electrical engineering and applied mathematics from Vanderbilt University, an MS in electrical engineering from the Georgia Institute of Technology, and a PhD in electrical engineering from the University of Maryland, College Park. His primary technical skills include detection and pattern recognition algorithms for electro-optical/infrared remote sensing systems, and his specialty is hyperspectral/multispectral imaging. Joshua's other research includes work on adaptive and semi-supervised classification methods, incorporation of physics models into pattern recognition systems, and statistical signal processing techniques. His email address is joshua.broadwater@jhuapl.edu.



Simulants for Chemical and Explosive Threats

David S. Lawrence and Kelly A. Van Houten

ABSTRACT

Studies using chemical warfare agents (CWAs) and explosives are dangerous and are therefore conducted only in specialized laboratories with highly controlled conditions and limited accessibility. Obtaining these materials for study is another challenge, as they are tightly regulated. Because of these challenges, simulants—molecules that mimic key characteristics of a specified CWA or explosive but lack toxicity—are often used in testing, sensor development, and decontamination studies. In the past, simulants have generally been selected on the basis of their historical use (with researchers sometimes simply choosing “convenient” materials that happen to provide a detector alarm, for example) rather than rational design. The Johns Hopkins University Applied Physics Laboratory (APL) created a simulant development approach, based on systems engineering concepts, that takes input from relevant parties and is scoped specifically for a project objective. This methodology can be universally applied to any type of simulant and includes down-selection criteria to identify specific simulant candidates that can be verified and validated according to the project’s required fidelity. This article describes the development approach, selection process, and demonstrated use cases for both CWAs and energetic materials.

INTRODUCTION

The use of chemical warfare agents (CWAs) is a growing threat. Between 1970 and 2020, more than 200,000 global terrorist attacks were reported in the Global Terrorism Database (GTD),¹ but just over 400 involved a CWA. However, from 2013 to 2017, a 500% annual increase of CWA-related incidents (193 attacks) was reported.¹ Recent events include the 2018 attack in Salisbury, United Kingdom, with a reported Novichok agent;² the 2017 assassination of the half-brother of Kim Jong Un with the nerve agent VX;³ and over 1,400 deaths attributed to chemical warfare in the Syrian conflict.^{4,5}

Adversarial use of energetic, or explosive, materials is also a continuing threat. For the calendar year 2022, the US Bureau of Alcohol, Tobacco, Firearms and Explosives (ATF) Bomb Arson Tracking System (BATS) reported 14,627 explosives-related incidents in the United States.⁶ Although the number of US incidents has varied slightly over the past couple of decades (since 9/11), it has been consistently high and reflects the much higher number of incidents occurring worldwide.

These trends highlight the need to study toxic CWAs and energetic materials and the consequences of their

use, but work with these materials is potentially hazardous and usually fraught with challenges—such as government regulation in gaining access to specialized laboratories, licensing, and accessing materials (especially chemical agents on the Chemical Weapons Convention list of scheduled chemicals⁷). For these reasons, it has become necessary to develop simulants—materials that mimic the relevant properties of the “target” chemical agent or energetic material. For example, simulant materials can be used for testing detection capabilities, exercising decontamination protocols, or training. Each application will have specific target attributes that need to be simulated with a required degree of fidelity. While some simulants may be adequate for more than one application, each simulant is generally tailored for a particular use case (such as detection).

Since 2006, APL researchers have been preparing simulants and test articles for explosives, CWAs, and narcotics threats for the Department of Defense and the Department of Homeland Security (DHS). In efforts for DHS and the Transportation Security Administration (TSA), APL developed simulants for explosives and synthetic opioids. This article focuses on APL’s simulant-based efforts for CWAs and energetic threats; APL’s work on simulants for illicit drugs is outside the scope of this article but is an active area of research.

APL has established guidelines for a rigorous and successful design and testing program, shown schematically in Figure 1 for test and evaluation (T&E) applications. The overarching approach to simulant development is based on a “systems engineering” philosophy that begins with understanding the intended use for the simulant and how it contributes to the entire T&E process. The first step, “technology knowledge,” requires end-user input to help establish selection parameters and includes relevant target data so that the target–simulant characteristics used for the application can be correlated during the selection process.

Simulant development for both CWAs and energetic materials follows equivalent design and development paradigms. It is important that the entire process—particularly, the operational use of the material—be kept in mind when designing simulant materials. Development of simulants for other applications, such as decontamination, follows similar approaches.

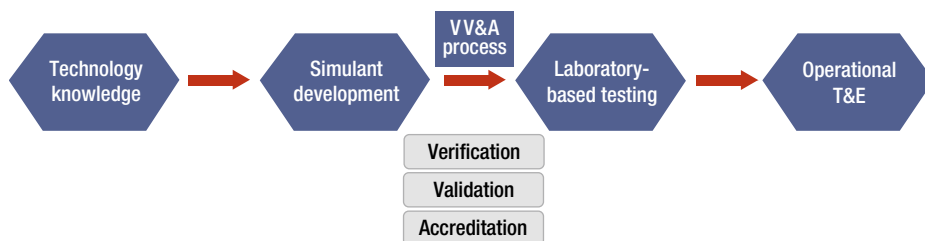


Figure 1. Standardized simulant development process for operational T&E. It is critical that the entire process, especially the operational use of the material, be considered during development.

EXPLOSIVE SIMULANTS

In 2007, APL developed a generic verification, validation, and accreditation (VV&A) methodology for use with any simulant and any detection technology. The VV&A methodology begins with a detailed understanding of the detection technology and algorithms of interest. **Verification** involves comparing relevant detection parameters for the energetic target and any candidate simulants. One key technology for detecting energetic materials is based on x-ray imaging. X-ray-based detection systems generally rely on material characteristics that include the effective atomic number and the density of the material (mass per unit volume). A related value, the CT (computed tomography) number, is also used in some x-ray screening systems as a way of describing the x-ray “texture” of a material. These characteristics can be calculated and/or measured for both energetic targets and simulant materials.

Validation of the candidate simulants involves side-by-side comparisons with the appropriate energetic target in the detection system under evaluation. For these purposes, the “system” includes not only the hardware but also the firmware and any software algorithms currently in place. A sufficient number of test runs with both the energetic target and the simulant must be performed using the system, in all relevant orientations of test samples (depending on the type of detection system), to ensure statistical significance of the probability of detection and probability of false alarm values within the desired level of confidence.

Accreditation involves the determination that the chosen simulant will perform appropriately under the conditions of its intended use. For an operational test, such as in an airport security checkpoint, the simulant will have to be usable in the local environment (e.g., in similar temperature and humidity conditions). It will also need to be nontoxic to humans and safe to use in indoor environments. The material’s shelf life should exceed the duration of the testing period, at a minimum. Finally, the material should be user-friendly for the intended application—for example, when contained in a piece of luggage with other background materials, such as clothing and electronics (“clutter”), the material should be packaged in such a manner that it can be manipulated to conform within the luggage and not leak onto other contents.

During its 15+ years of technical support to TSA, APL has cataloged physical and chemical properties of hundreds of explosives, precursors, and related materials, as well as simulants (commercial, APL developed, and component materials). These

Primary Name: Sodium Benzoate

Primary Abbreviation:

Chemical Names: Benzoic acid sodium salt;

Commercial Names: Purox S; Benzotron; FEMA 3025;

Abbreviations:

Common Names: Benzoansodny; Natrii Benzoas; Benzoate of soda; Antimol;

Variant Name:

CAS #(s): 532-32-1

Manufacturer: Aldrich

Category: Single Product

Images

Simulants

Physical Characteristics

Chemical Characteristics

Solubility

Detection Parameters

Edit

X-Ray-based Detection

Parameters

Values

Notes

Zeff (Calculated) (single) 7.600^[1]

Chemical Characteristics

Edit

	Formula	Elements
Molecular Formula	C ₇ H ₅ NaO ₂	C 68.3% H 3.5% O 22.2% Na 16.0%

Characteristics	Values	Notes
Bulk density (single)	0.78 g/cm ³ ^[53]	tamped in graduated cylinder
Bulk density (single)	0.77 g/cm ³ ^[53]	tapped density in graduated cylinder
Density (single)	1.440 g/cm ³ ^[54]	
Flash Point (single)	100.0°C ^[54]	100.0°C (>212°F)
Melting Point (single)	300.0°C ^[51]	>300°C
Molecular Weight (single)	144	

Figure 2. Example windows from the ALCHEMY database. This APL-developed database contains hundreds of records with referenced values as well as online tools to aid in simulant design.

properties include calculated and measured values for various detection technologies, such as x-ray, millimeter wave, optical, and nuclear-based systems (e.g., percentage of nitrogen density). Under tasking from TSA, APL developed a database that serves as a reference guide to enable efficient simulant development. The Augmentable Library of CHemicals, Explosives and other Materials for homeland securitY (ALCHEMY) database contains hundreds of records with referenced values (literature, measurement details, etc.) as well as online tools to aid in simulant design (Figure 2). The team also developed a quality management plan for ALCHEMY measurements that includes standard operating procedures for measuring properties during any simulant development activities.

In addition to developing the database and standard operating procedures for property measurement, the team constructed a simulant development process, shown as a flowchart in Figure 3, and an approach to independent verification and validation (IV&V). In general, the design of simulant candidates follows a methodical process, using information from the ALCHEMY database

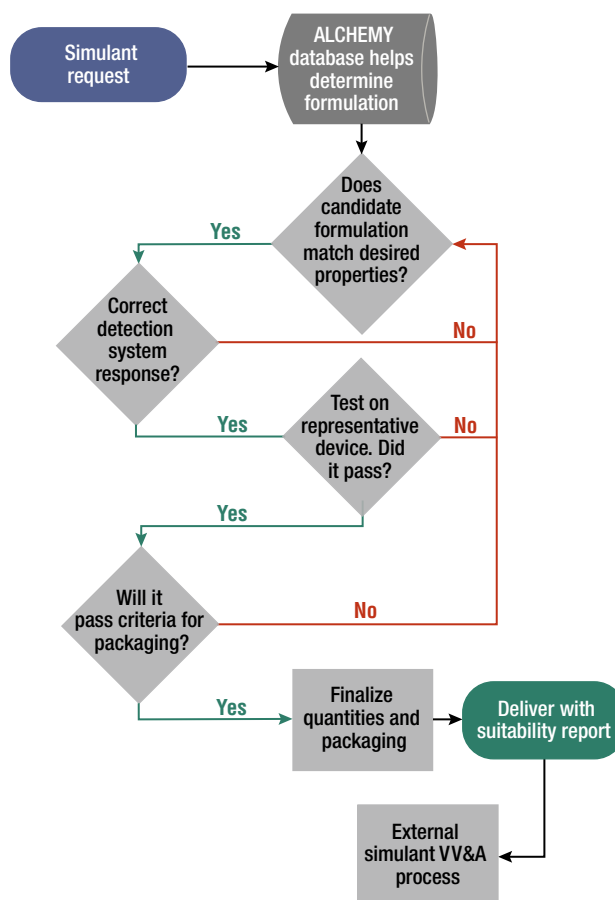


Figure 3. APL simulant development process. In general, this methodical process leverages an intake form that includes information on the simulant along with data from the ALCHEMY database to determine the formulation. Subsequent steps ensure thorough testing, and the process concludes with delivery of the simulant followed by IV&V.

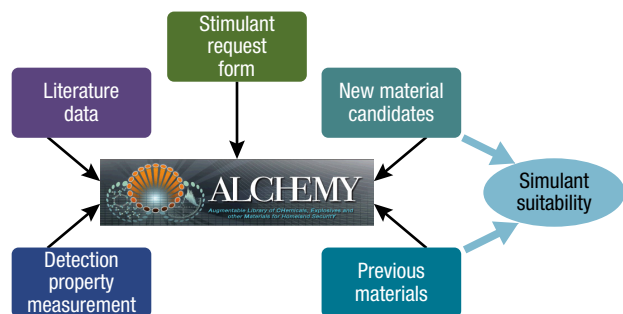


Figure 4. Another visualization of the simulant development process. Here the ALCHEMY database is used as the central tool. It takes input from the simulant request form, literature data, and detection property measurement to provide both previously developed materials and new material candidates.

to determine what commercial formulations might exist (and could be leveraged), what previously developed simulant formulations could be used, and what previously characterized materials could be combined.

This process has been implemented many times over the years to provide simulants and test articles to TSA and DHS for a variety of detection technologies. These technologies have included x-ray, millimeter wave, and neutron/gamma-based detection systems for applications in baggage, person-borne, and cargo screening. For the TSA-based simulants, the team created a form to capture all the relevant parties' requirements and priorities. The form documents basic information on the requested simulant and its application, required detection performance (particularly, the desired fidelity between target energetic and simulant materials), and operating conditions (for example, whether the material will be used indoors or outdoors, details on any interfering equipment, and how the material might be packaged into the test articles). While the specific process described in this article was developed by APL, several other organizations have developed similar approaches. All of the developers recently came together to draft the first-ever ASTM standard for the development of explosive simulants,⁸ which leverages input from APL.

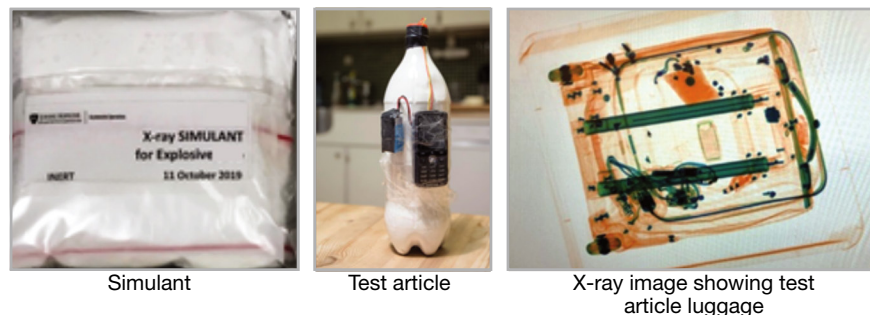


Figure 5. Detection-based application. Shown are a packaged simulant, a test article (an IED), and an x-ray image of a test article in luggage.

Figure 4 shows another way to visualize the simulant development process, where the ALCHEMY database is used as the central “tool” that takes input from the simulant request form, literature data, and detection property measurement. The ALCHEMY tool can be used to explore previously developed materials and to generate new material candidate mixtures (based on existing components) that can be used to examine simulant suitability in accordance with the desired target–simulant fidelity requirements.

As discussed above and illustrated in Figure 5, a detection-based application of simulant development for energetics includes the formulation of a simulant material, which can then be packaged into a test article (here, an improvised explosive device, or IED) and placed into luggage in order to generate an x-ray image for testing.

CHEMICAL SIMULANTS

The recent growth of CWA use described in the introduction highlights the need to develop novel methods for decontamination, destruction, and detection. The Chemical and Biological Weapons Conventions prohibit the widespread use of chemical and biological warfare agents for testing purposes, so simulants must be used. Even if agents were readily available, the needs of development and training programs are best met with simulants. Simulants minimize the risk to personnel and the contamination of equipment and the test location. In addition, working with agents can be cost prohibitive and is limited to certified locations. For these reasons, simulants for chemical and biological warfare agents are crucial for passive defensive research as well as developmental and operational testing. Simply put, simulants allow more testing and training in more settings over a shorter period of time and with fewer restrictions. The simulant data obtained can be used to inform final validation studies with CWAs.

Chemical simulants can facilitate the development of novel mitigation strategies since, by definition, they lack the toxicity of the agent. Chemical simulants may be structurally similar to the agent, may have similar reactivity under a given set of conditions, or both. Similar to the development of explosive simulants described above, the selection of the optimal chemical simulant for a given application combines the iterative activities of literature search, laboratory experimentation, and computational approaches.

APL has been developing CWA simulants since 2006 and has found that certain tasks are critical to all simulant selection

efforts. We have developed a tool set to aid in the simulant selection process. The tools used to down-select from candidate simulants provide a template to guide the chemist and the nonspecialist end user in identifying a CWA simulant that meets the end user's needs (Figure 6).

The simulant down-selection process starts with a series of questions, called the "Green Sheet" (Figure 7), designed to identify the simulant's intended use. Once the intended use has been determined, the next step is identification of agent properties relevant to that use. These properties, the most important components of the process, are then used to drive the simulant selection process. Selecting the proper simulant relies on the correlation of quality simulant and agent data, regardless of the ultimate use of the simulant. The higher the fidelity of the agent data, the more likely that the selected simulant will mimic the desired target agent behavior. Examples of agent data used in APL's simulant selections include chemical reactivity with decontamination solutions, physiochemical properties (e.g., solubility, vapor pressure, octanol-water partition coefficient, surface tension, viscosity, and thermal reactivity), and common synthetic pathways. If agent data are unavailable, they must be calculated computationally or collected at a government surety laboratory (a facility where agents are analyzed and other services are performed in a safe and secure environment; surety laboratories are used to analyze chemical, biological, and nuclear materials and to ensure the safety of the materials and the people working with them). These properties are prioritized to help

drive the development process. Simulant physiochemical data can be collected from open-source data or computationally determined. Wherever possible, simulants are also evaluated using the same experimental conditions that were used to collect agent data. Finally, the agent and simulant data are correlated. The process is discussed in more detail below.

As mentioned, the process begins with the Green Sheet, a series of questions that define the end user's simulant requirements. These include: What is the intended use? Will the simulant be used in a laboratory with trained chemists, or will it be used outside for fieldwork? If the simulant will be used in the laboratory by trained chemists, smaller quantities of simulant and higher levels of toxicity may be acceptable since engineering controls will be available. On the other hand, if the simulant will be used in outdoor fieldwork, larger quantities of simulant with lower toxicity levels are required, along with site location approvals. Determining how much simulant is needed will help determine whether the simulant can be purchased commercially or will need to be synthesized. Answering this question also helps in establishing timelines since it can take a long time to procure some chemicals.

Based on the end-user requirements defined in the Green Sheet, the agent properties required for the effort can be identified and prioritized. For example, using a simulant in an outdoor test may necessitate library updates to the detection equipment being used in the test. Obtaining the CWA data is the most critical part of the simulant selection process. These studies are

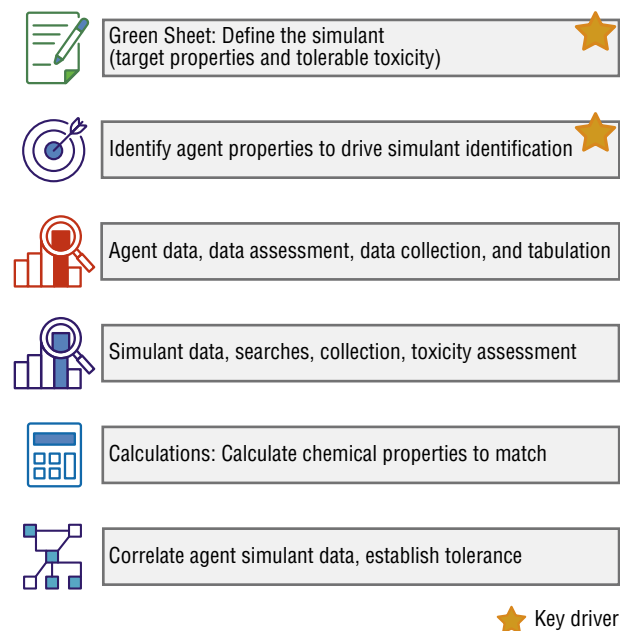


Figure 6. The simulant down-selection tool set. These tools guide the identification of a CWA simulant that meets end-user needs.

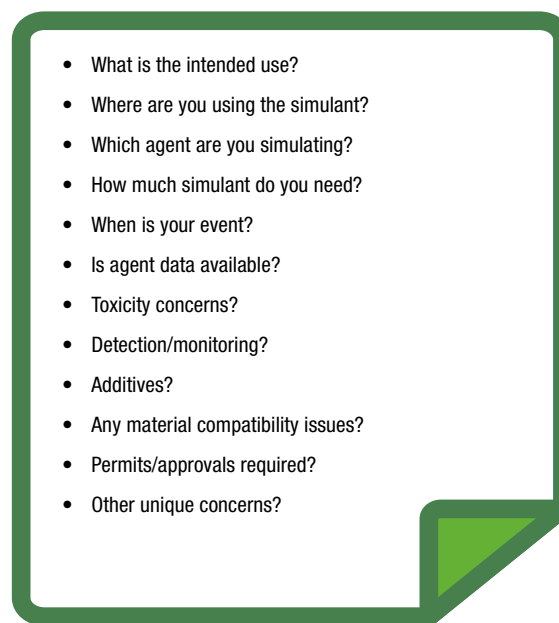


Figure 7. The Green Sheet. Answering a series of questions that define the end user's simulant requirements is the start and a key driver of the down-selection process.

expensive and can be performed only at government surety laboratories. If experimental data are unavailable, the physical properties can be modeled computationally.

Once the desired agent properties are selected, the simulant candidates are sought from the open literature. If any of the physical properties of the simulant are unavailable, they can be measured or computationally calculated. The simulant candidates are further down-selected by the criteria set by the Green Sheet. At this point, simulant candidates are narrowed to a short list. Laboratory studies are performed to evaluate simulant performance, ideally using the same procedures used to collect the agent data. For some simulant use cases, end users would like to be able to detect the simulant using their operator tools (specific detection technologies). In these cases, the simulant candidates can be further down-selected to be compatible with the detection technology. A colorimetric or fluorometric indicator is another option that can be added to the simulant formulation and provides a visual indication of simulant location. During the selection process, it is important to ensure that any additive has similar properties to the agent. For example, the additive would have a similar octanol–water partition coefficient to facilitate decontamination studies. Next, it is important to consider any material compatibility issues. For example, simulants used for testing on sensitive equipment should be compatible with the surface materials and should not damage the equipment.

Although each use case is unique and can have requirements that are not captured by the initial question list, a completed Green Sheet provides a template to identify the key agent properties that drive the simulant selection. The agent properties that must be retained in the simulant for a specific application vary considerably with the simulant use. Finally, the selected simulant formulation is evaluated under the experimental conditions used above and the results are correlated to the agent. This will show how the simulant compares to the agent. For example, compared with the agent, a decontamination simulant could correlate as x times easier or harder to remove from a given surface when following the use-specific instructions.

This is best illustrated with an example.

Chemical Simulant Example

The Defense Threat Reduction Agency (DTRA) Automated, Detailed Equipment Decontamination for Land Vehicles (Auto-Decon) advanced technology demonstration program required a chemical weapons simulant for use in large-scale outdoor training of the United States Army Chemical Corps. The simulant was used for a baseline detailed equipment decontamination and training of the 71st Chemical Company (Figure 8).

APL worked with the Auto-Decon team to define and prioritize the target properties of the simulant. The



Figure 8. Photo from a decontamination training exercise. APL supported this outdoor field test evaluating decontamination of military vehicles. (Used with permission from Esry.¹⁰)

Auto-Decon Green Sheet is shown in Figure 9. With the readily available agent data, as well as the protocol used for decontamination with hot, soapy water (HSW),⁹ the APL team developed a list of simulant candidates.

The initial simulant list included more than 100 candidates selected primarily from commercial off-the-shelf flavor and fragrance compounds. The simulant properties identified on the Green Sheet were molecular weight, melting point, boiling point, vapor pressure, octanol–water partition coefficient, and toxicity. The octanol–water coefficient is a first-principle descriptor of how a compound will interact in a mixed aqueous/

- ✓ Stimulant must be approved for open-air release.
- ✓ Simulant should have similar behavior to HD and/or VX on CARC-painted surfaces.
- ✓ Simulant should closely match physical properties (vapor pressure, viscosity, octanol–water partition coefficient) of HD and/or VX.
- ✓ Fluorophore detection reagent for decon is required.
- ✓ Materials must be commercial off-the-shelf and inexpensive.
- ✓ Materials must have extremely low toxicity ($LD_{50} > 1,000$ mg/kg).
- ✓ Simulant should behave and react like agent under HSW decontamination.
- ✓ Simulant solubility in water should increase upon decontamination.

Figure 9. The Green Sheet for DTRA's Auto-Decon training event. The sheet identifies simulant use and target properties. With this information, along with agent data and the protocol used for decontamination, the APL team developed a list of simulant candidates.

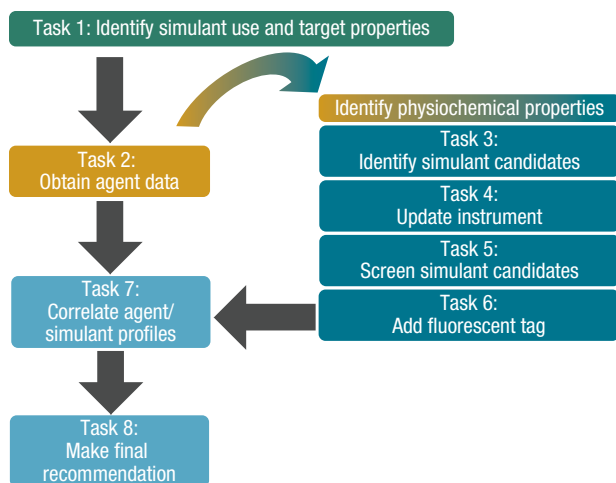


Figure 10. The Auto-Decon simulant down-selection process. The APL team initially selected candidate fluorophores that were expected to be colorless in solution under ambient light and to fluoresce blue under ultraviolet (UV) light irradiation.

organic system (like soapy water). For reference, compounds with a low octanol–water coefficient are more water soluble than organic soluble. Any molecule with an octanol–water coefficient between that for VX and HD was selected for further evaluation.

The Green Sheet indicated that the final simulant formulation must contain a fluorophore visible to the naked eye. The down-selection process is shown in Figure 10. The APL team initially selected candidate fluorophores on the basis of the criteria that they were expected to be colorless in solution under ambient light and to fluoresce under long-wave ultraviolet (UV) light irradiation. The fluorophores were required to be fluorescent when exposed to the long-wave UV light. The initial evaluation of the fluorophores involved dissolving each molecule in ethanol at a concentration of 50 mM (Figure 11). Fluorophores that gave brightly colored solutions and fluorophores that did not dissolve in ethanol were eliminated from consideration.

The APL team then evaluated the remaining simulant candidates' solubilities of the fluorophores. They evaluated various simulant–fluorophore pairs for their visibility under UV light on chemical-agent-resistant coating (CARC)-painted stainless

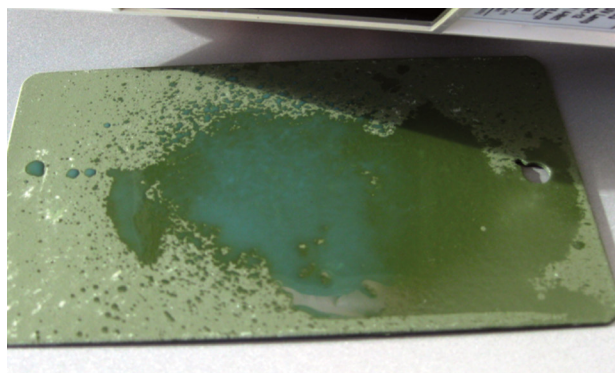


Figure 11. Representative simulant with an added fluorophore on a CARC coupon. This photograph was taken outside in direct sunlight. The blue fluorescence is readily visible from the hand-held UV light source.

steel coupons. Simulant–fluorophore pairs that were not readily visible on CARC were eliminated. Since the fluorophore serves as a marker for the simulant formulation, it is important that it behave like the simulant under HSW decontamination. The octanol–water coefficients were calculated for selected fluorophores using commercially available software. Finally, selected simulant–fluorophore pairs were evaluated in decontamination studies using the same protocols used to collect agent data. Figure 12 shows results from the Auto-Decon test. The top photos (a) show before decontamination and after successful decontamination of a part of a military vehicle. The bottom photos (b) show a failed decontamination. The vehicle shown in the bottom photos was returned to the decontamination line for additional

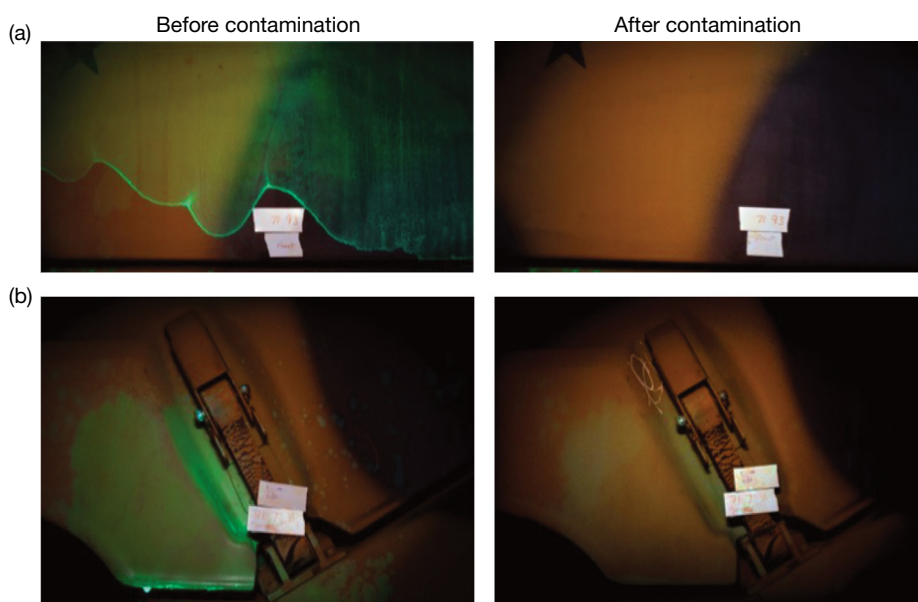


Figure 12. Photos from the Auto-Decon field test. Left, simulant formulation applied before decontamination. Right, after decontamination. (a) Successful decontamination; (b) unsuccessful decontamination. (Used with permission from Esry.¹⁰)

cleaning. The ability to quickly access decontamination efficiency in the field provided real-time feedback to end users so they could evaluate performance and protocols.

The Auto-Decon simulant use case had some unique requirements. Since the simulant was applied to military vehicles, it was important that it did not damage the vehicles. In addition to performing decontamination evaluation studies on CARC coupons, the APL team also tested with glass, cast acrylic, and extruded acrylic to determine whether these surfaces would be compatible with the simulant and the decontaminant. Additionally, because the field test's decontamination wash solutions were released into the environment, the simulant formulation had to be biodegradable to comply with requirements of the state where the simulant was used in training. These requirements represent the unique needs for this use case and demonstrate the need to account for simulant use during early stages of field test planning to ensure there is sufficient time to resolve any site-specific issues.

CONCLUSION

The hazardous nature of explosives and CWAs has driven the development of simulants, which mimic specific properties and characteristics of the materials of interest. The use of simulants facilitates development of tools and tactics to protect the warfighter and other frontline security professionals. Using a systems engineering approach, APL has created a simulant development process that includes a methodology for the design and selection of scenario-specific simulants. This process provides simulant materials that are ideally suited to a specific detection or other application, as defined by

the mission. Our selection process has been embraced by the user community and has been leveraged for numerous use cases. Because of the extreme safety risk and cost of studies using energetic materials and CWAs, simulant efforts will continue to provide valuable, impactful information to our sponsors.

REFERENCES

- ¹START (National Consortium for the Study of Terrorism and Responses to Terrorism), Global Terrorism Database 1970–2020 [data file], 2022, <https://www.start.umd.edu/gtd/>.
- ²J. A. Vale, T. C. Marrs, and R. L. Maynard, "Novichok: A murderous nerve agent attack in the UK," *Clin. Tox.*, vol. 56, no. 11, pp. 1093–1097, 2018, <https://doi.org/10.1080/15563650.2018.1469759>.
- ³P. R. Chai, E. W. Boyer, H. Al-Nahhas, and T. B. Erickson, "Toxic chemical weapons of assassination and warfare: Nerve agents VX and sarin," *Tox. Comm.*, vol. 1, no. 1, pp. 21–23, 2017, <https://doi.org/10.1080/24734306.2017.1373503>.
- ⁴R. Pita and J. Domingo, "The use of chemical weapons in the Syrian conflict," *Toxics*, vol. 2, no. 3, pp. 391–402, 2014, <https://doi.org/10.3390/toxics2030391>.
- ⁵J. Patočka, "Syria conflict and chemical weapons: What is the reality?," *Mil. Med. Sci. Lett.*, vol. 85, no. 1, pp. 39–43, 2016, <https://doi.org/10.31482/mmml.2016.006>.
- ⁶"2022 United States Bomb Data Center (USBDC) Explosives Incident Report (EIR)," DHS TRIPwire, Jun. 2, 2023.
- ⁷"Annex on chemicals," in the *Convention on the Prohibition of the Development, Production, Stockpiling and Use of Chemical Weapons and on their Destruction*, Jan. 13, 1993, <https://www.opcw.org/chemical-weapons-convention/annexes/annex-chemicals/annex-chemicals>.
- ⁸"Standard Guide for Development, Verification, Validation, and Documentation of Explosive and Contraband Simulants for Security Screening Systems," draft standard submitted to the ASTM International E54 Committee on Homeland Security Applications, Nov. 2023.
- ⁹Z. Zander, M. Waller, M. Shue, M. Sheahy, M. Hall, and P. Humphreys, "Evaluation of candidate decontaminants for automated decontamination program," Edgewood Chemical Biological Center Tech. Rep. no. 673, Apr. 2009.
- ¹⁰D. Esry, "Automated Detailed Equipment Decontamination (Auto Decon) Advanced Technology Demonstration (ATD) Baseline Demonstration Simulant Photo Report," KCP-613-8786, Honeywell, FM&T, Kansas City, MO, Aug. 2010.



David S. Lawrence, Asymmetric Operations Sector, Johns Hopkins University Applied Physics Laboratory, Laurel, MD

David S. Lawrence is a project leader and manager in APL's Asymmetric Operations Sector. He earned a BS in chemistry from Carnegie Mellon University and a PhD in organic chemistry from the University of

Rochester. David leads various programs involving detection instrumentation for chemical warfare agents and explosives analytical chemistry, as well as air and water sample preparation and analysis. He has more than 23 years of experience supporting homeland protection programs, including chemical, biological, radiological, nuclear, and explosives (CBRNE) sensor design and development, market surveys, evaluation, and deployment, as well as environmental analyses. He also has 20 years of experience in organic chemistry and biochemistry, specializing in the synthesis of complex organic and organometallic molecules, with research interests in spectroscopic analysis and detection. His email address is david.lawrence@jhuapl.edu.



Kelly A. Van Houten, Asymmetric Operations Sector, Johns Hopkins University Applied Physics Laboratory, Laurel, MD

Kelly A. Van Houten is the supervisor of APL's Applied Chemistry and Physics Group, which is responsible for developing solutions to detect, defeat, and deny chemical and nuclear threats. She has a BA in

chemistry from Johns Hopkins University, a PhD in chemistry from the University of Maryland, College Park, and an MBA from Johns Hopkins University. She has over 20 years of experience developing novel detection methodologies for organophosphates, designing and synthesizing chemical simulants, and developing chemistry-based warfighter tools. Her email address is kelly.van.houten@jhuapl.edu.

Large-Scale Production of Radiopure ^{135}Xe from Bremsstrahlung γ -Irradiation of Solid Xenon Difluoride

Evan P. Lloyd, Ciara B. Sivels, Alan W. Hunt, and Yenuel S. Jones-Alberty

ABSTRACT

The United States, together with the United Kingdom, signed the Limited Nuclear Test Ban Treaty in 1963. The Comprehensive Nuclear-Test-Ban Treaty was partially ratified by the United Nations General Assembly in 1996. A multifaceted worldwide monitoring network, in which the United States actively participates, continuously monitors treaty compliance. One of the tools this worldwide network uses is atmospheric sampling of radioxenon. During an underground detonation, noble gases, such as xenon, do not react with soil and can escape into the atmosphere. The detection of radioactive xenon in 2006 provided reliable proof of North Korea's underground testing. Because radioactive xenon is required for calibrating the detectors, the synthesis of high-purity radioxenon is of interest. In light of this interest, a team at the Johns Hopkins University Applied Physics Laboratory (APL) developed a novel production pathway for the ^{135}Xe isotope using APL's new linear accelerator facility.

INTRODUCTION

This article describes the use of bremsstrahlung radiation to induce $^{136}\text{Xe}(\gamma, p)^{135}\text{I}$ reactions, followed by milking of ^{135}Xe from β -decay of the ^{135}I product. To increase Xe density in irradiated samples, we used solid xenon difluoride, resulting in a yield of 80 nCi ^{135}I and 26 mCi ^{135}Xe from 122 mg XeF_2 after irradiation of 21.9 MeV over 30 min. Using XeF_2 , we were able to separate unreacted xenon from the ^{135}I product via aqueous sodium hydroxide decomposition of XeF_2 , followed by removal of evolved gaseous xenon by cryotrapping with liquid nitrogen. After decay, radiopure ^{135}Xe was recovered by cryotrapping.

Xenon-135, or ^{135}Xe , is required to calibrate the detectors that passively monitor the atmosphere for global enforcement of the 1963 Nuclear-Test-Ban Treaty. Radioactive xenon in the atmosphere can indicate nuclear explosions or testing; it is a clear marker of underground testing (because the unreactive noble gas escapes and persists after a test). Indeed, monitoring ^{133}Xe and ^{135}Xe ratios offered the most reliable proof of North Korea's 2006 underground nuclear test, providing a fission source term in contrast with seismic data that could have been produced with nonnuclear explosives.^{1,2} Optimized purification of xenon from atmospheric

sampling has been demonstrated using the automated radioxenon sampler-analyzer (ARSA) since 1999. ARSA was developed by the US Department of Energy's Office of Nonproliferation and the Pacific Northwest National Laboratory. Engineers have successfully purified and concentrated xenon from the atmosphere for analysis of radioxenon used to detect nuclear activity.

In experimental nuclear physics, a two-body nuclear reaction can be expressed as $A(a,b)B$, where, by convention, A represents the target nucleus; a is the incident particle; b is a lighter ejected particle, known as the ejectile; and B is a heavier ejected particle, known as the recoil. $^{134}\text{Xe}(n,\gamma)^{135}\text{Xe}$ transitions after exposure of low-density gaseous xenon, in which a neutron is incident on a ^{134}Xe nucleus, produce valuable ^{135}Xe samples for calibrating the worldwide detectors. These samples, however, contain mostly ^{134}Xe , which complicates the calibration process. Not only would radiopure and carrier-free ^{135}Xe samples improve the existing state of the art, but using an alternative, denser form of Xe would allow for production of greater yields.

$^{136}\text{Xe}(\gamma,p)^{135}\text{I}$ reactions have been described as a way to produce ^{135}Xe . Horkley et al. recently reported production of 592 Bq of ^{135}Xe after 6.5-h irradiation at 21.8 MeV.³ These experiments produced ^{135}Xe without detectable ^{133}Xe ; however, the yields were 10^3 times lower than would be required for practical use. If using a similar gamma source, concentrating the xenon substrate solves this limitation.

Xenon difluoride, or XeF_2 , is a colorless salt produced from the reaction of xenon and difluorine. These gases react when energy is added. XeF_2 has been synthesized from irradiation with ultraviolet (UV) light, heat, γ -rays, and other energy sources.⁴ Today XeF_2 is typically produced via UV irradiation of a xenon fluorine mixture in a 2:1 ratio with catalytic 1 mol % hydrogen fluoride,⁵ which forms pure crystals. Because of its volatility and reactivity, XeF_2 is best stored cold and in a sealed polyethylene or fluoropolymer container. Although xenon is a noble gas and therefore tends to be chemically inert, xenon difluoride is reactive; it will react with water but not rapidly, and it requires the presence of base to reliably dissociate and evolve xenon gas.⁶ XeF_2 is used as a niche fluorinating agent for research purposes⁷ but has limited industrial use synthetically. XeF_2 is available commercially from common chemical suppliers and can be purchased for less than \$200 per gram, although not in isotopically pure forms. Furthermore, purifying xenon from XeF_2 is simple by using liquid nitrogen for cryo-condensation.

Efforts to optimize the purification of xenon from atmospheric sampling have demonstrated reliable sequestration of radioxenon produced from $^{136}\text{Xe}(\gamma,p)^{135}\text{I}$ reactions and subsequent ^{135}I β -decay. In this article, we report a proof of concept for generating ^{135}Xe in large yields from a solid xenon-containing substrate, followed by purification and trapping of radiopure ^{135}Xe .

LINEAR ACCELERATOR FACILITY

We conducted experiments in APL's linear accelerator facility, a $\sim 4,000\text{-ft}^2$ laboratory that consists of a $\sim 1,000\text{-ft}^2$ heavily shielded accelerator hall, a $\sim 600\text{-ft}^2$ heavily shielded experimental hall, a $\sim 620\text{-ft}^2$ radiochemistry laboratory, and a $\sim 520\text{-ft}^2$ experiment staging area. The accelerator and experimental halls are both partially underground with walls and ceilings consisting of ~ 3 ft of concrete and 1.7 ft of steel, providing ample radiation shielding for radiation-producing machines and large radioactive sources. The accelerator is capable of delivering electron pulses with operator-selectable widths between 0.5 and 4 ms at a repetition rate up to 115 Hz. The maximum charge per pulse ranges from 40 nC for 0.5-ms pulses to 350 nC for 4-ms pulses. The electron energy can be varied from ~ 5 to 25 MeV with an energy resolution of 5%, which can be reduced using collimators or slits. The S-band standing wave radio frequency linear accelerator, which operates at ~ 2.8 GHz, was used to accelerate 21.9-MeV electrons that generate bremsstrahlung γ -radiation using a 2-mm tungsten source. With the electron linear accelerator's energy range and versatility, we were able to develop a novel solution for synthesizing radiopure ^{135}Xe .

EXPERIMENTAL METHODS

We placed xenon difluoride crystals (200 mg) into a 25-mL single-neck borosilicate glass Schlenk reaction tube fitted with a rubber septum. Next we submerged the sealed reaction tube in an ice water bath and then placed it directly in the γ -beam. This setup is pictured in Figure 1.

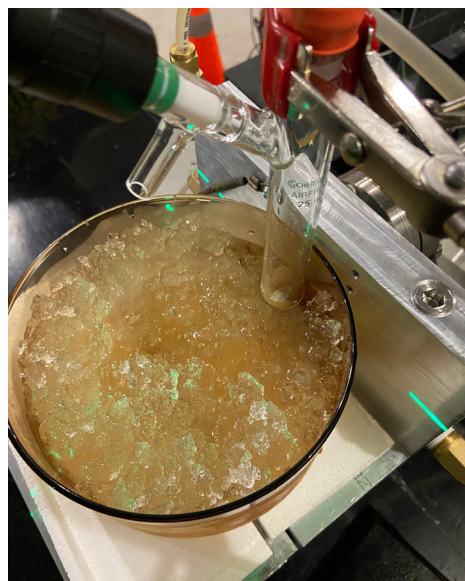


Figure 1. Placement of the reaction tube containing XeF_2 crystals in APL's linear accelerator facility γ -beam.



Figure 2. The apparatus used to purify xenon from XeF_2 . Inset, the U-tube fitted with a pressure gauge and valves on either end containing cryotrapped xenon.

We fit the sealed reaction tube containing irradiated XeF_2 to the apparatus pictured in Figure 2. The apparatus comprised the sealed reaction tube connected to a drying trap that facilitated visualization of moisture trapping. The drying trap connected to a stainless steel U-tube, also shown in Figure 2, and was fitted with a manual valve on both ends and a gauge to monitor internal pressure. We introduced into the reaction tube a steady stream of ultrahigh-purity nitrogen from a cylinder. Next, we opened the tube, drying tube, and reaction tube valves and then submerged the U-tube in liquid nitrogen before adding aqueous sodium hydroxide (1 N, 3 mL) to the XeF_2 crystals. Nitrogen flowed into the reaction solution to sparge the mixture and remove the entirety of dissolved xenon, as shown in Figure 3. We continued to purge the system with nitrogen for 1 min after we could no longer see xenon evolution, and then we shut off the gaseous nitrogen flow. Finally, we closed the reaction tube, drying tube, and tube valves and removed the U-tube from the liquid nitrogen bath, allowing the

tube to warm to room temperature. Figure 4 shows the XeF_2 -containing reaction tube at various stages during these experiments.

We piloted this procedure with unirradiated XeF_2 and examined the collected xenon by residual gas analysis, which is a form of mass spectrometry. During mass spectrometry, the mass-to-charge ratio (m/z) of an ion is measured, typically by manipulating the ion's trajectory using a magnetic field.⁸ The sensitivity of mass spectrometry techniques is such that individual ions of a given mass-to-charge ratio



Figure 3. Removal of dissolved xenon gas by sparging XeF_2 dissolved in 1N NaOH with gaseous nitrogen.

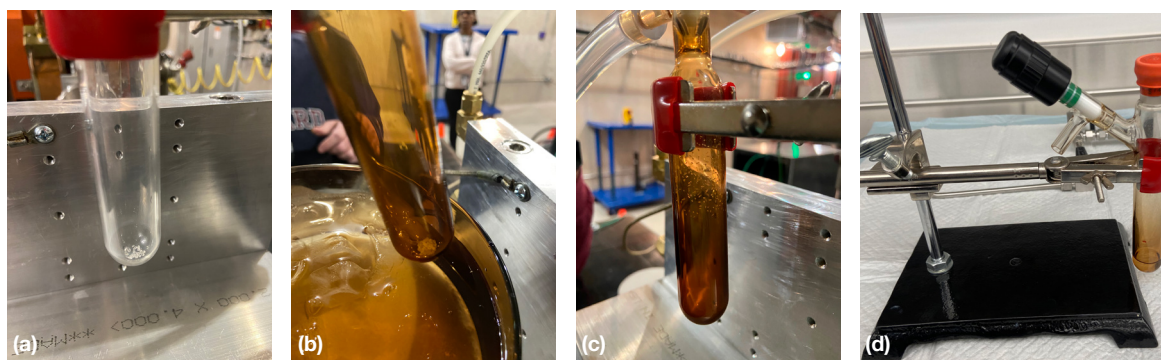


Figure 4. The XeF_2 -containing reaction tube. (a) Crystals before irradiation. (b) Intact crystals after irradiation at 0°C . (c) Sublimation of crystals after irradiation at ambient temperature. (d) Solution after dissociation with 1N NaOH.

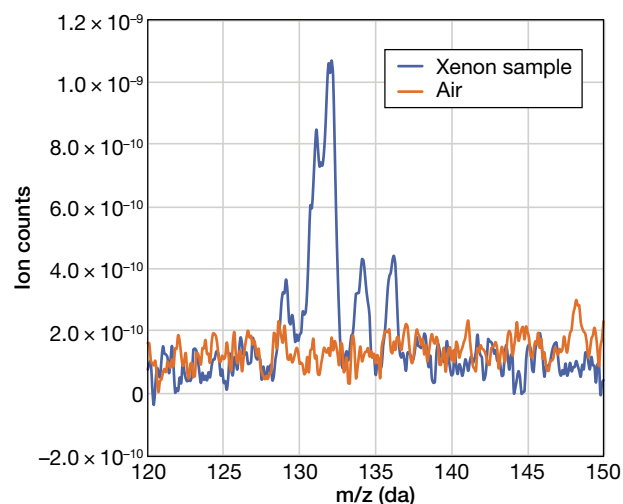


Figure 5. Residual gas analysis of cryotrapped xenon from XeF_2 .

can be counted. This analysis revealed xenon isotopes ranging from 126 to 136 Da, similar to the natural isotopic distribution for xenon, as shown in Figure 5. An increase in ion counts can be observed in this range for the xenon sample, shown in blue.

RESULTS

Irradiation of Xenon Difluoride

We sought to irradiate xenon difluoride crystals and determine the yield of ^{135}I and ^{135}Xe produced from a solid substrate. In a first-pass experiment, we added 100 mg XeF_2 to a borosilicate Schlenk tube. Processes to synthesize XeF_2 involve adding energy during the reaction, including γ -irradiation, and we did not know whether adding high amounts of ionizing radiation could reverse the reaction and produce hazardous gases.⁹

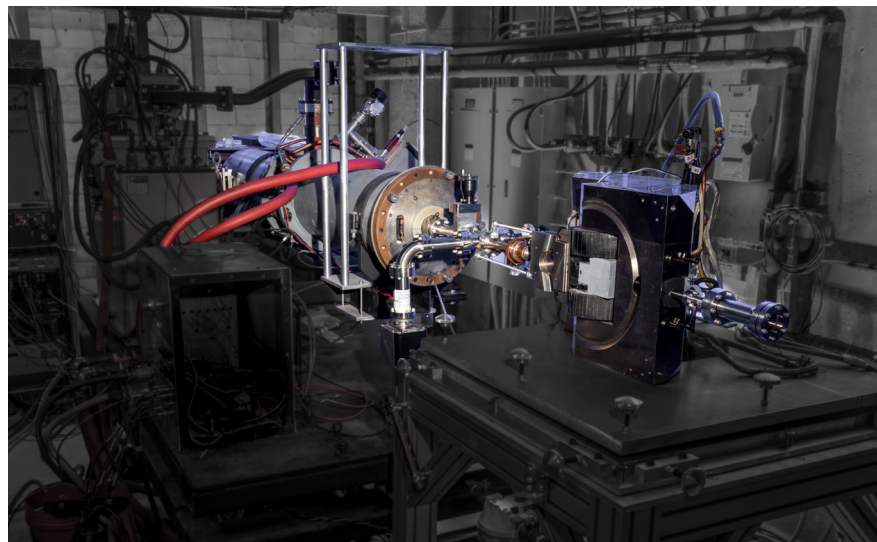


Figure 6. The 25-MeV linear accelerator in APL's facility.

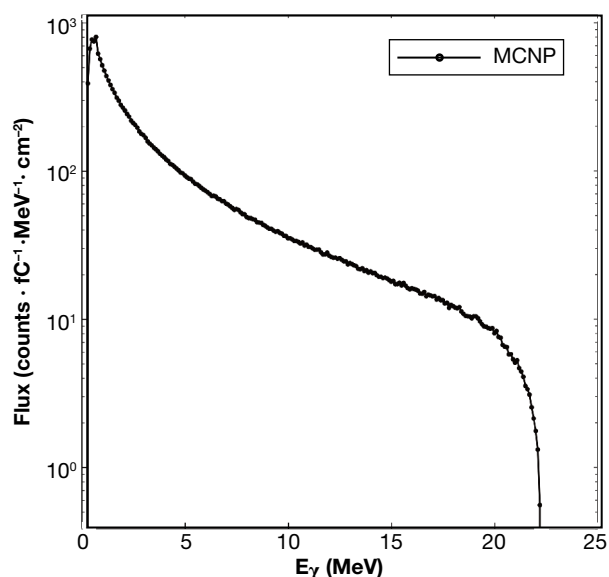


Figure 7. Monte Carlo N-Particle (MCNP)¹⁰ simulated bremsstrahlung spectrum for an incident 22-MeV electron beam.

Therefore, we fit the Schlenk tube to a gas scrubber to remove any produced hydrogen fluoride or fluorine vapors with aqueous 3N sodium hydroxide. This precaution turned out to be unnecessary, however, as we observed no bubbling during irradiation, and the XeF_2 crystals appeared intact after irradiation for 15 min at 21.9 MeV. Longer irradiations, at 1 h, resulted in visible sublimation of the XeF_2 substrate, so we performed future experiments at 0°C by using an ice water bath. With the temperature held constant at 0°C, we observed no sublimation, and the XeF_2 crystals remained intact and in place at the bottom of the reaction tube.

We measured the production yields of ^{135}I and ^{135}Xe at multiple energies by bombarding a 200-mg sample of XeF_2 with bremsstrahlung radiation. Measurements were taken at 16-, 19-, and 22-MeV end-point energies at 15-min irradiation intervals. Electrons were accelerated using the linear accelerator facility's 25-MeV linear accelerator (Figure 6), and bremsstrahlung radiation was generated by impinging a 2-mm-thick tungsten radiator. Also known as braking radiation, bremsstrahlung results from electrons decelerating in a medium.^{11,12} A 2.54-cm-thick block of aluminum served as a beamstop. A simulated bremsstrahlung spectrum for an incident 22-MeV electron beam is shown in Figure 7.

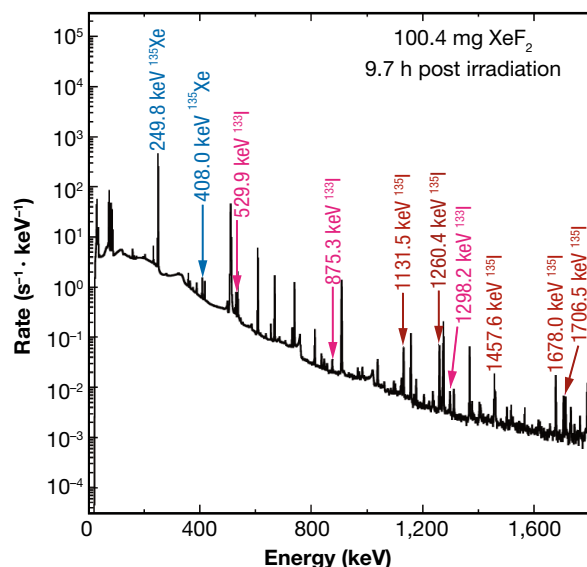


Figure 8. HPGe gamma spectrum for post-irradiated XeF_2 .

Purification of Xenon from Xenon Difluoride

We hypothesized that XeF_2 could be rapidly dissociated into xenon gas and fluoride salts upon addition of aqueous sodium hydroxide. Indeed, adding 3 mL 1N NaOH solution to the XeF_2 crystals caused vigorous bubbling in our initial tests with unirradiated material. We assembled an apparatus to remove xenon after irradiation by using positive flow of nitrogen gas from a cylinder into the sample-containing Schlenk tube, followed by drying of the flowed gases through anhydrous calcium sulfate desiccant and condensation of xenon gas into a stainless steel trap made from ¼-in. stainless steel tubing using liquid nitrogen. Xenon was cryotrapped from unirradiated XeF_2 using our apparatus, and successful xenon recovery was validated by residual gas analysis mass spectrometry.

The experimental workflow was repeated with irradiated XeF_2 and iodine was

successfully maintained in the aqueous sodium hydroxide solution. The isotopes of interest, ^{135}I and ^{135}Xe , have half-lives of 6.9 ± 0.4 h¹³ and 9.13 ± 0.5 h,¹⁴ respectively. Furthermore, it can be extrapolated that ^{135}I β -decays exclusively to ^{135}Xe based on the energies reported for this transition.¹⁵ Characteristic γ -decay energies associated with these radioisotopes were measured by analyzing the cryotrapped gases using a high-purity germanium detector (HPGe), which is a semiconductor γ -ray detector.¹¹ We observed prominent γ -ray decays of energy $E_\gamma = 1,260.409$, 1,131.511, and 1,457.56 keV, as shown in Figure 8. Decay curves, shown in Figure 9, were constrained for each isotope and are within error bars of known values. The production yields for ^{135}I and ^{135}Xe are shown in Figure 10. We determined that ^{135}Xe was successfully purified from the ^{135}I sample. After waiting for ~16 h, we repeated the procedure to sparge the solution and induce cryotrapping of the ^{135}Xe resulting from β -decay of the ^{135}I product during that period. Radiopure ^{135}Xe was recovered.

An additional insight resulted from these measurements. Currently, the experimental cross sections of the $^{136}\text{Xe}(\gamma, n)^{135}\text{Xe}$ and $^{136}\text{Xe}(\gamma, p)^{135}\text{I}$ reactions, which

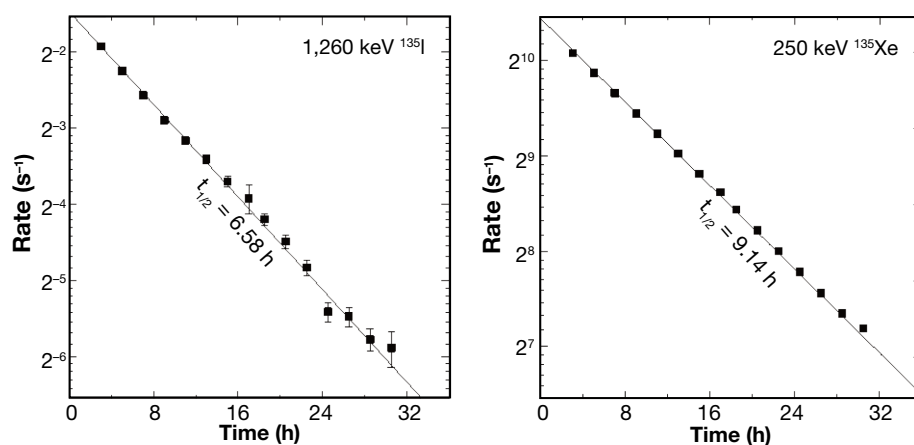


Figure 9. Decay curves for ^{135}I and ^{135}Xe produced from irradiation of XeF_2 .

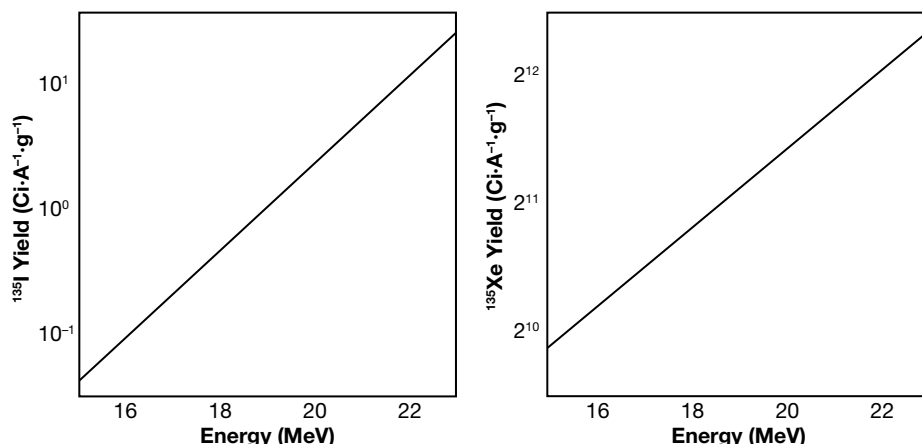


Figure 10. Production yields of ^{135}I and ^{135}Xe at 16, 19, and 22 MeV.

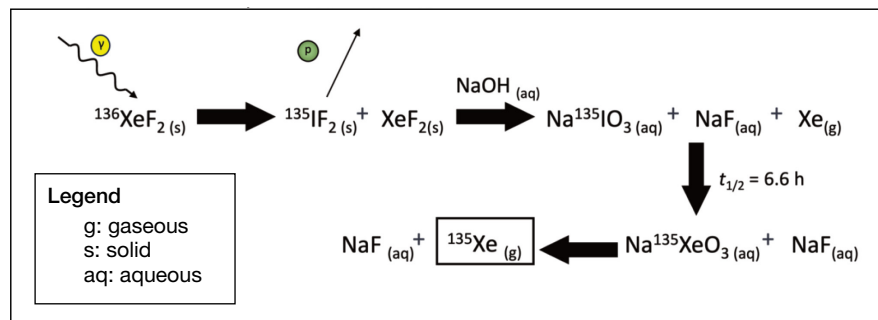


Figure 11. Radiochemical irradiation of XeF_2 and extraction chemistry.

describe the probability of these reactions taking place, have not been measured. As such, theoretical cross sections are used to predict the production yields of the ^{135}I and ^{135}Xe isotopes. Our measured ^{135}I production yield suggests a large discrepancy between the theoretical and experimental cross sections. Further measurements are needed to clarify this discrepancy and to constrain the experimental cross sections for these reactions; this work would be beneficial to the nuclear data community.

CONCLUSION AND OUTLOOK

Our hypothesis for how ^{135}Xe could be purified from the irradiated solid XeF_2 hinges on the passive evolution of gaseous xenon from aqueous solution. The overall radiochemical transition from ^{136}Xe to ^{135}I is shown in Figure 11. As the ^{135}I is likely stable as a salt in aqueous solution, the remaining xenon can be removed at this point by sparging the aqueous solution with an inert gas, such as nitrogen. The remaining aqueous ^{135}I will decay into ^{135}Xe with a half-life of 6.6 h and then can be removed by sparging the solution with gaseous nitrogen. Xenon's boiling point is 165 K, compared with nitrogen's boiling point of 77.3 K; therefore, the evolved ^{135}Xe can be trapped using liquid nitrogen.

The proposed chemistry in Figure 11 allows ^{135}Xe to be selectively purified if radiopure $^{136}\text{XeF}_2$ is used because the unconverted xenon is removed after the addition of aqueous sodium hydroxide (NaOH) followed by sparging of the solution with nitrogen. The removal of evolved ^{135}Xe after a waiting period through cryotrapping leaves behind the ^{135}I as an aqueous salt. The purity of the milked ^{135}Xe is measured using HPGe γ -spectroscopy, demonstrating the effectiveness of this approach for large-scale ^{135}Xe production. An example of the HPGe γ counting setup is shown in Figure 12.

These methods could be applied to a more refined production process using a custom-built and engineered apparatus. The techniques involved are simple and rely on separation of undesired xenon isotopes by removing them before the majority of the ^{135}I decay. If inert conditions are maintained through the use of a nitrogen atmosphere, using liquid nitrogen to cryotrap the

radioactive xenon product gas is a reliable approach to separating ^{135}Xe from the mixture without risking chemical release as a result of system overpressure.

Using XeF_2 as a substrate for radiochemical production of ^{135}Xe is a viable strategy to generate calibration samples for the comprehensive Nuclear Test Ban Treaty's atmospheric xenon detectors. Not only are production yields sufficient, but the

ability to chemically separate the produced ^{135}I allows for isolation of radiopure ^{135}Xe and removes the presence of problematic xenon isotopes. Cryo-condensation of these undesirable xenon isotopes allows for their safe handling and recycling, as well as bottling of radiopure ^{135}Xe for future sample preparation.

Future directions to refine this approach would involve designing a ^{135}Xe separation apparatus and using radiopure $^{136}\text{XeF}_2$. An apparatus for ^{135}Xe evolution and separation would require the use of an inert atmospheric environment, as previously stated, so the ability to load the irradiated XeF_2 material and purge the system with gaseous nitrogen is required, followed by the ability to add aqueous sodium hydroxide solution to the XeF_2 and sparge the resulting solution without opening the system to the atmosphere. Ideally, the evolved Xe that contains undesired ^{136}Xe from the sample would be cryotrapped and recycled into the synthesis of $^{136}\text{XeF}_2$. The apparatus should allow for an additional or replacement cryo-trap vessel so that pure ^{136}Xe can be collected after the ^{135}I decay process without opening the system to the atmosphere.



Figure 12. An example of the HPGe γ counting setup. The HPGe, shown on the right side of the image, is housed in lead bricks.

Radiopure $^{136}\text{XeF}_2$ can be synthesized through exposing UV light to a mixture of radiopure gaseous ^{136}Xe , available from chemical vendors in high purity, and fluorine gas, which is also commercially available. Although gaseous fluorine is highly corrosive and toxic, other researchers have described the synthesis of XeF_2 in a controlled laboratory setting.⁴ APL researchers could reproduce these settings in their laboratory or contract chemical manufacturers to do so (though the latter option would be more expensive).

We were able to demonstrate a novel production pathway for the synthesis of radiopure ^{135}Xe through three innovations: the milking of ^{135}Xe via the $^{136}\text{Xe}(\gamma, p)^{135}\text{I}$ reaction (where a XeF_2 target was bombarded with bremsstrahlung radiation generated by the 25-MV linear accelerator), the use of a solid XeF_2 target instead of a liquid solution (which increases the density of Xe in the target), and the chemical extraction of ^{135}I from the irradiated XeF_2 target. If implemented, our production pathway for radiopure ^{135}Xe could produce sufficient radioxenon to supply calibration material to the entirety of the worldwide network of detectors that passively sample radioxenon from the atmosphere.

REFERENCES

- ¹P. R. J. Saey, M. Bean, A. Becker, J. Coyne, R. d'Amours, et al., "A long distance measurement of radioxenon in Yellowknife, Canada, in late October 2006," *Geophys. Res. Lett.*, vol. 34, no. 20, art. L20802, 2007, <https://doi.org/10.1029/2007GL030611>.
- ²R. L. Garwin and F. N. von Hippel, "A technical analysis: Deconstructing North Korea's October 9 nuclear test," *Arms Control Today*, vol. 36, no. 9, pp. 14–16, Nov. 2006, <https://www.armscontrol.org/act/2007-03/features/technical-analysis-deconstructing-north-korea-s-october-9-nuclear-test>.
- ³J. J. Horkley, J. L. Brookhart, E. S. Cardenas, K. P. Carney, C. Hines, T. P. Houghton, T. A. Robinson, and M. G. Watrous, "Production of xenon-135 from isotopically enriched xenon-134 and xenon-136 targets," *J. Radioanal. Nucl. Chem.*, vol. 331, pp. 5447–5452, 2022, <https://doi.org/10.1007/s10967-022-08537-1>.
- ⁴M. Tramšek and B. Zemva, "Synthesis, properties and chemistry of xenon(II) fluoride," *Acta Chim. Slov.*, vol. 53, no. 21, pp. 105–116, 2006, <https://doi.org/10.1002/chin.200721209>.
- ⁵A. Šmalc, K. Lutar, and S. A. Kinkead, "Xenon difluoride (modification)," in *Inorganic Syntheses*, vol. 29, R. N. Grimes, Ed., New York: Wiley, 1992, pp. 1–4, <https://doi.org/10.1002/9780470132609.ch1>.
- ⁶E. H. Appelman, "Reaction of xenon difluoride with water and with xenon trioxide," *Inorg. Chem.*, vol. 6, no. 7, pp. 1305–1310, 1967, <https://doi.org/10.1021/ic50053a009>.
- ⁷C. A. Ramsden, "Xenon difluoride in the organic laboratory: A tale of substrates, solvents and vessels," *ARKIVOC*, vol. 2014, no. 1, pp. 109–126, 2014, <https://doi.org/10.3998/ark.5550190.p008.436>.
- ⁸G. Glish and R. Vachet, "The basics of mass spectrometry in the twenty-first century," *Nat. Rev. Drug Discov.*, vol. 2, pp. 140–150, 2003, <https://doi.org/10.1038/nrd1011>.
- ⁹D. R. MacKenzie and R. H. Wiswall Jr., "Compound formation by γ -irradiation of xenon-fluorine mixtures," *Inorg. Chem.*, vol. 2, no. 5, p. 1064, 1963, <https://doi.org/10.1021/ic50009a044>.
- ¹⁰M. E. Rising, J. C. Armstrong, S. R. Bolding, F. B. Brown, J. S. Bull, et al., "MCNP® code version 6.3.0 release notes," Los Alamos Nat. Lab. Tech. Rep. LA-UR-22-33103, Rev. 1, Jan. 2023.
- ¹¹J. E. Turner, *Atoms, Radiation, and Radiation Protection*. Wiley-VCH, Germany, 2007.
- ¹²G. F. Knoll, *Radiation Detection and Measurement*. 4th Ed. Wiley, 2010.
- ¹³Y. S. Popov, L. V. Zakharova, and G. A. Timofeev, "Half-lives of $^{131-135}\text{I}$ nuclides," *Radiochemistry*, vol. 43, pp. 5–7, 2001, <https://doi.org/10.1023/A:1012805618385>.
- ¹⁴F. Brown and L. Yaffe, "The independent yield of Xe^{135} produced in the fission of natural uranium by pile neutrons," *Can. J. Chem.*, vol. 31, pp. 242–249, 1953, <https://doi.org/10.1139/v53-035>.
- ¹⁵B. Singh, A. A. Rodionov, and Y. L. Khazov, "Nuclear data sheets for $A = 135$," *Nucl. Data Sheets*, vol. 109, no. 3, pp. 517–698, 2008, <https://doi.org/10.1016/j.nds.2008.02.001>.



Evan P. Lloyd, Asymmetric Operations Sector, Johns Hopkins University Applied Physics Laboratory, Laurel, MD

Evan P. Lloyd is an organic chemist in APL's Asymmetric Operations Sector. He has a BS in chemistry from Carnegie Mellon University and an MS and a PhD in chemistry from Johns Hopkins University.

He has experience in antibiotic drug development, medicinal chemistry, total synthesis, and enzymology. At APL, he has worked in the chemical and biological warfare agent defeat community, specializing in applied synthetic chemistry and testing. His email address is evan.lloyd@jhuapl.edu.



Ciara B. Sivels, Air and Missile Defense Sector, Johns Hopkins University Applied Physics Laboratory, Laurel, MD

Ciara B. Sivels is a nuclear engineer in APL's Air and Missile Defense Sector. She has a BS in nuclear engineering from the Massachusetts Institute of Technology (MIT) and an MS and a PhD in nuclear engineering from the University of Michigan. She

has experience in radiation detection and simulation, nuclear explosion monitoring for treaty verification using scintillation detectors, Monte Carlo radiation transport simulations, and high-resolution low-background measurements using semiconductor detectors. Her email address is ciara.sivels@jhuapl.edu.



Alan W. Hunt, Asymmetric Operations Sector, Johns Hopkins University Applied Physics Laboratory, Laurel, MD

Alan W. Hunt supervises the Radiation Systems Technologies Section within APL's Asymmetric Operations Sector. He has a BS in physics from the University of Michigan and a PhD in physics from Harvard University.

He led the effort to establish APL's linear accelerator and high-radiation facility. His research projects have spanned liquid semiconductors for novel power generation applications to electron/ion-induced spaceship charging. His most prolific research area has been investigating and developing nuclear techniques for security, nonproliferation, and nuclear forensics applications. The common theme in all his research endeavors is the interaction of ionizing radiation with matter and how to exploit the associated phenomenon for applications. His email address is alan.hunt@jhuapl.edu.



Yenuel S. Jones-Alberty, Asymmetric Operations Sector, Johns Hopkins University Applied Physics Laboratory, Laurel, MD

Yenuel S. Jones-Alberty is a post-doctoral fellow in APL's Asymmetric Operations Sector. He has a BS in physics from the University of Puerto Rico and an MS and a PhD in physics from Ohio University. He has worked on various projects in APL's linear accelerator facility, ranging from specific applications to basic science, and has operated the linear accelerator. His graduate research focused on studying nuclear reactions of astrophysical significance using neutron detection techniques. He operated a 4.50-MV tandem Pelletron accelerator when performing these experiments. His email address is yenuel.jones-alberty@jhuapl.edu.



APL's Contributions to the Odor Detection Canine Community

Shirley M. Klimkiewicz and David M. Deglau

ABSTRACT

Odor detection canines play a key role in ensuring our nation's security. For more than 15 years, the Johns Hopkins University Applied Physics Laboratory (APL) has supported research on and advancement of the community's efficacy and capabilities through the application of interdisciplinary solutions spanning chemistry, biology, data analytics, and engineering. Not only have APL's contributions resulted in strong collaborations across the research space, but they have also directly informed and impacted strategies and capabilities for operational deployments of odor detection canines.

INTRODUCTION

Odor detection canines (ODCs) are utilized as sensors in a variety of fields, from medical to military and defense to disaster relief, among others. Many people may have encountered ODCs at the airport, where the Transportation Security Administration (TSA) leverages them to scan luggage and passengers for explosive materials.¹ Similar to how TSA uses ODCs to scan luggage, other organizations, such as Customs and Border Protection, employ these canines to identify contraband and illicit substances at ports of entry.² The Federal Emergency Management Agency (FEMA) uses ODCs to locate survivors and human remains after a disaster.³ Researchers have explored the use of ODCs to detect specific biological conditions, including but not limited to diabetes, seizures, and various types of cancer.⁴ These select examples demonstrate the importance of ODCs in national security and infrastructure in the United States.

Building on natural biological characteristics and physiology, ODCs are trained from a young age to use

olfaction to detect a specific compound or class of compounds in a variety of environments and scenarios. Canines are the ideal candidate for detection applications, given their incredible olfactory abilities. They are able to detect substances at concentrations as low as one part per trillion, which is more sensitive than most analytical instruments.⁵ Additionally, canines have the dynamic capability of providing detection in different odor disciplines (e.g., narcotics, explosives, arson, human remains) based on which “library” of compounds is introduced via training. Utilization within an odor discipline requires a specialized training protocol to enable the canine to detect specific compounds related to the intended odor discipline without alerting to unrelated odors. In addition to their dynamic capabilities within odor disciplines, canines have a strong learning ability that enables their use in a variety of scenarios. Their initial training focuses on scanning static environments and stationary objects, such as stadium seats, luggage and packages, and vehicles. Some ODCs, such

as those the TSA uses at airport checkpoints, undergo additional training to scan people standing in queues or walking. ODCs' dynamic working ability also extends to the environment, as they can be deployed indoors and outdoors under a variety of weather conditions.

Like all analytical instrumentation, however, ODCs have limitations. One challenge of using biological detectors is establishing efficient, reliable communication between the ODC and the handler. Although canines within an odor discipline are generally trained to display a uniform response when alerting to a an odor they are trained to detect, each canine will likely exhibit different behavior leading up to the final trained response. Additionally, canines may display unique behaviors associated with a false alarm. Effective use of ODCs relies on experienced and attentive handlers to guide the canines and interpret their behavior, which is generally more difficult than interpreting results from nonbiological detectors. In preparation for working with an ODC, handlers undergo specialized training depending on the intended odor discipline. Typically, the final portion of this training involves pairing the handler and canine, which may require several attempts until an effective team is formed.

Another limitation, also related to communication, is that it can be difficult or even unfeasible for multiple handlers to pair with the same canine. During training, an ODC primarily works with trainers and its assigned handler, because it is important to form specific canine–handler pairs for efficient detection. Canine or handler reassignment typically requires additional training so that the handler can become familiar with the canine's behaviors and recognize patterns, making reassignment onerous. Whereas any operator with the appropriate skill set can use other analytical instruments, ODCs are typically most effective when paired with one handler.

Because of these complexities, ODCs are considered a qualitative sensor system, and thus, they are often used and relied on as a high-throughput but initial layer of screening. They are most effective when integrated into multiple layers of detection. For example, ODCs deployed at airports are layered with x-ray-based technologies to provide several layers of security. While canine detections are consistently used in security and medical applications, additional quantitative detections are still considered valuable as supportive or final determinations.

APL'S CONTRIBUTIONS TO CANINE DETECTION ADVANCEMENT AND ENGINEERING

APL's efforts within the ODC community have been as diverse as the range of staff members at APL itself. Over the course of more than 15 years, APL has established and grown a foundational approach to canine research and advancement through the efforts of an experienced and innovative interdisciplinary team bringing together:

- traditional disciplines (chemistry and biology);
- end users or operational teams and components; and
- nontraditional disciplines (engineering, computer science, and data analytics).

APL has performed, and continues to perform, research on every aspect of the canine's life, from informing the selection of matings to enhancing breeding outcomes to optimizing deployment. This breadth of scope is demonstrated across APL's various efforts, stemming from long-term relationships with sponsors driven by its Homeland Chemical, Biological, Radiological, Nuclear, and Explosives Defense portfolio, and is captured in Figure 1 and detailed below.



Figure 1. APL's ODC areas of effort.



Figure 2. APL staff members, University of Maryland Police Department officers, and Domestic Breeding Consortium (DBC) canines.

Domestic Breeding Consortium

As a key component of security measures in ports, airports, stadiums, and other public spaces, ODCs are critical to national security, public safety, and infrastructure in the United States. Explosives detection canines (EDCs) especially play a significant role in ensuring public safety and protection from explosive materials. Currently, most EDCs are sourced outside of the continental United States, a fact that Congress recognized as a potential threat to national security. In light of this, the House of Representatives passed the Domestic Explosives Detection Canine Capacity Building Act of 2017 directing the creation of a domestic breeding network to provide high-quality, effective EDCs.⁶ In 2019, APL started the Domestic Breeding Consortium (DBC) with the objective of meeting this congressional call. The DBC is a collaborative project focusing on developing evidence-based breeding and selection practices to strengthen and expand the domestic supply of ODCs, particularly EDCs.

The DBC has developed and deployed quantitative evaluations to monitor and support early and operational development as well as to create a more informed procurement structure. Additionally, APL has aggregated and documented a community best practices framework that both the private and public sectors can use to increase

the knowledge and capabilities of organizations raising ODCs. Over its 3 years of existence, through the collaborative efforts of five partner organizations across the private and academic sectors, the DBC has produced 125 canines and successfully developed and placed 60 into primary, 12 into secondary, and 19 into tertiary positions (as EDCs, operational ODCs, and research ODCs, respectively). Two graduates from the DBC, pictured in Figure 2, were placed with the University of Maryland Police Department.

The team plans to integrate all aforementioned knowledge, practices, and analytical developments into a common platform to be distributed and used by the develop-

ment, training, and deployment organizations. To fully understand the impact of applying scientific principles to breeding and developing ODCs, APL has created genetic references and is actively generating models to support the optimization of ODC discipline determination through not only development but also genetic optimization.⁷

Training Guideline

Another critical application of ODCs is person-borne explosives detection (PBED), which specifically involves the detection of explosive material carried by people,

Content:

- Introduction ▾
- Preparatory Training ▾
- Development Training ▾
- Maintenance Training ▾
- Remedial Training ▾
- Appendices ▾
- About the DHS S&T Detection Canine Program >

Dissemination of this training guideline outside of the law enforcement canine community, use or disclosure, in whole or in part, for any purpose, must have the written permission of the Department of Homeland Security, Science and Technology Directorate, Detection Canine Program.

Figure 3. APL-developed training guideline home page.

whether stationary or moving. Over the last decade, the Department of Homeland Security Science and Technology Directorate (DHS S&T) has prioritized research on the strengths and weaknesses of PBED canines, including factors that may impact their performance.⁸ In response to this call, APL developed a training guideline for uptraining traditional ODCs on expanded person-borne detection capabilities. The guideline, disseminated by DHS S&T,⁹ was developed based on input from ODC subject-matter experts and partner law enforcement agencies that deploy ODCs. Before this guideline was disseminated, many agencies relied on commercial sources for PBED training, and the training quality varied. The training guideline (Figure 3) provides detailed instructions as well as supplemental figures and videos, enabling agencies to conduct training in-house and ultimately giving more agencies the opportunity to deploy PBED canines.

Training Aid Development

The ODC training process requires the use of specialized training aids (TAs) for each odor discipline. The TAs contain the odor the canines are being trained to detect. In the case of EDCs, the conventional TAs are generally small amounts of neat (i.e., in the form that would be used operationally) explosive material. Although the amounts used vary according to explosive type and individual agency preference, the use of neat explosive material introduces considerable safety and logistical limitations across all agencies employing EDCs. While most agencies maintain a TA supply for ongoing maintenance training, the limited stability of certain explosive materials prevents agencies from keeping even small amounts in-house. In these cases, EDC training with the explosive material may be limited because it requires an agency to have the appropriate qualifications to handle and transport the material.

These limitations led to the development of alternative TAs that reproduce or mimic the neat material's odor profile but eliminate its safety hazards. These TAs can generally be categorized as dilution or derivative TAs. Dilution TAs contain the neat material, but it is rendered nonhazardous through means of altered concentration, mixture, or geometry. Derivative TAs do not contain the neat material, but rather a chemical derivative or product that is meant to be chemically or structurally analogous to the raw trained material.¹⁰ In contrast, TAs known as pseudo-TAs are the most common form of commercially available derivative TAs. They are primarily designed to reproduce the headspace generated by the neat material, as determined by gas chromatography–mass spectrometry (GC/MS).¹¹ This approach has several limitations, the most significant of which is the assumption that the compounds identified by headspace analysis are the same as those the canine identifies to make a positive detection. Given that

canines' detection ability is known to be more sensitive than that of analytical instrumentation, it is not unreasonable to presume that canine detection of the trained odor may rely on compounds that are not detected by gas chromatography–mass spectrometry or similar approaches, which may include but are not limited to binders, solvents, or tagents.⁵ For this reason, dilution TAs are generally preferred as alternative TAs, particularly for explosive detection. Dilution TAs often take on the format of a mixture of neat material in an inert matrix, such as diatomaceous earth or silica gel. Because the neat material is sufficiently dispersed in the inert matrix, the dilution TA does not pose the hazards the neat TA does. Furthermore, low-volatility inert matrices make minimum contributions to the headspace of the material. Therefore, usually the dilution TAs' headspace closely mimics the headspace of neat TAs and represents the entire odor profile rather than the profile of select compounds, as is generally the case with pseudo-TAs.

Because APL has experience in developing¹² and evaluating TAs using both traditional analytical and canine methods, it is often called on to review the state of the science as well as commercially available products. Findings are documented in market survey reports, the most recent of which was published for the ODC community and general public through a collaboration with the National Urban Security Technology Laboratory (NUSTL) System Assessment and Validation for Emergency Responders (SAVER)¹³ and paired with an additional succinct TechNote summary.¹⁴

Independent Operational Assessment

Regardless of odor discipline, ODCs are deployed in an operational environment after extensive training. Because deployment can introduce variables that may have been absent or controlled during training, the transition from training to an operational space can affect ODC performance. To solve this issue, APL has partnered with several local agencies deploying EDCs, such as the University of Maryland Police Department and the Pentagon Force Protection Agency, to optimize the operational assessment process and provide expert recommendations for optimizing team performance. With these local partners, APL has conducted small-scale pilots to test assessment methodologies and deployment optimization techniques before performing them in collaboration with national organizations such as TSA.

Operational assessments of ODCs can reveal the influence of any number of variables on performance and likelihood of success. The assessments are designed by APL and reviewed by external subject-matter experts to ensure that the complexity of assessing a biological detector is reflected in the experimental plan. As a trusted independent evaluator, APL is well positioned, given its partnerships with the end-user community, to conduct these assessments, interpret the results, and



Figure 4. Fogger kit. Left, fogger kit components; right, the kit deployed in a rolling suitcase.

provide tailored recommendations for potential improvements to canine training and deployment practices. This development cycle ensures that ODCs are trained and deployed through scientifically verifiable progressions.

Deployment Optimization

Many environmental factors are known or suspected to influence ODC performance in operational environments. One major factor of specific interest in the community is airflow. In light of this interest, APL undertook a substantial effort to develop airflow visualization and detection techniques to help handlers and trainers understand the potential impact of air movement in the dynamic operational environment. APL piloted the deployment of fieldable fogger kits (Figure 4) adapted from commercial off-the-shelf products.¹⁵ When using the fogger system during ODC training, handlers gained

a better awareness of typical air movement patterns or behaviors directly in the operational environment.

To further advance the capabilities and awareness of the ODC team, APL developed an advanced, fieldable sensor suite to give deployed teams and their agencies useful analytical knowledge of their operational environment. This knowledge is provided by a suite of self-contained anemometer-based units. These integrated units provide real-time situational awareness of their deployment environment through a graphical user interface. Handlers, trainers, and supervisors can then determine optimal deployment conditions with a more complete awareness of the environment and, when paired with knowledge ascertained through operational assessments, deploy with analytically informed and scientifically optimized efficacy. The anemometer array is shown in Figure 5 (green tripod structures) within the



Figure 5. APL's anemometer array concept.

deployed advance queue configuration developed in collaboration with and fielded by TSA.

CONCLUSIONS

While inherently it may seem that canine-based detection is more limited than continually advancing state-of-the-art equipment and sensors, ODCs have proven to be an effective, sensitive, and dynamically fieldable solution for the nation's defense against a wide range of threats. APL has contributed to the deployment, technologies, and information at all phases of the canine's life and deployment in order to ensure advancement in the state of the science and capabilities of an invaluable fielded sensor platform that is integral to the safety and security of our nation.

ACKNOWLEDGMENTS: The authors acknowledge the DHS S&T Detection Canine Program for its long-standing support. Key to the efforts described in this article are the invaluable partnerships with the University of Maryland Police Department, Pentagon Force Protection Agency, Fort Lauderdale Police Department, Maryland State Police, and the TSA. Additionally, the authors greatly appreciate collaborations with Aspen Creek Kennels, Auburn University, Katalyst Kennels, Project One Retrievers, Kreator LLC, and especially Person-Borne Detection K9. Key APL staff members who contributed to the work discussed in this article include Neal Baker, Jordan Johnson, Ashley Kilhefner, Karen Meidenbauer, Kathy Santos, and Megan Toms, with foundational work done by Mike House and Trang Vu.

REFERENCES

- ¹"TSA Canine Training Center." Transportation Security Administration. <https://www.tsa.gov/news/press/factsheets/tsa-canine-training-center> (last updated May 19, 2021).
- ²"Canine Program." US Customs and Border Protection. <https://www.cbp.gov/border-security/canine-program> (last modified Dec. 21, 2023).
- ³"National US&R Response System." FEMA Canine. <https://fema.canine.org> (accessed Jul. 5, 2024).

- ⁴P. Jendry, F. Twele, S. Meller, A. D. M. E. Osterhaus, E. Schalke, and H. A. Volk, "Canine olfactory detection and its relevance to medical detection," *BMC Infect. Dis.*, vol. 21, art. 838, 2021, <https://doi.org/10.1186/s12879-021-06523-8>.
- ⁵A. Kokocińska-Kusiak, M. Woszczyło, M. Zybala, J. Maciocha, K. Barłowska, and M. Dzieciol, "Canine olfaction: Physiology, behavior, and possibilities for practical applications," *Animals*, vol. 11, no. 8, art. 2463, 2021, <https://doi.org/10.3390/ani11082463>.
- ⁶US House, 115th Cong. (2017-2018), H.R.4577, *Domestic Explosives Detection Canine Capacity Building Act of 2017*. <https://www.congress.gov/bill/115th-congress/house-bill/4577>.
- ⁷R. A. Player, E. R. Forsyth, K. J. Verratti, D. W. Mohr, A. F. Scott, and C. E. Bradburne, "A phased *Canis lupus familiaris* Labrador retriever reference genome utilizing high molecular weight DNA extraction methods and high resolution sequencing technologies" (preprint), *bioRxiv*, 2020, <https://doi.org/10.1101/2020.08.26.269076>.
- ⁸"Detection canine." US Department of Homeland Security Science and Technology Directorate. <https://www.dhs.gov/science-and-technology/detection-canine> (last updated Jun. 14, 2024).
- ⁹"Canine person-borne explosive detection training guideline." US Department of Homeland Security Science and Technology Directorate. <https://www.dhs.gov/science-and-technology/publication/canine-person-borne-explosive-detection-training-guideline> (last updated Aug. 16, 2022).
- ¹⁰M. Cerreta, "The creation and evaluation of novel canine training aids for cocaine using molecularly encapsulated sol-gel polymers and an investigation of canine field accuracy," PhD dissertation, Florida International University, Miami, FL, 2015, <https://doi.org/10.2514/etd.FI15032132>.
- ¹¹A. Simon, L. Lazarowski, M. Singletary, J. Barrow, K. Van Arsdale, T. Angle, P. Waggoner, and K. Giles, "A review of the types of training aids used for canine detection training," *Front. Vet. Sci.*, vol. 7, art. 313, 2020, <https://doi.org/10.3389/fvets.2020.00313>.
- ¹²D.-T. T. Vu, Process for producing non-detonable training aid materials for detecting explosives, US Patent US20140097551A1, filed Feb. 25, 2013, and issued Aug. 18, 2015. <https://patents.google.com/patent/US20140097551A1/en>.
- ¹³National Urban Security Technology Laboratory and Johns Hopkins University Applied Physics Laboratory, "Non-detonable training aids for explosives detection canines: Market Survey Report," Washington, DC: US Department of Homeland Security Science and Technology Directorate, Feb. 2024. https://www.dhs.gov/sites/default/files/2024-03/24_03_12_st_caninetraingaid_msr.pdf.
- ¹⁴National Urban Security Technology Laboratory, "Non-detonable training aids for explosives detection canines," SAVER TechNote, Feb. 2024. https://www.dhs.gov/sites/default/files/2024-02/24_02_14_st_caninetraingaid.pdf.
- ¹⁵D. Deglau and S. Klimkiewicz, "Airflow visualization tools for optimized search patterns in person-borne scenarios (A)," in *Proc. Canine Olfaction and Detection Sci. Conf.*, May 25, 2023, <https://eventsignup.fiu.edu/event/abstractdetails/991>.



Shirley M. Klimkiewicz, Asymmetric Operations Sector, Johns Hopkins University Applied Physics Laboratory, Laurel, MD

Shirley M. Klimkiewicz is an organic chemist in APL's Asymmetric Operations Sector. She has a BS in chemistry from Princeton University and is pursuing a master's in biotechnology, with a concentration in biodefense, at Johns Hopkins University. She has significant experience working with odor detection canines, specifically in designing and executing field assessments. She also has experience in biological assays, cell culture, and small-scale synthesis and analytical techniques, including nuclear magnetic resonance spectroscopy and gas chromatography-mass spectrometry. Her email address is shirley.klimkiewicz@jhuapl.edu.



David M. Deglau, Asymmetric Operations Sector, Johns Hopkins University Applied Physics Laboratory, Laurel, MD

David M. Deglau is a chemical engineer in APL's Asymmetric Operations Sector. He has a BS in biochemistry from Saint Vincent College and an MS in chemical and biomolecular engineering from Johns Hopkins University. His professional focus is testing, evaluating, and developing prototype chemical detection systems. He has a broad range of experience with odor detection canines, gas and liquid control systems, carbon nanotubes, nanopore, and nanowires. His email address is david.deglau@jhuapl.edu.

Using Knowledge Graphs to Counter Weapons of Mass Destruction

Ray H. Mariner, Timothy P. Lippa, Phillip T. Koshute, David W. Boyce,
Josef C. Behling, and Michael J. Peters

ABSTRACT

This article describes the development of a data-driven approach to map adversarial activity into machine-readable models. Specifically, this approach is grounded in well-structured knowledge graphs and uses a semantic representation of domain-specific pathways implementing formal ontology and Resource Description Framework (RDF) and Web Ontology Language (OWL). In addition, the article describes a web-based application through which a user can interact with the underlying knowledge graph. The application also allows for development of analytics that use these data to answer questions about adversarial activity.

INTRODUCTION

Many US government agencies and organizations are involved in countering weapons of mass destruction (CWMD). While overall goals and specific mission objectives vary, the US government typically requires access to experts on WMD production. When experts are not readily available, however, especially in operational settings, the government has typically supplemented expert knowledge with printed material, such as note cards or books. In a field environment, these printed materials can be cumbersome to carry and use effectively, especially for new operators. Additionally, materials are often severely outdated because adversaries have evolved their tactics, techniques, and procedures (TTPs).

Another factor complicating CWMD missions is the lack of a common vocabulary to describe adversary TTPs. This, coupled with the many disparate and stove-piped data systems, makes sharing information difficult. As a result, everything from retrieving information to developing advanced artificial intelligence and machine

learning algorithms is inefficient and costly. APL recognized the potential of semantic data models to enable a revolutionary shift in CWMD knowledge management and analysis.

Based on an Independent Research and Development experiment, APL researchers developed a semantic data model using domain-specific ontologies. Without ontologies, analysts typically rely on the natural language to describe the world, and natural language lacks the precision required for machine interpretation. The formal representation of knowledge through ontologies allows for greater clarity among both individuals and computer agents. For instance, consider the difficulty a system (or human) would face in understanding the intent of the word *tank* in the following example: “Tanks found at grid coordinates x,y, along with heavy-duty press and several kilograms of calcium chloride.” Because natural language is inherently overloaded, this one simple example quickly grows in confusion when attempting to

describe and model a domain of interest in any detail. To address the associated problems described above for supporting CWMD missions, APL developed several domain-specific ontologies to define and represent the relationships between entities within the field of WMD agent production.

Existing US Department of Defense and Intelligence Community systems provide information (e.g., observations of entities and events of interest). APL's semantic models allow us to organize and relate this information, and the organization and relationships then allow us to reliably interpret the information and build analytical tools.

In 2009, the US Defense Threat Reduction Agency (DTRA) funded the creation of a broader set of CWMD adversary models in pursuit of the following objectives:

- Characterize threats with meaningful definitions, health and safety information, and physical properties
- Identify and document adversary TTPs for WMD production, weaponization, and employment
- Provide a standard vocabulary for CWMD missions
- Provide analytical capabilities to aid analysts looking for WMD activity

APL, on behalf of DTRA, created these models and developed a comprehensive knowledge graph known as the Chemical, Biological, Radiological, Nuclear, Explosive Semantic Framework (CBRNE-SF). This graph contains the information related to processes (actions taken by an adversary) and observables (things needed and used by an adversary) to perform a specific action in pursuit of WMD. Pathways for more than 100 threat agents have been modeled, with more than 20,000 observables and more than 100,000 multilingual alternative labels and synonyms for the observables.

A simple example is presented in Figure 1. The activities are represented by rectangles, whereas observables are in blue type beneath each activity. If someone had made fresh orange juice, one could expect to observe oranges, a juicer, and a pitcher.

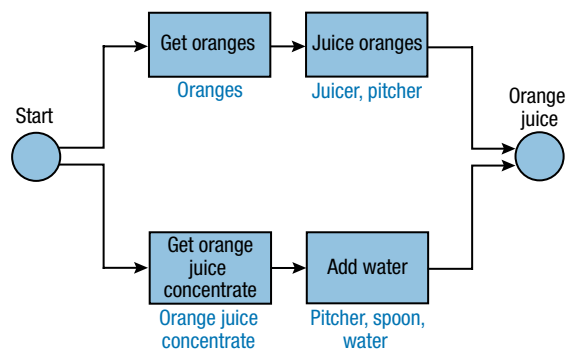


Figure 1. Example of the process of making fresh orange juice. Observables are listed below each boxed activity.

Powered by the CBRNE-SF, APL also created a user interface for DTRA, which is currently deployed in several environments across many federal agencies. The application allows the user, or even other systems, to access the CBRNE-SF to quickly complete the following tasks:

- Identify observables using a comprehensive list of synonyms and imagery for WMD agents, precursors, and equipment to help standardize the vocabulary used to describe WMD TTPs
- Understand how observables are associated with adversary activities related to WMD production, weaponization, and employment
- Understand health and hazard information on the effects of WMD agents and precursors, including chemical exposure, biological disease, and symptoms

CBRNE-SF CONSTRUCTION

The CBRNE-SF knowledge base contains the interconnected series of actions an adversary would likely take when producing, weaponizing, or employing a WMD. In many cases, there are several different synthetic approaches to produce a WMD, so the knowledge base must contain all possible approaches. The knowledge base is not meant to provide precise step-by-step instructions for producing, weaponizing, or employing a WMD; instead, it provides a road map to the most essential actions that present opportunities for discovery. Additionally, it leverages a diverse range of authoritative sources. Subject-matter experts (SMEs) consulted online databases, specialized dictionaries, reference texts, peer-reviewed journals, and other trusted resources to develop each process. Whenever possible, our workflows are grounded in, and enriched by, peer-reviewed literature.

To codify the steps an adversary would use to carry out some activity or set of activities, we developed the following lexical constructs: pathways, processes, activities, observables, and signatures.

A pathway is the interconnected series of actions that are performed and lead to some intended outcome. In CBRNE-SF, this takes the form of a unidirectional flowchart comprising processes and activities.

A process allows for collecting related activities used to get to a specific end state. These processes can be nested as subprocesses in a bigger overall process.

An activity defines the lowest level of discrete action modeled in the pathway. Activities contain all the relevant information required for that activity to be completed successfully and, subsequently, all the information that would allow the activity's discovery. These activities are assembled in processes that themselves can

be nested in higher-level processes. Similar to Unified Modeling Language (UML),¹ we provide constructs in the data model that allow for decisions to be made when multiple choices are available in carrying out a set of activities and also allow capture of activities that can be performed asynchronously. Supplemental information, such as activity descriptions, references, drawings, and illustrations, is also captured and associated as appropriate. Within the CBRNE-SF, processes and activities can be reused to gain efficiency in modeling new threats. A SME can leverage these previously modeled items containing hundreds or thousands of nodes simply by copying them. This saves considerable time and standardizes the processes for commonly used precursors, as well as allows for quick updates to the models as the threat landscape changes.

A key innovation for the construction of the data model is the idea that the pathways themselves should be instantiations of ontological classes. This led to the development of a pathway modeling ontology, with the resulting behavior that, as the pathways are constructed, the processes, activities, decisions, etc., end up as connected nodes in the knowledge graph. This allows for a fully interconnected graph that can be easily traversed in a query. This enables the kinds of analysis described later in this article.

A pathway allows for activities to be associated with the set of items, or observables, required to carry out the activity successfully, and each of these observables in turn can be associated with many signatures (e.g. spectral). These signatures are data representations of how the observable “appear” when analyzed by a specific sensor.

Here, similar to the construction of the pathways, each association of an observable to an activity or signature to observable, expands the knowledge graph by creating additional nodes and edges in the data model.

Observables can most simply be thought of as anything that can be sensed (e.g., smelled, tasted, seen, heard, touched). Observables are divided into three distinct groups:

1. **Preconditions:** Observables that must be present for the activity to succeed
2. **Effects:** Observables produced as a result of performing the activity, regardless of whether they are detected (Example: A reaction produces chlorine, but a mechanism is used to remove the chlorine from the waste stream. Chlorine is still called out as an effect.)
3. **Incidentals:** Observables that are not absolutely required for an activity but are likely to be present given what is typically used to conduct the activity (Example: In the chemistry domain, many reactions are carried out in a fume hood. The fume hood, while

ideal for safety reasons, is not absolutely required and is therefore called out as incidental because it may or may not be present. If present, it does provide significant clues to the type of activities being conducted.)

Each observable contains the following information if available from a vetted source:

- Definition/description
- Nefarious and legitimate manufacturing uses
- English, foreign-language, and language-independent alternative labels, synonyms, and colloquialisms
- Description of entity relationships (e.g., potential uses)
- Classification
- Source information (e.g., bibliographic citations)
- Pictures/illustrations

For biological and chemical entities, the following information is also included:

- Health and hazard statements, where appropriate
- Physical properties, where appropriate
- Industrial uses
- Cross-references to chemical and biological datasets
- Machine-readable identifiers (e.g., Chemical Abstract Service registry numbers)

Observables, like processes and activities, are modeled as instances of classes defined within ontologies tailored to specific CBRNE-SF domains. These ontologies are built using the Resource Description Framework (RDF) and the Web Ontology Language (OWL), standards endorsed by the World Wide Web Consortium (W3C).^{2,3} RDF structures data as a graph composed of subject–predicate–object triples, each expressing a simple fact (e.g., Bill isFatherOf Steve). These statements are linked to form dynamically growing graphs, enabling rich semantic modeling, inference, and graph analytics, capabilities particularly well-suited for representing adversarial activity.

To enhance semantic precision and structure, RDF is extended through RDF Schema (RDFS) and OWL, which introduce class- and property-based constructs for building ontologies. In this framework, classes define conceptual entities, and properties express the relationships among them, together forming a flexible, machine-readable vocabulary for each domain of interest.

The CBRNE-SF knowledge base is fundamentally a composition of such ontologies. These are not limited to

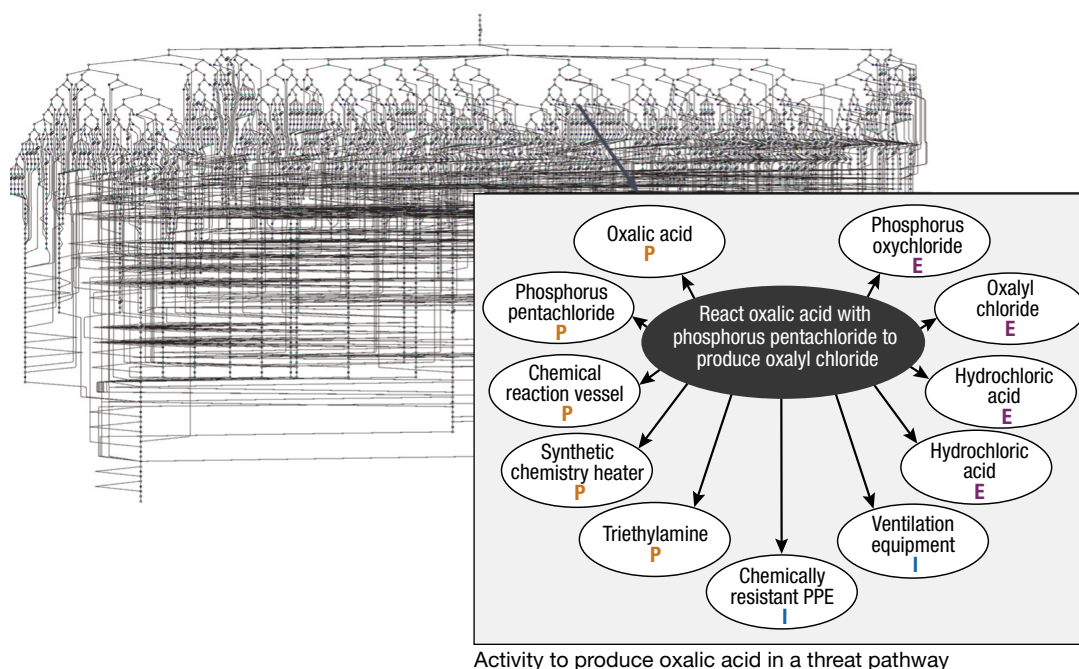


Figure 2. Example of a threat pathway within the broader knowledge graph and details of a specific activity.

taxonomic hierarchies; rather, concepts can assert facts about other concepts, creating a richly interconnected semantic model. To ensure consistency and expressiveness across domains, the domain-specific ontologies are aligned under foundational upper ontologies. These upper ontologies provide additional structure and rigor to the knowledge representation, though their detailed description lies beyond the scope of this overview.

Combining processes, activities, observables and signatures for a single threat agent creates a complex data model that a human would have difficulty understanding as a whole. However, given the structure of the CBRNE-SF, the application interface allows a user to easily query the graph in real time to explore complex relationships among observables, activities, and processes for WMD production, weaponization, and employment. This interface provides deeper insights and more comprehensive answers to complex mission-critical questions. Figure 2 shows an example of a single threat pathway as an illustration of the scale and complexity of more than one hundred of these pathways modeled in the overall graph.

ANALYTICS ENABLED BY CBRNE-SF

A web application was developed to provide analysts with an interface to quickly retrieve, explore, and query the complex data enabling them to answer the most mission-relevant questions with ease. Several analytical workflows assist system users as they

answer mission-critical questions about observables. For example:

1. What is it?
 - Basic definition
 - Uses and regulations
 - Exposure information
 - Physical characteristics
 - Alternative identification
2. What can it be used for?
 - Possible nefarious WMD production routes
 - Possible non-nefarious industrial/commercial uses
3. What else should I look for?
 - A prioritized list of unique observables to guide further search activities

Given the machine-readable knowledge graph, queries are returned in real time and dynamically rendered on a web page. A user's primary workflow involves searching for an observable and scrolling through the Details page. In another workflow, the user enters observables into the Evidence Bag and scrolls through the returned output. To give some insight to the information returned to an analyst, a few examples are provided below.

Observable Detail Page Workflow

The observables Details page varies slightly by the WMD threat type, but, in general, all Details pages contain similar information pulled dynamically from

(U) A molecular entity that appears as a greenish-yellow gas at room temperature and as a clear amber-colored liquid in condensed conditions. Chlorine gas is recognized by a pungent, irritating odor (cf. chloramine) like that of "bleach". It occurs widely as chloride compounds in salts dissolved in seawater. Elemental chlorine, however, exists as a diatomic molecule which occurs very rarely in nature. Industrial quantities of chlorine are produced mainly via the electrolysis of brine, a process for making sodium metal. It is normally stored as condensed liquefied gas in steel tanks/cylinders. It can also be generated in small scale by acidification of widely available hypochlorite salts. Chlorine is used in manufacturing, as a reagent in synthetic chemistry, for water purification, and in the production of chlorinated lime, which is used in fabric bleaching. It is a strong oxidant and a powerful irritant that can cause fatal pulmonary edema. Its main route of entry is inhalation.

Figure 3. Excerpt from the Details page for the chlorine gas observable.

CBRNE-SF through queries that traverse the knowledge graph to retrieve the requested information. When accessing the Details page for a toxic industrial chemical (e.g., chlorine gas), the user will see a definition of the chemical, as shown in Figure 3. Definitions, typically written by a SME, provide basic information in an easy-to-understand paragraph. They are designed to be helpful to nonexperts and provide context for why the observable is part of a CWMD knowledge graph.

In the view shown in Figure 4, the user is presented with the activities associated with chlorine. These activities are separated by the function that chlorine plays in the activity (e.g., "Activity as precondition"). Chlorine is used in 28 activities as a precondition, indicating that while chlorine itself is toxic, it is also used as a precursor. Chlorine functions as an effect in 21 activities, indicating that there are 21 general ways to generate chlorine either as the intended product or as an incidental by-product. Chlorine functions in one activity as an incidental, indicating that it may or may not be present. While not shown in the figure, a user can expand each section to access a collapsible list of specific activities. The user can further click a link to a particular activity to see all of the content, such as activity definitions, images, durations, reference material, and bibliographic citations.

The CBRNE-SF also contains information on manufacturing uses, and similarly, if the observable is on any control lists, the lists will be provided in a dedicated section. If the user needs more information on other observables within a manufacturing industry or on a list, they simply need to click the linked text in the relevant section to view all of the observables in the CBRNE-SF with that industrial use or on that control list.

Information on uses and regulations allows the user to understand whether there are dual uses for the observable and whether there any restrictions on its use. This information provides critical context and situational awareness for the user.

Exposure information

The application also dynamically displays exposure information in two sections of the Details page. The first section lists information extracted from safety data sheets, which are globally standardized documents detailing the harmful effects of chemical exposures. For all chemical threats and precursors included in the CBRNE-SF, such as chlorine, a safety data sheet was obtained and the information extracted. Figure 5 shows an example of the type of extracted information that is

Associated Activities

- 28 Activities as precondition
- 1 Activities as incidental
- 21 Activities as effect

Manufacturing Uses

<ul style="list-style-type: none"> Algicide Manufacturing Antifreeze Manufacturing Battery Manufacturing Bleaching Agent Materials Manufacturing Disinfectant Materials Manufacturing Flame Retardant Materials Manufacturing 	<ul style="list-style-type: none"> Food Industry Manufacturing Fungicide Manufacturing Gasoline Additive Manufacturing Herbicide Manufacturing Pesticide Manufacturing Pharmaceutical Manufacturing 	<ul style="list-style-type: none"> Plastic Manufacturing Pulp And Paper Manufacturing Refrigerant Materials Manufacturing Rubber Manufacturing Textile Manufacturing Water Treatment Materials Manufacturing
---	---	--

Watchlists

- CSAC Agent of Concern
- ERSH-DB Agent
- High Hazard Index TIC

Figure 4. Activities associated with chlorine.

Health Hazards <ul style="list-style-type: none"> • Causes damage to organs • Causes damage to organs through prolonged or repeated exposure • Causes serious eye damage • Causes severe skin burns and eye damage • Fatal if inhaled
Physical Hazards <ul style="list-style-type: none"> • Contains gas under pressure; may explode if heated
Prevention Precautions <ul style="list-style-type: none"> • Do not breathe dust/fume/gas/mist/vapours/spray. • Do not eat, drink or smoke when using this product. • Use only outdoors or in a well-ventilated area. • Wash hands thoroughly after handling. • Wear protective gloves/protective clothing/eye protection/face protection • Wear respiratory protection.
Response Precautions <ul style="list-style-type: none"> • Get medical advice/attention if you feel unwell. • IF exposed: call a POISON CENTER or doctor/physician. • IF IN EYES: Rinse cautiously with water for several minutes. Remove contact lenses, if present and easy to do. Continue rinsing. • IF INHALED: Remove person to fresh air and keep comfortable for breathing. Call a POISON CENTER or doctor/ physician. • IF ON SKIN (or hair): Remove/Take off Immediately all contaminated clothing. Rinse SKIN with water/shower. • IF SWALLOWED: Rinse mouth. Do NOT induce vomiting. • Wash contaminated clothing before reuse.
Storage Precautions <ul style="list-style-type: none"> • Protect from sunlight. • Store in a well-ventilated place. Keep container tightly closed. • Store locked up.
Disposal Precautions <ul style="list-style-type: none"> • Dispose of contents/container to an approved waste disposal plant.

Figure 5. Example of the type of information extracted from a safety data sheet.

included for each chemical and biological precursor, when available.

Physical Properties

The scientific community and the US government have made considerable investments to understand physical properties of chemical and biological threat agents and precursors. Knowledge of these properties is critical for certain missions, such as modeling and simulating potential releases to assess consequences. Some of these data can be found in open sources, such as PubChem,⁴ while other data can be found only in restricted government reports. The web application provides the user with a single location to access both open-source data and US government-furnished data. Each data point has a button indicating where the data originated. For instance, Figure 6 displays the boiling point of chlorine, as obtained from PubChem.⁵

Boiling Point Temperature	-34.04 °C	PubChem
---------------------------	-----------	---------

Figure 6. Example of physical property data from PubChem.

While the user can simply view the displayed values dynamically returned from the knowledge graph, it is also possible to create a custom query that traverses the CBRNE-SF to return all chemicals with a certain boiling property.

Alternative Identification

Language is complex, with multiple ways to refer to the same object. Chemicals can be described using system identifiers and multilingual terms. The CBRNE-SF contains all known system identifiers, such as the Chemical Abstracts Service (CAS) registration numbers and reference numbers for popular open-source databases, such as ChemSpider.⁶

Multilingual terms, like the ones in Figure 7 for chlorine, are typically extracted from data sources such as PubChem. All multilingual terms that are encoded for a given observable are also searchable. This allows the user to access information on an observable without needing to know the name used in the CBRNE-SF. As an example, each chemical in the CBRNE-SF has a unique URI with alternative label data semantically linked as a series of nodes and edges.

Multilingual Terms							
Language Independent	(U) 231-959-5	(U) 7782-50-5	(U) 7782-50-5, chlorine gas, cl	(U) Bertholite	(U) Chlor	(U) Chlor	(U) Chlore
	(U) Chlorine mol.	(U) Cl2	(U) Cloro	(U) Diatomic chlorine	(U) Molecular chlorine	(U) UN 1017	
English	(U) Bertholite	(U) Chlorine	(U) chlorine diatomic	(U) Chlorine Gas	(U) Chlorine Gas (Common Form)		
	(U) chlorine molecule	(U) Diatomic Chlorine	(U) dichloran	(U) dichlorine	(U) molecular chlorine		
Arabic	(U) الكلور						
Chinese	(U) 氯						
Chinese (Latin, pinyin)	(U) lu qi						

Figure 7. Example of multilingual terms in the CBRNE-SF.

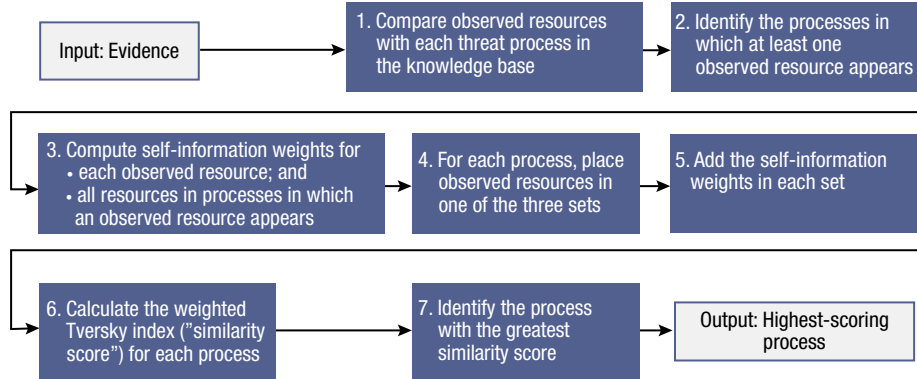


Figure 8. Steps involved in the process-ranking algorithm.

Set Similarity Algorithm for Evidential Reasoning

A user is able to look for threat agent production processes associated with the set of entered observables. The application traverses the knowledge graph and presents a table of processes ordered by a calculated similarity score. In set theory, this similarity score is called a weighted Tversky index.⁷ Similarity scores are described in more detail below.

Algorithm Overview

Figure 8 summarizes the steps involved in the process-ranking algorithm.

The three sets described in step 4 are related to the overlap of the observed resources within an Evidence Bag and the resources within a given process. Given an evidence set E and process p , three sets of resources must be identified:

1. The overlap set contains all of the resources that appear in E and either appear directly in p or are an instance of a resource that appears in p .
2. The evidence-only set contains resources that are in E but are not in p .
3. The process-only set contains resources that are in p but not in E .

These sets are illustrated in Figure 9.

In step 3, each resource r is given a weight X_r that is inversely related to its prevalence

$$X_r = -\log(F_r), \quad (1)$$

where F_r is the resource's prevalence (i.e., the proportion of processes in which r appears). This weight is equivalent to the resource's "self-information."⁸

Step 7 in the algorithm computes a similarity score for each process with respect to the observed evidence set. The similarity score for each process is computed as

$$W_p = T_{\text{OVERLAP}} / (T_{\text{OVERLAP}} + \alpha * T_{\text{EVIDENCE-ONLY}} + \beta * T_{\text{PROCESS-ONLY}}). \quad (2)$$

In Eq. 2, parameter α determines the size of the penalty for resources from the evidence set that do not appear in process p . Parameter β determines the size of the penalty for resources in p that were not recorded within the evidence set.

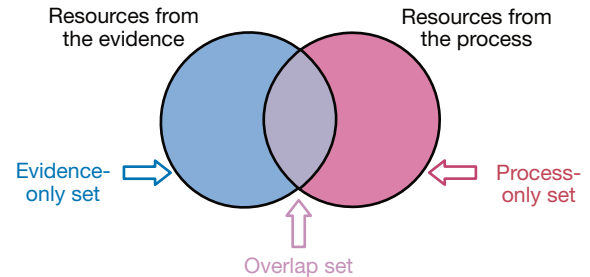


Figure 9. Sets of resources.

The process with the greatest similarity score is ranked the highest and can be considered the most likely. The score for each process is determined from the scores of the resources within that process, the scores of the resources within the given set of evidence, and the extent to which these sets of resources overlap.

Example Computations

To demonstrate the evidence algorithm, consider the following example for making iced tea, lemonade, and orange juice. Figures 10 and 11 each contain a single process, as does Figure 1 shown earlier. Blue boxes indicate activity nodes, and blue type outside the boxes describes resources used in the activities. In this example, α and β are both set to 0.5, suggesting that it is equally important for a resource to be missing from the Evidence Bag or from a process.

Each time evidence is collected, the observables are compared with the resources in each process, and a corresponding score is assigned to each process. The steps enumerated below correspond to the algorithm description in Figure 8.

- Evidence set = {cup, ice cube tray, pitcher, sugar}.
- Steps 1 and 2: The resources within this evidence set overlap with the iced tea, lemonade, and orange juice processes. Therefore, weights must be calculated for all resources in these processes.
- Step 3: Table 1 provides the weights for each resource that appears in at least one process. If a resource appears in one of three processes, its

weight is $-\log(1/3) = 1.097$. Similarly, if a resource appears in two of three processes, its weight is $-\log(2/3) = 0.405$. If a resource appears in all three processes, its weight is $-\log(3/3) = -\log(1) = 0$.

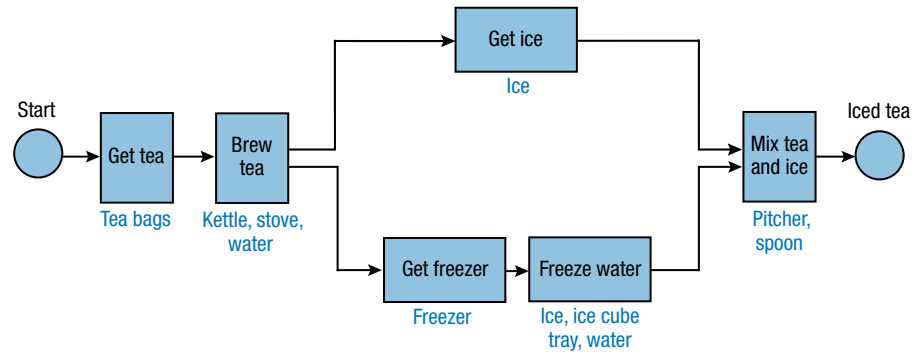


Figure 10. Iced tea process example.

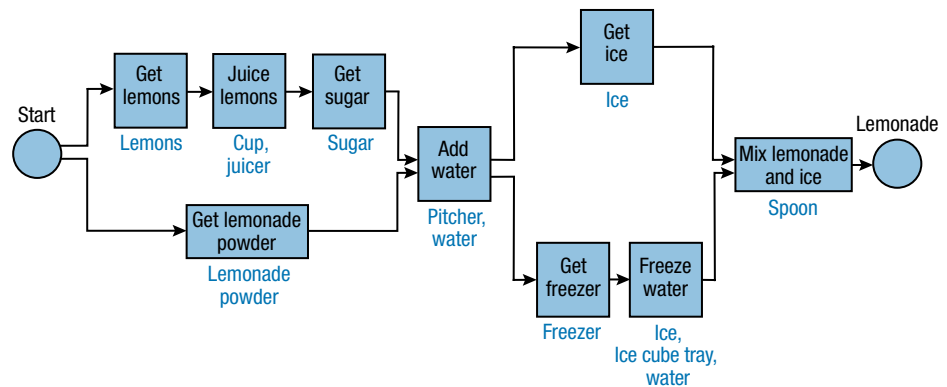


Figure 11. Lemonade process example.

Table 1. Weights by resource for example

Resource	Appears in			Resource Prevalence	Weight
	Iced Tea Process	Lemonade Process	Orange Juice Process		
Cup		✓		1/3	1.097
Freezer	✓	✓		2/3	0.405
Ice	✓	✓		2/3	0.405
Ice cube tray	✓	✓		2/3	0.405
Juicer		✓	✓	2/3	0.405
Kettle	✓			1/3	1.097
Lemonade powder		✓		1/3	1.097
Lemons		✓		1/3	1.097
Orange juice concentrate			✓	1/3	1.097
Oranges			✓	1/3	1.097
Pitcher	✓	✓	✓	3/3	0
Spoon	✓	✓	✓	3/3	0
Stove	✓			1/3	1.097
Sugar		✓		1/3	1.097
Tea bags	✓			1/3	1.097
Water	✓	✓	✓	3/3	0

Table 2. Weights for each set (from example 1)

Process	Set		
	Overlap	Evidence-Only	Process-Only
Iced tea	1.502	1.097	4.180
Lemonade	2.599	0	3.527
Orange juice	0	2.599	2.635

- Step 4: The resources that appear in the evidence are compared separately with each process.
 - For the iced tea process, the resources that appear both in the evidence set and the process (overlap set) are {cup, ice cube tray, pitcher}. The resources that appear in the evidence but not in the iced tea process (evidence-only set) are {sugar}. The resources that appear in the iced tea process but not in the evidence (process-only set) are {freezer, ice, kettle, spoon, stove, tea bags, water}.
 - For the lemonade process, the overlap set is {cup, ice cube tray, pitcher, sugar}; the evidence-only set is the empty set (i.e., there are no resources in this set); and the process-only set is {freezer, ice, juicer, lemonade powder, lemons, spoon, water}.
 - For the orange juice process, the overlap set is {pitcher}; the evidence-only set is {cup, ice cube tray, sugar}; and the process-only set is {juicer, orange juice concentrate, oranges, water}.
- Step 5: Table 2 provides the total weight for each set. These totals are obtained from the sum of the weights of the resources in each set. For instance, the weight for the overlap set in the iced tea process is 1.097 (cup) + 0.405 (ice cube tray) + 0 (pitcher) = 1.502 . Since the pitcher resource appears in all three processes, its weight is 0 (i.e., it does not provide any information on which process is most similar to be active).
- Step 6: Given $\alpha = \beta = 0.5$, the similarity scores for each process are calculated as follows:
 - $W_{IT} = 1.502 / (1.502 + 0.5 * 1.097 + 0.5 * 4.180) = 0.363$
 - $W_{LM} = 2.599 / (2.599 + 0.5 * 0 + 0.5 * 3.527) = 0.596$
 - $W_{OJ} = 0 / (0 + 0.5 * 2.599 + 0.5 * 2.635) = 0$
- Step 7: $W_{LM} = 0.596$ is greater than W_{IT} or W_{OJ} (i.e., the lemonade process has the greatest similarity score). Therefore, the lemonade process is identified as the most similar.

CONCLUSION

APL has worked with the US government for more than 15 years to create the most comprehensive set of CBRNE ontologies to enable CWMD missions worldwide. As a machine-readable representation of reality,

the CBRNE-SF is continuing its evolution as a shared CWMD resource. It is poised to support next-generation generative artificial intelligence and large language model capability. The CBRNE-SF has contributed to DTRA's position as a locus of authority for CBRNE ontologies, enabling tighter integration of and interoperability within the broader US government CWMD mission space.

REFERENCES

- Object Management Group, "What is UML?" <https://www.uml.org/what-is-uml.htm> (accessed Jun. 23, 2025).
- World Wide Web Consortium (W3C), "RDF 1.1 primer," W3C Working Group Note, Jun. 24, 2014, <https://www.w3.org/TR/rdf-primer>.
- World Wide Web Consortium (W3C), "RDF 1.2 schema," W3C Working Draft, Jun. 13, 2025, <https://www.w3.org/TR/rdf12-schema>.
- National Library of Medicine, PubChem, <https://pubchem.ncbi.nlm.nih.gov/> (accessed Jun. 23, 2025).
- S. Kim, J. Chen, T. Cheng, A. Gindulyte, J. He, et al. "PubChem 2025 update," *Nucleic Acids Res.*, vol. 53, no. D1, pp. D1516–D1525, 2025, <https://doi.org/10.1093/nar/gkaf1059>.
- H. E. Pence and A. Williams, "ChemSpider: An online chemical information resource," *J. Chem. Educ.*, vol. 87, no. 11, pp. 1123–1124, 2010, <https://doi.org/10.1021/ed100697w>.
- C. Gao, H. Ye, F. Cao, C. Wen, Q. Zhang, and F. Zhang, "Multiscale fused network with additive channel-spatial attention for image segmentation," *Knowl.-Based Syst.*, vol. 214, art. 106754, 2021, <https://doi.org/10.1016/j.knsys.2021.106754>.
- G. Katona and O. Nemetz, "Huffman codes and self-information," *IEEE Trans. Inf. Theory*, vol. 22, no. 3, pp. 337–340, 1976, <https://doi.org/10.1109/TIT.1976.1055554>.



Ray H. Mariner, Air and Missile Defense Sector, Johns Hopkins University Applied Physics Laboratory, Laurel, MD

Ray H. Mariner is a program manager in APL's Homeland Defense Mission Area. He has a BS in chemistry from Loyola University in Maryland (now Loyola University Maryland) and an MS in homeland security management from the University of Maryland Global Campus. Ray has more than 25 years of experience as an analytical chemist and data scientist, and other areas of expertise include semantic modeling, threat modeling, and threat prioritization. His email address is ray.mariner@jhuapl.edu.



Timothy P. Lipa, Asymmetric Operations Sector, Johns Hopkins University Applied Physics Laboratory, Laurel, MD

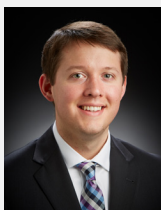
Timothy P. Lipa is the head of APL's Electromagnetic Sensing Systems Branch. He holds a BS in chemistry from Loyola University and an MS and a PhD in chemistry from Johns Hopkins University. He leads three technical groups and has led a broad portfolio of technical projects focused primarily on countering the proliferation and use of chemical warfare agents. His work includes the development of chemical sensors, integrated

sensing systems, and sensor test beds. He has also collaborated with computer scientists to merge natural sciences with data science, producing software systems that enhance understanding of potential adversarial threats and inform methods to counter them. His email address is timothy.lippa@jhuapl.edu.



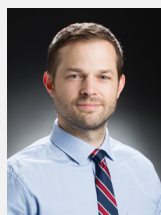
Phillip T. Koshute, Asymmetric Operations Sector, Johns Hopkins University Applied Physics Laboratory, Laurel, MD

Phillip T. Koshute is a data scientist and statistical modeler in APL's Asymmetric Operations Sector. He earned a BS in mathematics from Case Western Reserve University and an MS in operations research from North Carolina State University. He is pursuing a PhD in applied statistics at the University of Maryland. He provides statistical expertise to data science projects with a wide range of applications, including biology, chemistry, and additive manufacturing. His email address is phillip.koshute@jhuapl.edu.



David W. Boyce, Asymmetric Operations Sector, Johns Hopkins University Applied Physics Laboratory, Laurel, MD

David W. Boyce is physical and material scientist in APL's Asymmetric Operations Sector. He has a BS in chemistry from Villanova University and an MS and PhD in chemistry from the University of Minnesota. David's primary interests include creating models and multi-domain ontologies to support counter-weapons of mass destruction data science applications. He has experience in synthetic techniques, catalysis, and spectroscopy. His email address is david.boyce@jhuapl.edu.



Josef C. Behling, Asymmetric Operations Sector, Johns Hopkins University Applied Physics Laboratory, Laurel, MD

Josef C. Behling is the program area manager of APL's Counter CBRNE Program Area. He has a BS in operations and information systems management from Pennsylvania State University and an MS in computer science from American University. He has expertise in melding software engineering, knowledge representation, natural science, and machine learning. As research lead, Joe shapes, communicates, and assesses cutting-edge research in natural science, sensing, artificial intelligence, autonomy, and data analytics for the counter-weapons of mass destruction mission. He is chair of the Department of Defense/Intelligence Community Ontology Working Group and the Internationalized Resource Identifier (IRI) Naming and Resolution Committee and is APL's advisory committee representative to the World Wide Web Consortium (W3C). His email address is Josef.Behling@jhuapl.edu.



Michael J. Peters, Asymmetric Operations Sector, Johns Hopkins University Applied Physics Laboratory, Laurel, MD

Michael J. Peters is a senior software engineer and data scientist as well as the assistant supervisor of APL's Threat Analytics Systems Group. He has a BS in computer science from Pennsylvania State University and an MS in computer science from Johns Hopkins University. Michael's research interests include software design, applied machine learning, ontologies, and distributed software architectures. His email address is michael.peters@jhuapl.edu.

MLM: Machine Learning for Threat Characterization of Unidentified Metagenomic Reads

Benjamin D. Baugher, Phillip T. Koshute, N. Jordan Jameson, Kennan C. Lejeune, Joseph D. Baugher, and Christopher M. Gifford

ABSTRACT

Forensics and military investigators often assess sites of interest, searching for evidence of biological hazards. The application of metagenomics provides genomic data for all microorganisms present in a sample, enabling advanced analysis for detection of biological signatures and threat detection from such sites. DNA sequence segments (digitally represented as “reads”) from metagenomics samples are commonly compared with reference libraries in order to identify microorganisms present in the sample. However, this approach does not capture the complete biological signature, as there always remains a subset of reads that are unable to be successfully mapped to a known organism. The Johns Hopkins University Applied Physics Laboratory (APL) Machine Learning for Metagenomics (MLM) pipeline characterizes these unidentified reads in terms of composition and alignment with sequences of known organisms. Since these reads are unable to be mapped directly to a known organism, our models classify each read according to one of five threat levels, ranging from 0 to 4 (with threat level 4 the most severe). Our pipeline consists of random forest, Bayesian network, and clustering models. When testing this pipeline against simulated and real sequencing data, we achieved high threat level classification accuracy: 95% for clusters of related reads. Based on these results, we are preparing for deployment of our pipeline on far-forward devices, providing investigators with real-time threat assessment of biological materials to inform an appropriate rapid response.

INTRODUCTION

Forensics and military investigators often assess sites of interest, searching for evidence of biological hazards due to malicious actors or natural phenomena.¹ When hazards are present, it is ideal to identify them precisely. However, if this is not possible, characterizing the severity of the threat provides vital insights for guiding the investigators’ response.

Metagenomics enables detailed screening of biological samples from sites of interest. Collected samples can be passed through a sequencer, yielding reads of DNA nucleotides. A read is a digital representation of a segment of a DNA molecule. In an attempt to identify the organisms present in a sample, the reads are compared with reference libraries of DNA sequences from known

organisms. Close matches with reference sequences infer the presence of specific organisms in the sample. However, there always remains a subset of reads that are unable to be successfully mapped to a known organism based on the set of matches, if any, to reference sequences. For instance, emerging, mutated, or modified threats all potentially pose concern to investigators but often do not have matches within reference libraries. Additionally, reference sequences exist only for a small percentage of microorganisms.

Our Machine Learning for Metagenomics (MLM) project focuses on these unmapped reads (i.e., “unidentified” reads). We developed a pipeline of models that characterizes unidentified reads in terms of composition and alignment with sequences of known organisms. Since these reads are unable to be mapped directly to a known organism, our models classify each read according to one of five threat levels (TLs), ranging from 0 to 4. We developed this scale of TLs by combining the bioterrorism categories from the US Centers for Disease Control and Prevention² and the biosafety risk groups from the US National Institutes of Health.³ Within our scale, organisms that pose the greatest threat have TL4, while organisms that do not pose a threat have TL0. By predicting the TL of the organism(s) represented by unidentified reads through carefully trained classification models, MLM provides rapid TL assessments of unidentified organisms present in biological samples (e.g., organisms that are unknown or are not represented within a reference library). We focus specifically on detecting bacterial and viral threats because they comprise the large majority of organisms that pose threats to human health.

The remainder of this article proceeds as follows. We first give a detailed overview of the components of our MLM model pipeline. Then, we describe how we trained the models within the pipeline, enabling the models’ training algorithms

to search for patterns between reads with the same TLs. Next, we highlight the pipeline’s results on both simulated and real reads and offer observations on practical considerations for deploying our pipeline. Finally, we suggest possible next steps for ongoing and future research.

MODEL SETUP

Our MLM pipeline consists of interconnected processing steps, random forest (RF) models, Bayesian network (BN) models, and clustering steps. Figure 1 illustrates the progression of reads through these steps and models. Within the pipeline, unidentified reads are gathered and filtered, features are extracted from

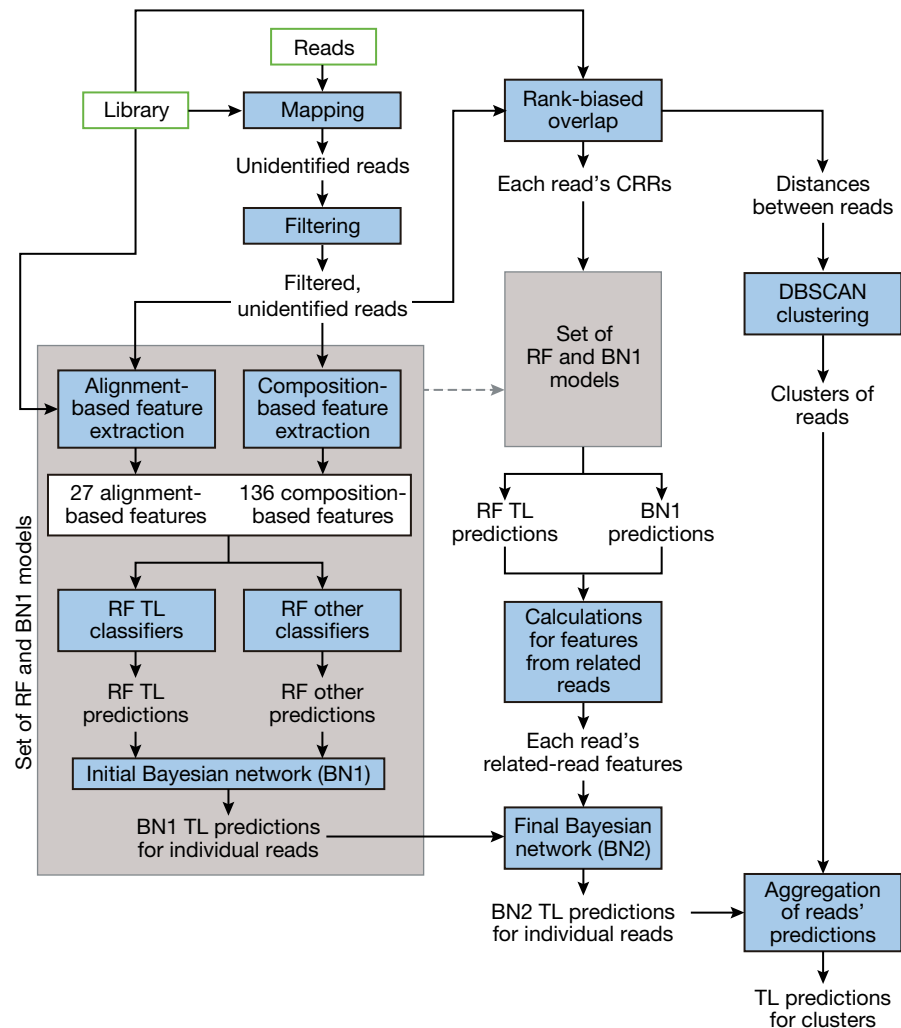


Figure 1. Data flow through model pipeline. Unidentified reads are gathered and filtered, features are extracted from remaining reads, and these features are passed through a combination of models. The ensemble of RF models provides preliminary prediction of the TLs of the reads’ organisms, as well as other characteristics. The initial BN (BN1) fuses the RF predictions. The final BN (BN2) incorporates features computed from the predictions of each individual read’s closely related reads (CRRs). The clustering step is based on the density-based spatial clustering for applications with noise (DBSCAN) method and enables a single aggregate TL prediction for the organisms represented in each cluster of reads.

remaining reads, and these features are passed through a combination of models. The ensemble of RF models provides preliminary prediction of the TLs of the unidentified organisms represented by the reads and of other characteristics. The initial BN (BN1) fuses the RF predictions. The final BN (BN2) incorporates features computed from the predictions of each individual read's closely related reads (CRRs). The clustering step is based on the density-based spatial clustering for applications with noise (DBSCAN) method and enables a single aggregate TL prediction for the organisms represented in each cluster. Each of these steps is further described in the following subsections.

Read Source

Among the multitude of available sequencing devices, we focus our analysis on sequencing data from the Oxford Nanopore MinION sequencer.⁴ We opted for the MinION device because of its portability, low cost, and ease of use—characteristics that are important in many use cases for military investigators. All of the reads within this analysis have either come from a MinION simulator (refer to the Read Simulation subsection) or have been collected with a MinION device or similar nanopore sequencing device (refer to the Results on Real Reads subsection).

If desired, our process for extracting features and developing and evaluating models could be similarly implemented for reads from other sequencing platforms for which data are available. For instance, we have previously demonstrated this capability for Illumina's MiSeq and iSeq platforms.

Read Mapping with Reference Library

Before mapping, we pass reads through an algorithm that flags reads that are highly likely to originate from macroorganism (host organism) contamination. This algorithm searches for matches in a set of short overlapping k-mers between the read and a database of plant and animal reference sequences that are extremely unlikely to have occurred by chance. (A k-mer is a subsequence of nucleotides of length k .) We discard reads that correspond to such matches.

To identify remaining reads that can be mapped to known microorganisms, we developed a pair of matching and alignment algorithms. Relying on clever indexing of large reference libraries and overlapping short k-mer matches, the first algorithm is very fast but at the cost of some accuracy. The second algorithm verifies matches identified by the first algorithm by performing targeted alignments between a given read and the portion of the reference sequence in which the potential match was found.

The matching algorithm yields an alignment score between each read and the top N reference sequence matches, where N is a user-defined parameter.

Ultimately, an alignment hit occurs when the alignment score between the read and a reference sequence exceeds a specified threshold. This alignment score is also used for feature extraction in the cases where the scores do not exceed the threshold (refer to the Feature Extraction subsection).

Currently, we use as our reference library the October 2, 2021, version of the Nucleotide database from the National Center for Biotechnology Information.⁵ We plan to update our reference library periodically as we move forward with this project.

After this matching step, we annotate reads for which we have identified alignment hits with known organisms and provide them to the end user for analysis. The remaining reads without alignment hits (i.e., unmapped reads) are then processed by our MLM pipeline to search for any undetected threats from emerging, mutated, or modified microorganisms. By assessing the unmapped reads, our MLM pipeline aims to complement the insights obtained from reads mapped to known organisms. The MLM pipeline can also be used to assess the unidentified reads from any other alignment or taxonomic classifier tool.

Filtering Unidentified Reads

To select the best set of reads from a given sample to run through our model pipeline, we employ a variety of filtering steps.

First, we check the number of nucleotides that are suitable for assessment. After masking likely MinION sequencing adapters⁶ and low complexity regions,⁷ we discard reads that do not have at least 100 unmasked nucleotides.

We also consider the quality scores of each read, checking whether a read has enough high-quality nucleotides and a sufficiently long sequence of contiguous high-quality nucleotides. We discard reads that do not meet both of these conditions.

Each of the filtering steps is based on parameters that can be tuned to be more or less aggressive based on the use case and end user needs. Our default parameter values are somewhat conservative, yielding greater confidence in the results. In contrast, a more liberal approach would enable greater sensitivity to traces of potential threats, but at the cost of an increased false alarm rate (FAR). A false alarm (FA) occurs when the MLM pipeline predicts a high TL but the true TL is not high. We regard TL2, TL3, and TL4 as high TLs.

Feature Extraction

For all unidentified reads remaining after filtering, we extract 163 features, including 19 alignment-based features and 144 composition-based features. These features are ultimately used as inputs to six subsequent RF models.

We obtain the alignment-based features by comparing each read with sequences of reference organisms for which we know the TL. These alignment-based features include the TL of the reference sequence most closely aligned to the read under consideration, the top alignment scores for reference sequences from each TL (i.e., one feature for each of the five TLs), and the percentage of alignment hits from each TL.

While alignment-based features seek to quantify and represent a read's similarities to known organisms, composition-based features focus directly on the nucleotides that make up a given read. Most of the composition-based features correspond to the frequencies of the 136 unique tetramers. Other composition-based features include the GC (guanine-cytosine) content of the read and minimum compositional distances to reference sequences from each TL.

Taken together, the alignment- and composition-based features provide a detailed representation of each read. Subsequent supervised machine learning (ML) models leverage this representation to find patterns between reads' features and the TLs of the organisms from which they have come.

Random Forest Classifiers

RF models are supervised ML models consisting of numerous decision trees, each trained by a statistically strategic random subset of the available data.⁸ The random selection of each tree's training data reduces the correlation in the trees' prediction, amounting to less prediction variance and less overall prediction error for the RF. Within the RF, each decision tree yields a separate prediction based on a set of logical rules, which can be evaluated by progressing down the tree. For our data, examples of such logical rules might include "top normalized alignment score for a TL3 reference sequence < 0.4" or "normalized frequency of tetramer #1 > 0.05."

Our MLM pipeline includes six RF classification models (or "classifiers"). Four of the RF classifiers predict TLs. Each of these TL classifiers is trained with a different set of simulated reads. (We describe our simulation process in the Read Simulation subsection.) Each set is characterized by whether its reads originated from a bacterium or virus and which clade (species or strain) of "neighbors" has been removed from the reference library before those reads' features have been computed. We remove the neighbor clade as a way to mimic the scenario in which a read from a previously unseen species or strain is collected. We refer to the RF TL classifiers according to the set of reads on which they were trained: BSp (bacteria reads with their species removed from the reference library), BStr (bacteria reads with their strains removed from reference library), VSp (virus reads with their species removed from the reference library), and VStr (virus reads with their strains removed from

reference library). We train separate RF classifiers for each set of reads to cover a range of possible unidentified organisms from which reads might be collected. The predictions from these RFs are ultimately fused (along with other values) by the BNs later in the pipeline.

The other two RF classification models predict other characteristics of the reads. The BV classifier predicts whether a given read corresponds to bacterium or virus. Likewise, the NN classifier predicts whether the closest related organism in the reference library is in the same species or not ("nearest neighbor"). The outputs of these additional RF classifiers also are inputs to the BNs within the MLM pipeline.

Initial Bayesian Network

BNs represent probability relationships between variables, enabling the state of one or more variables to be assessed as data are observed. In particular, BNs provide an estimate of the "belief level" for each possible state of each variable, based on prior knowledge of these variables and observed data.

In a BN, each variable is defined by a node, which has two or more possible discrete states. The "target" node has special importance; this node represents the variable for which the state is being estimated. Pairs of nodes with conditional probability relationships have a directed edge between them; the edge originates at the node corresponding to the variable on which the other variable is conditioned. A node may be the terminus for more than one directed edge (i.e., a variable may be conditioned on more than one other variable).

The structure of a BN's nodes and edges may be determined through expert knowledge or "learned" via training data. We determined through experimentation that learning the BN structure yields better prediction performance. Our approach for training our BNs is described in the Model Training Details subsection.

Each node also has a conditional probability table (CPT), which describes the conditional probability relationships between nodes connected by edges. The dimension of each node's CPT is determined by the number of variables on which the variable corresponding to that node is conditioned. In general, the values in each column of a CPT sum to 1.

BN1 includes nodes for nine variables: the outputs of the six RF classifiers, the true type of read (bacterium or virus), the true removed clade (species or strain), and the read's TL (i.e., TL of the organism from which the read has come). For each read, we compute values for the first six variables. When these values are propagated through BN1, the BN1 inference step estimates values for the remaining three variables, including the read's TL. Figure 2 gives an example of a possible structure for BN1. Based on this particular BN1 structure, Table 1 gives an example of a CPT for one of the nodes (BSp RF TL Prediction).

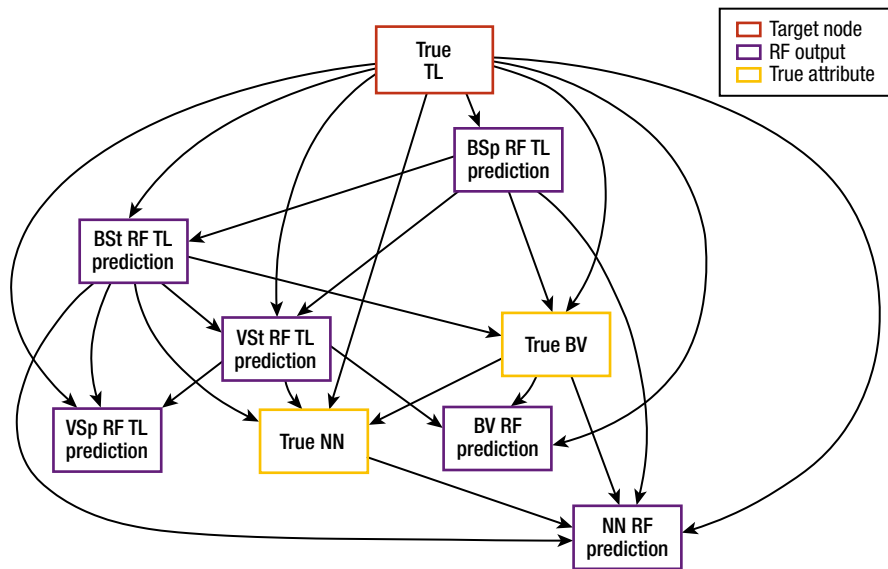


Figure 2. Example of BN1 with learned structure. Included are nodes for nine variables: the outputs of the six RF classifiers, the true type of read (bacterium or virus), the true removed clade (species or strain), and the TL.

Table 1. Example of BN1 CPT

BSp RF TL Prediction	True TL				
	0	1	2	3	4
0	0.9442	0.5895	0.1863	0.3639	0.8501
1	0.0185	0.3672	0.0351	0.5391	0.0954
2	0.0018	0.0379	0.6970	0.0280	0.0348
3	0.0277	0.0046	0.0001	0.0665	0.0003
4	0.0077	0.0008	0.0816	0.0023	0.0194

Rows correspond to TLs predicted by the BSp RF model for each read, and columns correspond to the true TL of the organism that each read represents. Each cell shows the probability of the TL predicted by the BSp RF (indicated by the row), given the true TL (indicated by the column). Hence, the values within a given column sum to 1.

The output of the BN is a set of belief values for each node, with one belief value for each state of the variable represented by that node. The belief values range from 0 to 1 and must sum to 1 for a given node. (In Table 1, the sum of each column may slightly differ from 1 because of rounding.) For BN1, these values can be used to predict a discrete TL by identifying the state in the target variable's node ("Threat Level") with the largest belief value.

Identifying Closely Related Reads

Within metagenomic analysis, reads are not collected in isolation but rather in samples with sets of thousands to millions of other reads from many different organisms. These sets generally include multiple reads obtained from each organism present. To predict the TL for an individual read, we use features from the read itself as well as from other CRRs that are likely to have

come from the same organism or a very closely related one. This mix of features helps us to fine-tune our threat assessment for each read and ultimately reduce FA assessments. Our methods for computing features based on CRRs is described in the Features Based on Closely Related Reads subsection. The model for which these features are inputs is described in the Final Bayesian Network subsection.

To determine the CRRs for each read, we use a method based on rank-biased overlap (RBO).⁹ For each read, we use segments within the read to match the read with sequences from our reference library. For the reference sequences that match, we align the reads with targeted portions within the reference sequences based on where the segments matched to obtain alignment scores characterizing how well the reads match the reference sequences. These alignment scores are used to produce a ranked list of similar organisms for each read. The list consists of the reference library organisms with the best alignment scores. We repeat this process, obtaining rankings or reference library organ-

isms for each unidentified read. Given these rankings, we compute "distances" between pairs of unidentified reads by comparing the reads' lists using the RBO method. These distances do not correspond to physical space but instead measure the dissimilarity between reads; reads with similar lists have smaller distances. Originally developed for comparing results of internet search engines, the RBO method enables comparison of ranked and possibly incomplete lists to identify similarities between lists.

For each read, we identify up to 1,000 CRRs from among those with the smallest distances to the read. Not all reads have the full set of 1,000 CRRs. This occurs when there are a limited number of reads present from a given organism. It can also occur with reads that have fewer matches with the reference library. Some reads may even have no CRRs.

Table 2. Summary of neighbor-based features for BN2

Feature	Description	Possible Values
CRR_RF_TLPred_Mode	The most common output for all RF TL classifiers for all CRRs	0, 1, 2, 3, 4
CRR_RF_PredLevel_TL0	Discrete categories of the proportion p of the RF TL predictions for CRRs with a given TL (the feature value is <i>Low</i> if $p < 0.2$ for that TL, <i>medium</i> if $0.2 \leq p < 0.5$, and <i>high</i> if $p \geq 0.5$)	Low, medium, high
CRR_RF_PredLevel_TL1		
CRR_RF_PredLevel_TL2		
CRR_RF_PredLevel_TL3		
CRR_RF_PredLevel_TL4		
CRR_BN1_TLPred_Mode	The most common BN output for CRRs	0, 1, 2, 3, 4
CRR_BN1_TLPred_Max	The highest TL among BN1 outputs of all CRRs	0, 1, 2, 3, 4
CRR_BN1_PredLevel_TL0	Discrete categories of the proportion p of the BN1 predictions for CRRs with a given TL (the feature value is <i>low</i> if $p < 0.2$ for that TL, <i>medium</i> if $0.2 \leq p < 0.5$, and <i>high</i> if $p \geq 0.5$)	Low, medium, high
CRR_BN1_PredLevel_TL1		
CRR_BN1_PredLevel_TL2		
CRR_BN1_PredLevel_TL3		
CRR_BN1_PredLevel_TL4		

Features Based on Closely Related Reads

Given each read's CRRs, we compute 13 additional features for use as inputs for BN2. These features characterize the predictions of the RF TL classifiers and BN1 for the neighbor reads. Table 2 summarizes these additional features. If a read has no CRRs, CRR_BN1_TLPred_Mode and CRR_BN1_TLPred_Max are set to the BN1 prediction for that read. Likewise, CRR_RF_TLPred_Mode is set to the most common prediction from the RF TL classifiers. All other CRR-related features are set to 0.

BNs expect features with discrete states. Thus, a discrete value must be set for each feature, and special care is needed when there are ties for TL-based features. For the CRR_RF_TLPred_Mode and CRR_BN1_TLPred_Mode features, ties are handled by computing the mean value among all TLs involved in the tie and rounding to the nearest TL. A tie may occur for a given read if multiple TLs are predicted equally often by the CRRs for that read.

Final Bayesian Network

BN2 is similar to BN1 but leverages information from CRRs and incorporates additional features. BN2 involves the 9 nodes from BN1, as well as nodes for the 13 features from Table 2. Similar to BN1, the output of BN2 is a predicted TL for the given read, determined from the TL with the largest belief value in the target node ("Threat Level").

Clustering

The unidentified reads within our pipeline are composed of very noisy data with a variety of limitations, such as low quality. There are also errors in the reference library. Additionally, reads from low-threat organisms that are somewhat closely related to high-threat organisms may be assessed as posing higher threat than is warranted because of shared genomic regions. As a result, TLs may be incorrectly predicted for individual reads.

To provide a robust alternative to predictions for individual reads, we group the reads within a sample into clusters using the DBSCAN method.¹⁰ For each resulting cluster, we obtain cluster-level TL predictions by identifying the most commonly predicted TL for individual reads within the cluster.

The DBSCAN method uses high- and low-density data regions to identify clusters and outliers, characterizing density in terms of reads' distances from each other. We compute distances between reads as part of the RBO-based CRR identification step (refer to the Identifying Closely Related Reads subsection).

DBSCAN involves two parameters that generally guide the size and number of clusters. The assignment of points to clusters is determined by whether they are in the "neighborhood" of one or more core points. (For our analysis, each read corresponds to a point.) The *eps* parameter defines the radius of each point's neighborhood. It can be set as any positive number. Larger values of *eps* permit more points to be included in a single neighborhood, thus prompting more points to be clustered together and encouraging smaller numbers of clusters. We typically use *eps* = 0.1. Secondly, the *minPts* parameter sets the minimum number of other points within a given point's neighborhood to qualify that point as a "core point." A point is within another point's neighborhood if the distance between the points is less than *eps*. As a result, larger values of *minPts* make the requirements for a core point to be regarded as a core point more strict and therein also encourage smaller numbers of clusters. Wanting to encourage detection of smaller clusters, we typically set *minPts* as the minimum of 100 and $0.05N_p$, where N_p is the number of points in a given sample.

Within DBSCAN, points that are not within the neighborhood of any core point are assigned to a "noise cluster." The points in this cluster are not necessarily similar to each other, but rather are relatively unlike other points assigned to other clusters. Smaller values of *eps* and larger values of *numPts* promote

more points to be assigned to the noise cluster. In our case, the noise cluster most likely includes reads from contaminating organisms.

MODEL TRAINING

We train and evaluate models using simulated reads, which provide the benefit of knowing the TLs of the organisms from which they have come. We use the DeepSimulator tool to simulate reads. We split the training reads into multiple sets to separately train the RF models, BN1, and BN2. The following subsections describe our training process in further detail.

Read Simulation

DeepSimulator^{11,12} is the first deep learning-based MinION read simulator. It seeks to accurately simulate the reads by simulating the entire sequencing process. DeepSimulator directly models the raw electrical signals produced by nanopores, rather than simply trying to mimic the sequencing results. In particular, it builds a context-independent pore model using deep learning methods to simulate the electrical signals produced by the actual nanopores. Given these signals, it uses standard base-calling software to convert the simulated signals into reads.

To train and evaluate the version of our pipeline shown in this analysis, we ran DeepSimulator version 1.5 on selected reference sequences from the Nucleotide database, using the built-in error profile for the MinION sequencer. Additionally, we specified a mean read length of 8,000 nucleotides, a read coverage of 50× for bacterial genomes, and a read coverage of 250× for viral genomes. Read coverage refers to the average number of simulated reads in which a given nucleotide is included. These runs ultimately yielded approximately 372 million simulated reads for bacteria and approximately 70 million reads for viruses.

Simulating Unidentified Reads

To train models to make accurate predictions about unidentified organisms, we construct simulated datasets of “unknown” organisms by removing known organisms from the reference databases (i.e., “sanitizing” the databases). To do this, we remove each clade one by one, compute the features on the simulated reads obtained from the organisms within the removed clade, and then put it back before removing the next clade. For both bacteria and viruses, we construct two datasets apiece. The first one set mimics the case in which an entire new species is encountered without being represented in the reference library. The second set similarly mimics the case in which a new strain is encountered.

We use our read mapping algorithm (refer to the Read Mapping with Reference Library subsection) to classify

and then align each of the simulated reads with the sanitized reference database. We discard reads that align well to any reference sequence that remains in the database because these would not be considered to be unidentified reads. The remaining reads are those that would be unidentified if the given clade was in fact unknown; we use these reads for training and testing our models. We set the threshold for regarding a read as unidentified to a 90% alignment match.

Defining Training and Test Sets

We gathered slightly more than 1.4 million unidentified reads from the simulated data described above. We set aside ~25% for testing and separated the rest into different training sets: 136,446 reads for BSp RF; 84,056 for BSt RF; 52,138 for VSp RF; 15,419 for VSt RF; 284,925 for BN1; and 490,522 for BN2. The different types of reads used to train our four TL RF classifiers are described in the Feature Extraction subsection. We formed an additional training set as the union of the four training sets for RF TL classifiers (amounting to 288,059 reads) and used this aggregate set to train both the BV and NN RF classifiers.

For each training set we extract 163 features from each read within the set (refer to the Feature Extraction subsection). Training ML models involves allowing computerized algorithms to find patterns that link input features to the target value. We train six RF models using the feature data extracted from their individual training sets. As described in the Random Forest Classifiers subsection, the first four RF models predict the read's TL; these models differ in the type of reads used to train them (BSp, BSt, VSp, VSt). The other two RF models predict whether the read is from a bacterium or virus for the BV classifier and whether the closest related organism in the reference library is in the same species or not for the NN classifier. Subsequently we run the feature data extracted from the BN1 training set through the trained RF models and use the outputs of these models to train BN1 to predict TL. As a final training step, we run the feature data from the BN2 training set through the trained RF and BN1 models, compute CRR-based features (summarized in Table 2), and use the resulting 19 features to train BN2 to predict TL for individual reads (refer to the Final Bayesian Network subsection).

To assess performance, we ran the 346,373 reads from the test set through the entire MLM pipeline. Because these reads were not at all involved in model training, the pipeline's performance against them provides an estimate of the pipeline's performance against unidentified threats. The pipeline's performance against these reads is described in the Results on Simulated Reads subsection.

Model Training Details

We use various R packages to train our models: *ranger* for the RF models¹³ and both *bnlearn*¹⁴ and *gRain*¹⁵ for BN1 and BN2.

For the RF models, we use 50 trees per model and *ranger* default values for all other settings. The minimum number of reads at a terminal node in each decision tree is one, and trees are set to grow as large as the data permit. For each tree, reads are randomly sampled with replacement (i.e., reads can be sampled more than once for a given tree). Each split within each tree considers a subset of 12 randomly selected features (equal to the floor of the square root of the total number of features, $\text{floor}(\sqrt{163}) \approx 12$).

For training the BN models, we use the hill-climbing algorithm from the *hc* function within the *bnlearn* package to learn the structure of the models. To aid the learning, we specify an initial network (with edges originating from the “Threat Level” node and terminating at each of the other nodes) and a list of forbidden edges (e.g., those that terminate at the “Threat Level” node). For BN2, we also limit the number of edges terminating any given node to 3. This constraint limits the size of any given node’s CPT and also decreases the time required to run the model. Likewise, we use the *extractCPT*, *compileCPT*, and *grain* functions within the *gRain* package to fit the nodes’ CPTs. To account for the possibility in which a given cell in the CPT has zero instances, we specify a smoothing constant of 0.01.

Supporting Evidence Check for False Alarm Reduction

During model development, we observed that FAs occurred because in certain cases reads from the training set with true high TL did not have any supporting evidence for the high TL (i.e., the extracted RF features corresponding to high TLs had low values, suggesting that there were no similarities to high-threat organisms for these reads). As a result, the BN models had learned to associate features that did not reflect similarities to high-threat organisms with high TL predictions. This aspect of the models can lead to FAs because these associations do not generalize well. While there are reads from true high-threat organisms for which we do not find any similarities to known threats, we generally have low confidence in any high TL predictions for which such similarities have not been found.

To account for this phenomenon, we implemented a postprocessing step after BN2 to adjust predicted TLs for which there was no supporting evidence. In particular, if a predicted high TL is not consistent with RF feature values corresponding to that TL, we adjust the belief values for that TL so that it is no higher than any belief value for a low TL and renormalize all TLs’ belief values so that they sum to one. We repeat this step until the highest belief value for the read is for a low TL or for a high TL with supporting evidence. This step substantially reduces the MLM pipeline’s FAR without impacting cluster-level TL predictions for real reads (refer to the Results on Real Reads subsection).

RESULTS

To assess the performance of the MLM pipeline, we evaluated it on both simulated and real reads. For simulated reads, the true TL of the organism from which each read has come is known. The real reads come from collected samples for which the primary organisms present are known. Thus, the true TL for each organism within a set of real reads is known, but the true TLs for individual reads are not necessarily known.

Results on Simulated Reads

As described in the Read Simulation subsection, we simulated reads using the DeepSimulator tool. To account for the randomness in how RF classifiers are constructed, we trained 10 sets of models, tracking results for the test set reads (refer to the Defining Training and Test Sets subsection) on each set of models. We measure performance in terms of accuracy (the proportion of correctly predicted TLs across all reads), sensitivity (the proportion of reads with true high TL for which we predict high TL), and positive predictive value (PPV, the proportion of reads for which we predict high TL that have a true high TL). In other contexts, sensitivity and PPV are also called recall and precision, respectively.

Because the simulated reads are not grouped into samples, we analyzed these metrics at the read level. We did not conduct the clustering step as part of our analysis of simulated reads. While operational decisions are unlikely to be made in practice on individual reads, different models’ PPV and sensitivity on these reads characterize the models’ relative performance and point to which model is most promising for use with clusters of reads.

Figure 3 shows the accuracy results for each model type within our pipeline for each set of models. These models undertake the five-class classification problem of predicting a TL for each read from among one of five possible TLs. Incorporating the outputs of the RF models (Figure 1), the BN models perform better than the RF TL classifiers, consistently achieving classification accuracy among the five TLs of 70% or greater and averaging near 75% accuracy. Since the BN models leverage the predictions of the RF TL classifiers, the improved performance with the BN models is expected.

We also assessed the models’ ability to accurately predict high TLs, i.e., to predict whether or not a read has come from an organism with a TL of 2 or higher. Since this amounts to a binary classification problem, the model’s prediction is determined by comparing its output score (i.e., sum of belief values for TL2, TL3, and TL4) with the decision threshold. It is important for models to not miss true TLs (i.e., achieve high sensitivity) and also to not falsely predict high TLs (i.e., achieve high PPV). Figure 4 shows the trade-off between sensitivity and PPV for each model with a decision threshold of 0.5. Again,

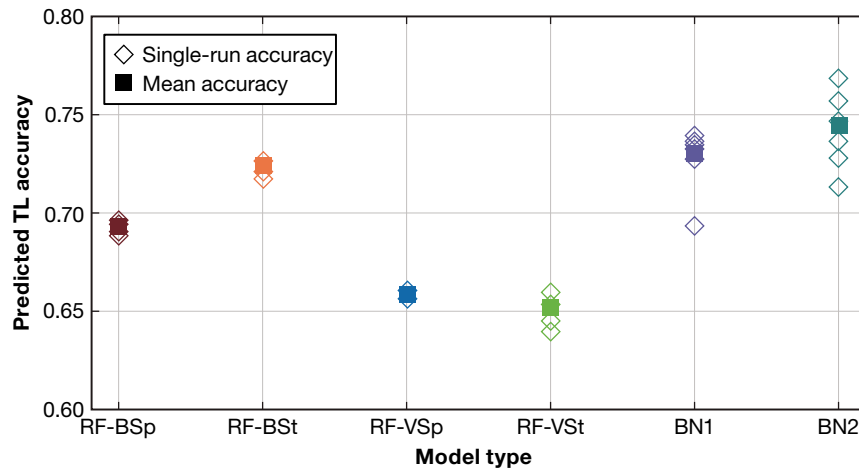


Figure 3. TL classification accuracy (out of five TLs) by model type. The BN models perform better than the RF TL classifiers, consistently achieving 70% or greater classification accuracy and averaging near 75% accuracy.

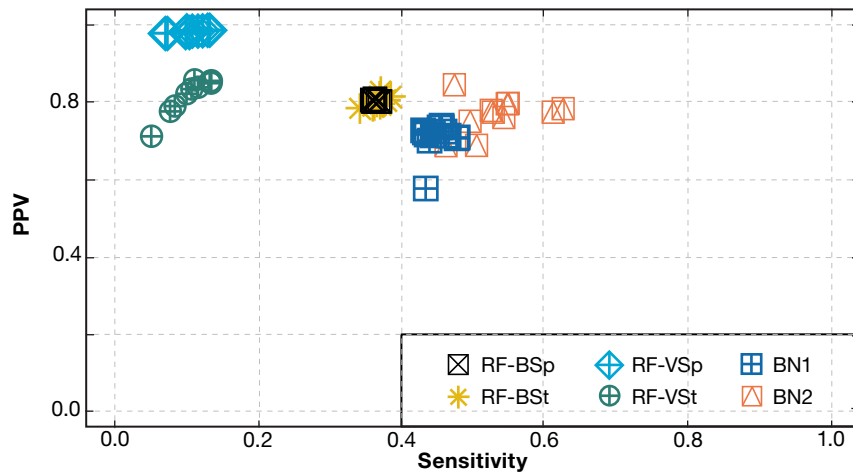


Figure 4. Trade-off between sensitivity and PPV by model type (with five original TLs consolidated to two low and high TLs). BN2 performed best, with relatively high sensitivity and moderate PPV. Other models showed higher PPV but very low sensitivity.

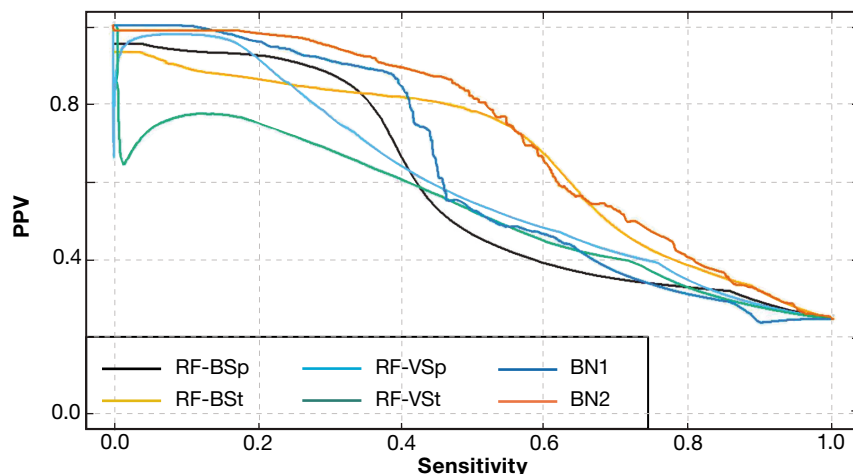


Figure 5. PPV-sensitivity curves (precision-recall curves) by model type. BN2 again performed best. The RF-BSt model also shows good performance.

BN2 showed the best results, with relatively high PPV and moderate sensitivity. Other models, including RF-VSp, showed higher PPV but very low sensitivity.

For some operational decisions, these values (PPV ~ 0.8 , sensitivity ~ 0.5) may be unsatisfactory. Nevertheless, given the 3-to-1 class imbalance within our test set (with more low TLs than high TLs), they still point to the potential of BN2 to efficiently detect high-TL organisms. Refer to the Results on Real Reads subsection for details on how these read-level performance values translate to success on clusters of reads.

In Figure 5, each model's PPV-sensitivity curve (also known as a precision-recall curve) shows the values of PPV and sensitivity as the decision threshold is varied. These curves are constructed by aggregating the results from all 10 sets of models. BN2 and RF-BSt show the best performance.

Results on Real Reads

We also assessed the MLM pipeline using 21 samples of real reads that were prepared, sequenced, and analyzed by an external organization. The samples were analyzed using a bioinformatics pipeline based on *minimap2*,¹⁶ and the unidentified reads were given to us for analysis. We ran each sample through the MLM pipeline (Figure 1). The number of unidentified reads ranged between thousands and hundreds of thousands per sample, and we first ran these through our filters (refer to the Filtering Unidentified Reads subsection). After filtering, the number of reads remaining for analysis from each sample ranged from several dozen to several hundreds of thousands.

From each sample, we applied DBSCAN clustering (refer to the Clustering subsection) and predicted TLs at the cluster level. Accordingly, we evaluated our

Table 3. Confusion matrix of TL predictions by real read sample

Highest Predicted TL	True Highest TL for Sample				
	0	1	2	3	4
0	<u>5</u>	<u>1</u>	0	0	0
1	0	<u>7</u>	0	0	0
2	0	0	0	0	0
3	0	0	0	<u>2</u>	0
4	0	0	0	0	<u>6</u>

Nonzero counts are shown in boldface and underlined.

predictions at the cluster level, comparing the true TL of the highest threat organism (i.e., the true highest TL) with the highest TL predicted for any cluster within the sample. Table 3 shows this comparison, with nonzero counts shown in boldface and underlined for easy reference.

We correctly predicted the highest TL for 20 of 21 samples (95%). These results include correct predictions for 8 of 8 samples with TLs of 2 or higher. The one misclassified sample could arguably have been counted as correct as it contained a TL1 organism but only at a very low abundance (0.01%). Based on this abundance level, the expected number of reads present would be well below the MLM pipeline's specified level of detection. For a given sample, the level of detection is determined by the minimum cluster size (refer to the Clustering subsection). For this sample, the minimum cluster size and level of detection would be 100 reads (i.e., 0.06% of this sample).

We also achieved low FAR against these samples. We did not predict a high TL (TL2 or above) for any of the 13 samples with true low TLs (TL0 or TL1). Thus, our FAR for these cluster-level predictions was 0%. Moreover, for the ~1 million reads within these samples, we had a 0.01% read-level FAR.

DEPLOYMENT CONSIDERATIONS

Based on the results of the MLM pipeline on both simulated reads and collected samples, we are considering requirements for deployment, including physical size, cost, adaptability, runtime, and interpretability.

Requirements for size, weight, and power depend on whether our model pipeline is run at a nearby mobile laboratory as part of a follow-up analysis or in the field amid a real-time investigation. If the models are run in a laboratory, minimizing size, weight, and power needs is less crucial. Conversely, if the models are run in the field, they must be able to be implemented on devices carried during military missions and other investigations.

For the scenario in which our pipeline is run in the field, the computational requirements must not result in

the need for a device that is overly heavy or that requires additional batteries. We are mindful of these constraints, and have selected more efficient design options whenever possible, and made numerous improvements to reduce the memory footprint and runtime of the pipeline. Some examples include a fourfold reduction of our overall memory footprint by implementing a database decimation technique developed for plagiarism detection; an analysis of the effect of the number of trees in our RF models that resulted in substantially smaller models, improving both memory use and runtime; and a redesign of our BN inference implementation that reduced the inference runtime by three orders of magnitude.

The devices must also have a low enough cost and size that they can be feasibly included within an investigator's tools. In its current setup, the MLM pipeline can run smoothly on a laptop or a miniature personal computer (mini-PC). For instance, we demonstrated that the MLM pipeline can run on a mini-PC (connected wirelessly to the sequencing device) that has a footprint of 20 in.², weighs 1 lb., and draws only 6 W of power. We also developed a user-friendly web application to enable follow-up analysis on a laptop when desired.

New threats are prone to emerge at any time, and the reference library leveraged by our pipeline may fall out of date. Nevertheless, insofar as we target reads that are not mapped to reference organisms, our approach is robust to intervals without library updates. Moreover, we are able to update the reference library whenever new information becomes available, enabling the models to be retrained if time permits. Several weeks are typically required to fully train and validate the models.

Some investigators may need insights within short time frames to inform their decisions. Thus, we aim for our models to have efficient runtime. The current pipeline can process and analyze approximately 3,200 unidentified reads per minute on a laptop and approximately 1,800 unidentified reads per minute on the mini-PC. For context, MinION sequencers yield about 20,000 reads per hour. Our pipeline does not fully process all of these reads but only those that are unidentified. Although the percentage of unidentified reads can vary considerably between samples, on average the pipeline can process an hour's worth of sequencing data in approximately one minute on a laptop and in less than two minutes on a mini-PC.

Decision support insights are also enhanced by complementing TL predictions with explanations of how the predictions are determined. To achieve this, we incorporated SHAP (SHapley Additive exPlanations) into our pipeline, which is a popular ML technique for explaining the particular influence that values of individual features have had on the overall TL predictions.^{17,18} These explanations provide additional information to support decision-making and to increase user confidence in the models.

POSSIBLE NEXT STEPS

The models within our MLM pipeline show promising performance, achieving over 74% accuracy in TL classification of individual simulated reads and 95% accuracy for predicting the highest TL present in real samples based on clusters of related reads (refer to the Results section). At the same time, work for this project is ongoing, and several additional capabilities or analyses are underway or planned. These next steps focus on possible new features for the RF models, new features for BN2, and possible alternatives to BN2. Complementing the deployment considerations described in the preceding section, these steps are aimed at further improving the accuracy of the pipeline.

Currently, we have 136 features tracking the frequency of unique tetramers within each read. These features only consider DNA sequence segments of 4 nucleotides. Considering sequences of different numbers of nucleotides might offer a broader space within which the pipeline models can find TL patterns, but increasing the sequence length greatly increases the number of possible sequences and, thus, the number of corresponding features. For instance, there are 8,192 unique 7-mers. Deep autoencoders are neural networks that compress higher-dimensional inputs to a much smaller d -dimensional representation that is still able to reconstruct the original inputs. We envision using the smaller-dimensional representation (e.g., with $d = 25$) from such a model to replace the high-dimensional feature space arising from frequencies of tetramers, 5-mers, 6-mers, and 7-mers. This representation would replace the current 136 tetramer frequency features.

The current set of 19 BN2 input features builds on the results of the RF models and BN1, but additional metrics reflect other aspects of these models' results and may be used as potential BN2 input features. For instance, rather than extracting features from the TL classifications for all of a given read's 1,000 CRRs, complementary features could consider only the 100 or 200 closest CRRs. Also, the TL predicted by BN1 for a given read could be used as an input for BN2. These additional features could enable BN2 to more precisely identify patterns distinguishing different TLs.

We previously opted to use BNs to fuse the predictions of the RF models because of their ability to explicitly quantify the probabilistic relationships between the models' outputs. However, as the space of BN2 input features (potentially) expands, other types of models may provide greater flexibility. For instance, we have considered replacing BN1 or BN2 or both BNs with one or more additional RF models. Alternative model types such as neural networks¹⁹ or gradient-boosted models²⁰ might also yield performance improvement.

CONCLUSIONS

As sequencing technology continues to increase in speed and portability, rapid threat assessment of unidentified organisms in complex biological samples has become increasingly desirable. Our MLM pipeline builds on the vast amount of available sequencing data, enabling objective characterization of the TL of any unidentified organisms present in the samples through the use of ML models that have been carefully trained to recognize patterns in sequencing reads that correspond to threat signatures. These insights offer the potential to provide crucial information for investigators in identifying appropriate responses to emerging, mutated, and modified threats.

ACKNOWLEDGMENTS: We acknowledge the contributions of Steven Borisko, Brant Chee, Erhan Guven, Benjamin Klopčic, Francisco Serna, Dana Udwin, and Charles Young to the development of the MLM system. Our efforts have been funded through various sources: Before 2019, we received funding from the APL Homeland Protection and Special Operations Mission Areas' Independent Research and Development programs. Since 2020, we have received funding from the United States Defense Threat Reduction Agency (DTRA).

REFERENCES

- ¹A. A. González, J. I. Rivera-Pérez, and G. A. Toranzos, "Forensic approaches to detect possible agents of bioterror," in *Environmental Microbial Forensics*, R. J. Cano, G. A. Toranzos, Eds., Washington, DC: American Society for Microbiology, 2018, pp. 191–214, <https://doi.org/10.1128/9781555818852.ch9>.
- ²US Centers for Disease Control and Prevention, "Bioterrorism agents/diseases," <https://emergency.cdc.gov/agent/agentlist-category.asp> (last reviewed Apr. 4, 2018).
- ³National Institutes of Health, "NIH guidelines for research involving recombinant or synthetic nucleic acid molecules (NIH guidelines)," Apr. 2019, https://osp.od.nih.gov/wp-content/uploads/NIH_Guidelines.pdf.
- ⁴M. Jain, H. E. Olsen, B. Paten, and M. Akeson, "The Oxford Nanopore MinION: Delivery of nanopore sequencing to the genomics community," *Genome Biol.*, 17, art. 239, 2016, <https://doi.org/10.1186/s13059-016-1103-0>.
- ⁵National Center for Biotechnology Information, Nucleotide database, <https://www.ncbi.nlm.nih.gov/nucleotide/>.
- ⁶R. R. Wick, L. M. Judd, C. L. Gorrie, and K. E. Holt, "Completing bacterial genome assemblies with multiplex MinION sequencing," *Microb. Genom.*, vol. 3, no. 10, 2017, <https://doi.org/10.1099/mgen.0.000132>.
- ⁷A. Morgulis, E. M. Gertz, A. A. Schäffer, and R. Agarwala, "A fast and symmetric DUST implementation to mask low-complexity DNA sequences," *J. Comput. Biol.*, vol. 13, no. 5, pp. 1028–1040, 2006, <https://doi.org/10.1089/cmb.2006.13.1028>.
- ⁸L. Breiman, "Random forests," *Mach. Learn.*, vol. 45, pp. 5–32, 2001, <https://doi.org/10.1023/A:1010933404324>.
- ⁹W. Webber, A. Moffat, and J. Zobel, "A similarity measure for indefinite rankings," *ACM Trans. Inf. Sys.*, vol. 28, no. 4, pp. 1–38, 2010, <https://doi.org/10.1145/1852102.1852106>.
- ¹⁰M. Ester, H.-P. Kriegel, J. Sander, and X. Xu, "A density-based algorithm for discovering clusters in large spatial databases with noise," in *Proc. 2nd Int. Conf. on Knowl. Discov. Data Mining (KDD-96)*, 1996, pp. 226–231, <https://dl.acm.org/doi/10.5555/3001460.3001507>.

- ¹¹Y. Li, R. Han, C. Bi, M. Li, S. Wang, and X. Gao, "DeepSimulator: A deep simulator for Nanopore sequencing," *Bioinform.*, vol. 34, no. 17, pp. 2899–2908, 2018, <https://doi.org/10.1093/bioinformatics/bty223>.
- ¹²Y. Li, S. Wang, C. Bi, Z. Qiu, M. Li, and X. Gao, "DeepSimulator1.5: A more powerful, quicker and lighter simulator for Nanopore sequencing," *Bioinform.*, vol. 36, no. 8, pp. 2578–2580, 2020, <https://doi.org/10.1093/bioinformatics/btz963>.
- ¹³M. N. Wright and A. Ziegler, "Ranger: A fast implementation of random forests for high dimensional data in C++ and R," *J. Statist. Softw.*, vol. 77, no. 1, pp. 1–17, 2017, <https://doi.org/10.18637/jss.v077.i01>.
- ¹⁴M. Scutari, "Learning Bayesian networks with the bnlearn R package," *J. Statist. Softw.*, vol. 35, no. 3, pp. 1–22, 2010, <https://doi.org/10.18637/jss.v035.i03>.
- ¹⁵S. Højsgaard, "Graphical independence networks with the gRain package for R," *J. Statist. Softw.*, vol. 46, no. 10, pp. 1–26, 2012, <https://doi.org/10.18637/jss.v046.i10>.
- ¹⁶H. Li, "Minimap2: Pairwise alignment for nucleotide sequences," *Bioinform.*, vol. 34, no. 18, pp. 3094–3100, 2018, <https://doi.org/10.1093/bioinformatics/bty191>.
- ¹⁷S. M. Lundberg and Su-In Lee, "A unified approach to interpreting model predictions," in *Proc. 31st Int. Conf. Adv. Neural Inf. Process. Syst. (NIPS'17)*, 2017, pp. 4768–4777, <https://dl.acm.org/doi/10.5555/3295222.3295230>.
- ¹⁸S. M. Lundberg, "An introduction to explainable AI with Shapley values." 2018. https://shap.readthedocs.io/en/latest/example_notebooks/overviews/An%20introduction%20to%20explainable%20AI%20with%20Shapley%20values.html (accessed Aug. 26, 2024).
- ¹⁹C. M. Bishop, *Neural networks for pattern recognition*. New York: Oxford University Press, 1995. <https://dl.acm.org/doi/10.5555/235248>.
- ²⁰J. H. Friedman, "Greedy function approximation: A gradient boosting machine," *Ann. Statist.*, vol. 29, no. 5, pp. 1189–1232, 2001, <https://doi.org/10.1214/aos/1013203451>.



Benjamin D. Baugher, Asymmetric Operations Sector, Johns Hopkins University Applied Physics Laboratory, Laurel, MD

Benjamin D. Baugher is a project manager and machine learning scientist in APL's Asymmetric Operations Sector. He earned a BS in mathematics from Cedarville University and an MS and a PhD in mathematics from Johns Hopkins University. His contributions include

the development of innovative machine learning solutions to complex challenges across diverse domains including genomics, epidemiology, underwater acoustics, remote sensing, and the social sciences. His email address is benjamin.baugher@jhuapl.edu.



Phillip T. Koshute, Asymmetric Operations Sector, Johns Hopkins University Applied Physics Laboratory, Laurel, MD

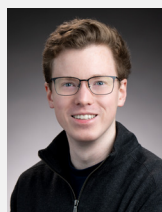
Phillip T. Koshute is a data scientist and statistical modeler in APL's Asymmetric Operations Sector. He earned a BS in mathematics from Case Western Reserve University and an MS in operations

research from North Carolina State University. He is pursuing a PhD in applied statistics at the University of Maryland. He provides statistical expertise to data science projects with a wide range of applications, including biology, chemistry, and additive manufacturing. His email address is phillip.koshute@jhuapl.edu.



N. Jordan Jameson, Asymmetric Operations Sector, Johns Hopkins University Applied Physics Laboratory, Laurel, MD

N. Jordan Jameson is a data scientist in APL's Asymmetric Operations Sector. He earned a BA in commercial music from Belmont University, a BS in mechanical engineering from Tennessee State University, and a PhD in mechanical engineering from the University of Maryland, College Park. He studies and applies methods to understand, characterize, and dissect datasets to achieve mission readiness and advance operational opportunities. His email address is jordan.jameson@jhuapl.edu.



Kennan C. LeJeune, Asymmetric Operations Sector, Johns Hopkins University Applied Physics Laboratory, Laurel, MD

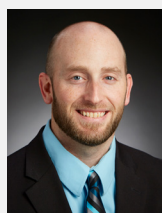
Kennan C. LeJeune is a software engineer in APL's Asymmetric Operations Sector. He earned a BS and MS in computer science from Case Western Reserve University. His work focuses on developing tools

for biothreat analytics and their integrations with biosurveillance systems. His email address is kennan.lejeune@jhuapl.edu.



Joseph D. Baugher, Office of Analytics and Outreach, Center for Food Safety and Applied Nutrition, US Food and Drug Administration, College Park, MD

Joseph D. Baugher is a biological scientist with expertise in bioinformatics and computational genomics, currently focusing on pathogen surveillance and foodborne illness outbreak investigations. He earned an MS in applied molecular biology from the University of Maryland, Baltimore County and a PhD in biochemistry, cellular, and molecular biology from Johns Hopkins University School of Medicine. His contributions to the work detailed in this manuscript were not funded by the US Food and Drug Administration. His email address is joseph.baugher@fda.hhs.gov.



Christopher M. Gifford, Asymmetric Operations Sector, Johns Hopkins University Applied Physics Laboratory, Laurel, MD

Christopher M. Gifford is a principal remote sensing and machine learning scientist in APL's Asymmetric Operations Sector and the acting assistant group supervisor for the Imaging Systems

Group. He earned a BS, an MS, and a PhD in computer science from the University of Kansas. He leads Department of Defense and Intelligence Community efforts to deploy automatic target recognition, real-time scene understanding, and autonomy capabilities to low size, weight, and power platforms at the tactical edge. He is a demonstrated leader in applying and fielding computer vision and machine learning algorithms in constrained environments for intelligence, surveillance, and reconnaissance and geospatial intelligence applications. His email address is christopher.gifford@jhuapl.edu.

Assessment of Sequencing for Pathogen-Agnostic Biothreat Diagnostics, Detection, and Actionability for Military Applications

Christopher E. Bradburne, Robert A. Player, Sarah L. Grady, Ellen R. Forsyth, Kathleen J. Verratti, and Jeffrey B. Bacon

ABSTRACT

Biothreat detection strategies have historically focused on cheap, specific, and deployable assays that detect a small but specific nucleic acid or protein component of a threat organism. Genomic sequencing technologies that have emerged over the past 15 years are poised to find their place in the biothreat detection tool kit for military and civilian use. Here we describe efforts to compare and contrast sequencing to traditional polymerase chain reaction (PCR) assays for diagnostics and detection of biothreat agents of concern in military applications. We show that after direct spiking of human blood and serum with biothreat simulants, agnostic sequencing can achieve detection. However, for known agents, PCR is still superior in terms of speed, cost, scale, and reliability for military applications. Although PCR should still be the first choice for diagnostics and detection when an agent is known or suspected, for unknown agents, agnostic sequencing can be a powerful addition to identify causative agents in soils, aerosols, and biothreats in patient samples. APL developed and conducted this work for the Department of Defense to address the basic question of when to use PCR versus when to use sequencing for field-forward infectious disease diagnostics and environmental detection.

INTRODUCTION

Over the past 30 years, rapid biological threat detection and identification has been enabled by small, mobile, cheap, and specific polymerase chain reaction (PCR) assays for DNA and RNA¹ and lateral flow assays (LFAs) for proteins and antigens.² The advantage of PCR for detection is that it can be made to target DNA sequences that are specific to a pathogen while also excluding closely related, but nonpathogenic microbes and viruses (i.e., “near neighbors”). PCR enables enzymatic amplification from, in theory,

a single DNA molecule to millions of copies. This allows the target signal to be amplified from very low levels relative to background noise. In addition, the abundance of pathogen target can be estimated based on how long it takes the signal to cross a threshold of detection (termed a cycle threshold, or Ct, value) in a quantitative PCR (qPCR) assay. A Ct value can therefore constitute both a detection signal and an abundance signal, with lower values indicating higher amounts of initial material.

Because PCR is a moderately complex molecular assay, an automated PCR platform (FilmArray) that can run several targeted pathogens is currently used across the military. A simpler, hand-held option is the LFA. An LFA is a paper-based chromatography assay that uses the wicking properties of paper to separate sample components and then expose biothreat target proteins or antigens to a detection antibody. Those antibodies are linked to a chromatographic indicator that gives either a positive or negative indication if the antibody comes into contact with the antigen. LFAs are simple and robust and include such widespread applications as home pregnancy tests. As such, they are excellent for quick answers but can struggle with sensitivity and low-abundance target samples.

Genomic sequencing involves assessing a sample for the genomic content and the specific sequence of nucleotides of each genomic fragment in that sample. Because early Sanger sequencing could sequence only one DNA fragment at a time, throughput, scale, time, and cost made it untenable for field-forward diagnostics. The field changed in 2007 with the commercial development of a massively parallel genome sequencer able to generate millions of sequencing reads of varying lengths. Since then, a handful of technology companies have pushed the market forward.^{3,4} Their products vary in terms of ease of use, lengths of individual DNA reads, per-base quality, and throughput. The cost of sequencing per base has also been driven down by at least four orders of magnitude since 2007.⁵

Despite these advances, sequencing still has not made it into widespread use in field-forward disease diagnostics or in environmental biothreat detection for military applications. The major barriers are the cost and complexity of individual sequencing runs and difficulties in analyzing and interpreting results. All sequencing technologies produce immense amounts of data (on the order of a hundred megabytes to hundreds of gigabytes), and the analysis can typically be done only on highly capable laptops, the cloud, or high-performance computers. Considerable technical knowledge and skill are required to perform bioinformatics, and interpretation can be difficult even when automated pipelines are employed. Examples of bioinformatic complexity include the presence of many near-neighbor sequences in a sample, faulty and mis-curated reference genomes, and differences in the abundance of the target versus background that result in the target not being detected. Because these and other challenges have been difficult to solve, the US Food and Drug Administration (FDA) has not fully approved genomic sequencing technologies for diagnostic use, even though it issued “draft guidance” for the industry in 2016 with the expectation that sequencing for diagnostics would eventually be approved.^{6,7} To our knowledge, there has been no updated guidance since this draft document was released.

One of the simple questions the Department of Defense (DoD) seeks to answer is when to employ LFA and/or PCR-type technologies and when to employ genomic sequencing technologies. In 2019, just before the start of the COVID-19 pandemic, the Defense Threat Reduction Agency (DTRA) tasked APL to address this question, using data and experience to guide DoD stakeholders on when, where, why, and how to utilize this emerging capability. Partners at the US Army Medical Research Institute of Infectious Diseases (USAMRIID) had developed and/or adopted three protocols employing different methodologies to enrich viral sequences in metagenomic samples so that they could be detected, counted, and characterized:

1. Sequence-independent, single-primer amplification (SISPA)⁸ employs single primers targeting a virus, with random hexamers to allow virus taxa amplification without knowledge of the viral genome beyond the single target primer. This allows a mostly sequence-agnostic enrichment of the virus in a sample undergoing next-generation sequencing (NGS).
2. Sequence-independent, single-primer amplification, and rapid amplification of cDNA ends (SISPA-RACE)⁸ employs SISPA, but includes rapid amplification of the cDNA ends after reverse transcription.
3. Hybrid oligonucleotide enrichment amplification⁹ involves utilizing bioinformatics optimization to select many primer oligonucleotide sequences to enrich for a variety of viruses.

A challenge in agnostic diagnostic sequencing is determining which strategy to select to optimize the chances of detection. In true field-forward settings, field personnel may be able to draw or obtain diagnostic samples, but they may not know whether to target bacteria, viruses, or even fungi as the causative agent. Of these agents, viruses are typically the most difficult to detect using NGS because of their small genome size relative to the host and the fact that they may not be present in high titers in a clinical sample. Therefore, employing a sequencing protocol to enrich viruses would enable virus detection while still generating enough sequencing reads to detect any bacterial pathogens present. With this concept in mind, APL designed a test bed to evaluate these viral-enrichment, yet pathogen-agnostic, sequencing pipelines. The data generated gave the DoD important insights into the performance of sequencing versus PCR, and one of the protocols, hybrid enrichment, was a forerunner of the ARTIC protocol that clinical laboratories and researchers used to enrich and sequence SARS-CoV-2 viruses from clinical diagnostic samples during the COVID-19 pandemic.¹⁰

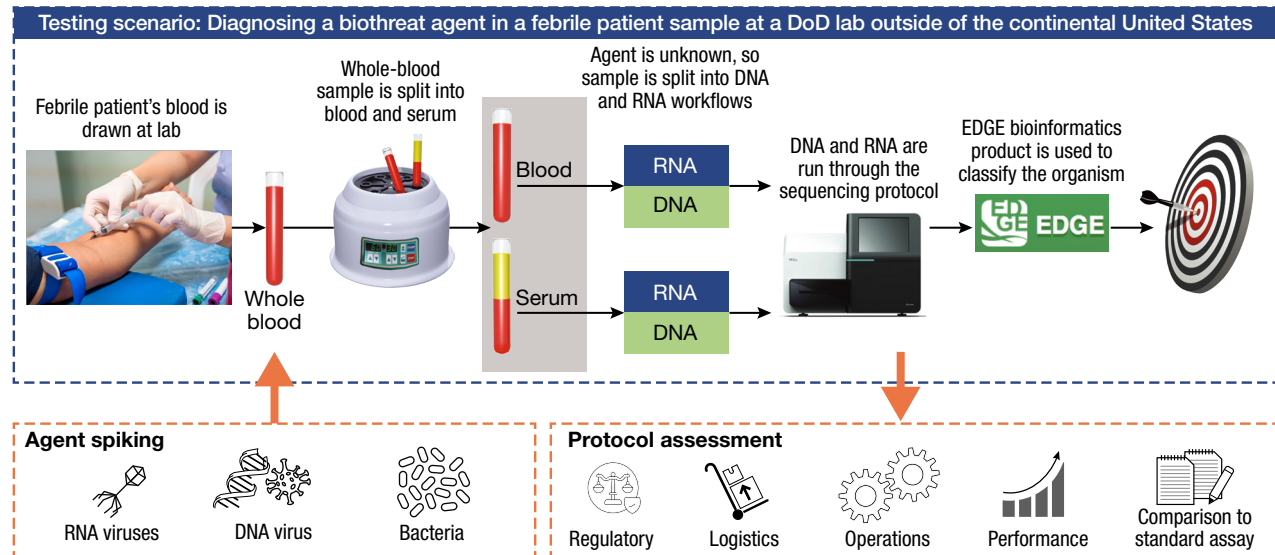


Figure 1. APL testing scenario for comparison of pathogen-agnostic sequencing assays for use in field-forward diagnostics. The use case is a febrile patient who walks into a forward, remote, low-resource clinic. An agnostic sequencing approach is initiated to look for the presence of RNA and DNA viruses and bacteria. Sequencing protocols are assessed against the PCR standard assay for performance, ease of use, cost, speed, and regulatory considerations.

APPROACH

Biothreat Diagnostics

For testing, APL designed a scenario-based test that envisions a febrile patient infected with an unknown biothreat agent (Figure 1). The patient provides a blood sample, which is divided into whole blood and serum. This biothreat scenario is applicable to many potential select agents that achieve bacteremia/viremia at or beyond the febrile phase, but other clinical specimens could also be appropriate. (“Select agents are biological agents and toxins that have been determined to have the potential to pose a severe threat to public health and safety, to animal and plant health, or to animal or plant products.”¹¹) In this scenario, since the causative agent

is not known, each sample is probably split by a lab technician for DNA and RNA processing and then entered into the NGS protocol. After sequencing, the sample is analyzed using a DTRA-funded analysis software, Empowering the Development of Genomics Expertise (EDGE) Bioinformatics, to determine the presence and abundance of an agent. APL was the project integration lead involved in initiating the development of this software with Los Alamos National Laboratory and the Naval Medical Research Command in 2013. To test this pipeline against an array of pathogen genomes, four Biosafety Level (BL) 2 or BL3 agents are used: *Bacillus anthracis* Ames (Ba), a bacterium; vaccinia virus (VV), a double-stranded (ds) DNA virus; Venezuelan equine encephalitis virus (VEEV), a (+) single-stranded (ss)

Table 1. Pathogens chosen for spiking blood and serum and the corresponding human clinical disease concentrations targeted

Organism in the Literature	Equivalent Test Organism	Host	Range of Clinical Concentration	Measured in	Reference	Concentration Chosen for Testing
<i>Bacillus anthracis</i> Ames ancestor	Ba	African green monkeys	40 to > 1e3 CFU/mL	Blood	Rossi et al. ¹²	1e5 CFU/mL
<i>Sin Nombre</i> (Hanta)	HV	Human	1e4.5 to 1e7.5 PFU/mL	Blood	Terajima et al. ¹³	7.5e3 PFU/mL
<i>Puumala</i> (Hanta)			3 to 1.8e6 PFU/mL	Serum	Evander et al. ¹⁴	
Venezuelan equine encephalitis virus	VEEV	Human	1e5 to 1e7 PFU/mL	Blood	Sellon and Long ¹⁵	
			1e2 to 1.8e4 PFU/mL	Serum	Vilcarromero et al. ¹⁶	
			3e2 to 6.7e5 PFU/mL	Serum	Quiroz et al. ¹⁷	
Variola virus	VV	Macaques	1e1.7 to 1e1.56 PFU/mL	Serum	Weaver et al. ¹⁸	
Variola virus			Up to 1e4 PFU/mL	PBMC	Rubins et al. ¹⁹	1e5 PFU/mL
Monkeypox			Up to 2e7 genomes/mL	Blood	Mucker et al. ²⁰	
			Up to 4.8e6 genomes/mL	Blood	Barnewall et al. ²¹	

PBMC, peripheral blood mononuclear cell.

RNA virus; and Seoul hantavirus (Ha), a (–) ssRNA virus. Each agent is tested with each sequencing protocol, as well as with agent-specific qPCR assays, at a concentration in blood or serum corresponding to human clinical concentrations reported in the literature (Table 1). This helps to ensure some fidelity of the use case of a febrile patient who might appear with an infection from that pathogen.

To support application to real-world scenarios, all protocols were evaluated for cost and operational time of use. Lastly, even though the scenario was for a use case outside the continental United States, there was an interest in mapping to regulatory requirements for the use of diagnostic tests in US jurisdictions. FDA regulatory oversight of sequencing for clinical diagnostics has been challenging because sequencing is so sensitive and can reveal so much information that the results can often be difficult to interpret. For example, nearly every metagenomic sample will have sequence reads that map to pathogens, and yet those pathogens may not constitute a threat for a number of reasons: they may be identical to nonpathogenic near-neighbor organisms, associated with nonviable threats, or associated with nonvirulent variants of an infectious agent, or they may constitute pathogenic sequences that appear across many different microbial taxa. As mentioned earlier, the FDA's draft regulatory guidance provides a comprehensive assessment

of a diagnostic test using sequencing, in anticipation of eventual approval, but as of this publication date, there is still no official FDA approval of sequencing for infectious disease diagnostics as described here. Nevertheless, we compared the operation of these three protocols with the draft FDA guidance document.

Performance metrics for each protocol are shown in Figure 2. Each protocol was evaluated using spiked agent from blood and serum and compared directly with qPCR and droplet-digital PCR (ddPCR) for extensive quantification. This enabled direct comparison of the protocols' performance and sensitivity.

Fielded Biothreat Detection

Aiming to put sequencing technologies in the hands of service members in far-forward environments, DTRA has funded efforts to transition a small, portable sequencing capability to special operations teams. APL has supported components of these efforts by providing subject matter expertise and participating in exercises demonstrating these capabilities. In February 2024, DTRA and the US Army Combat Capabilities Development Command Chemical Biological Center (DEVCOM CBC) hosted a testing and training exercise just south of the Arctic Circle in Fox, Alaska, to support testing and evaluation for the Army's Far Forward Advanced Sequencing Technology (F-FAST), led

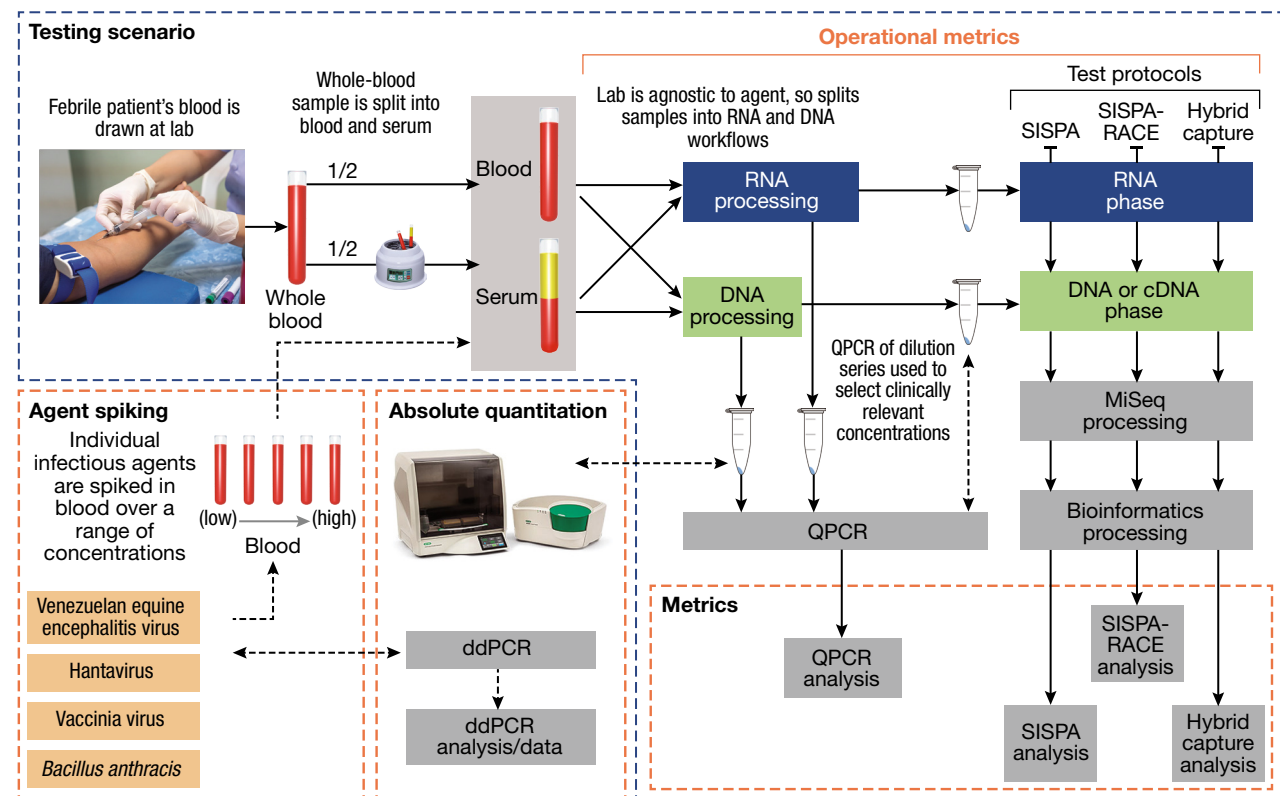


Figure 2. Compartmentalization of performance metrics and process quality control for the APL diagnostic sequencing test scenario. Spiked pathogen concentrations are confirmed by droplet-digital PCR (ddPCR) and qPCR.

by Dr. R. Cory Bernhards of DEVCOM CBC. F-FAST, which has now transitioned into the Far Forward Bio-detection System (FFBS), uses an Oxford Nanopore platform called the M1kC, a handheld device that contains a readout display and flow cell cartridge. Supporting materials for sample and library preparation are labeled in a kit that is deployed with the M1kC. This system is designed to agnostically provide the genetic content of a noncomplex sample and information about a potential threat agent in under an hour for microbial pathogens and DNA viruses and in 90 min for RNA-based viruses. At the time of the exercise, the F-FAST system had the ability to identify known biological pathogens by using a custom database containing the full genomes of ~5,000 organisms.

The F-FAST system has already been tested and evaluated in multiple environments, including Dugway Proving Ground during the peak of summer when temperatures were over 100°F. This exercise sought to test performance in the extreme cold at Fort Wainwright, Alaska, home to the Army's 11th Airborne Division "Arctic Angels." The division's mission is to conduct expeditionary operations within the Indo-Pacific theater, but it is specialized to conduct multi-domain operations in the Arctic.²²

RESULTS

Biothreat Diagnostics

The results of the scenario testing support the general idea that when the agent being tested for is known, qPCR—and not sequencing—should be used. Only cases with an unknown causative agent could begin to justify the cost and time required to implement sequencing to detect microbial and viral infections. Table 2 demonstrates the significant cost and time to obtain results for the Illumina-based sequencing protocols tested. All protocols took between 88.2 and 107.3 h to reach a result, and the minimum materials cost was \$1,730. In contrast, qPCR took only 4.25 h to reach a result on average, while costing only \$420. Furthermore, this qPCR cost estimate is probably high, as the materials would

Table 2. Time and cost per answer for sequencing vs. qPCR

Sequencing Protocol or qPCR	Source	Time to Answer (h)	Materials Cost per Answer (\$)
Nextera XT	Illumina	92.85	2,906
SISPA	USAMRIID	88.5	3,069
SISPA-RACE	USAMRIID	88.2	1,730
Hybrid Capture	USAMRIID	107.3	2,352

generally be bought and implemented at scale, whereas this was a single-usage test.

qPCR performance was also excellent, with zero false positives and nominal detection of each organism consistent with the amount of spiked material (Table 3). This supports the case for qPCR to continue to be the gold standard when using the diagnostic test to confirm or deny the presence of a known agent.

The sequencing tests generally performed well, but some conflicting results made interpretation difficult. As shown in Table 4, all sequencing protocols detected the *Bacillus anthracis* Ames ancestor bacteria, generating no false positives or false negatives. SISPA and SISPA-RACE failed to detect the vaccinia dsDNA virus infectious agent in both whole blood and serum. For VEE, the ssRNA (+) virus, SISPA was adequate, but SISPA-RACE failed to detect the virus in whole blood. The most difficult taxon to detect was clearly the ssRNA (–) hantavirus. This pathogen typically grows to low titers in the lab and in infections, so it was expected to be difficult to detect. Hantavirus reads were detected in the SISPA-RACE protocol, but not enough to fall above the threshold of the EDGE bioinformatic filter that makes the decision to call the organism present in the sample (data not shown).

Across all tested protocols, the hybrid capture protocol performed the best and failed to detect only the hantavirus. This was not surprising because, as noted above, hantavirus typically grows to low titers in clinical infections and can be difficult to detect in clinical samples. The ability to enrich viral targets in large amounts of background was a core strategy of the ARTIC protocol

Table 3. qPCR performance for detection of spiked organisms

Target Organism	Spiked Organism Concentration (PFU/mL)	Ct Value	
		Whole Blood	Serum
<i>Bacillus anthracis</i> Ames ancestor	1.00E + 05	27.8	28.7
BA-negative control	0.00E + 00	0	0
Vaccinia virus Wyeth	1.00E + 05	23.1	22.9
VV-negative control	0.00E + 00	0	0
Venezuelan equine encephalitis virus TC-83	7.50E + 03	27.2	24.0
VEEV-negative control	0.00E + 00	0	0
Seoul hantavirus Baltimore	1.10E + 03	29.6	29.6
HA-negative control	0.00E + 00	0	0

Table 4. Performance of agnostic sequencing workflow without enrichment (Nextera XT) and with the three enrichment protocols (SISPA, SISPA-RACE, and Hybrid Capture)

Protocol	Database	Target Organisms							
		gram+ bacteria: <i>Bacillus anthracis</i> Ames ancestor		dsDNA virus: Vaccinia virus Wyeth		ssRNA (+) virus: Ven- ezuelan equine enceph- alitis virus TC-83		ssRNA (–) virus: Seoul hantavirus Baltimore	
		Whole Blood	Serum	Whole Blood	Serum	Whole Blood	Serum	Whole Blood	Serum
Nextera XT	Bacterial	TP,TN,TP	TP,TN,TP	TN,TN,TN	TN,FP,TN	FN,TN,–	TN,TN,–	TN,TN,–	TN,TN,–
	Viral	TN,TN,TN	TN,TN,TN	TP,TN,TP	TP,TN,TP	TN,TN,–	TN,TN,–	TN,TN,–	TN,TN,–
SISPA	Bacterial	TN,TN,–	TN,TN,–	TN,TN,–	TN,TN,–	TN,TN,TN	TN,TN,TN	TN,TN,–	TN,TN,–
	Viral	TN,TN,–	TN,TN,–	FN,TN,–	FN,TN,–	TP,TN,TP	TP,TN,TP	FN,TN,–	FN,TN,–
SIS- PA-RACE	Bacterial	TN,TN,–	TN,TN,–	TN,TN,–	TN,TN,–	TN,TN,TN	TN,TN,TN	TN,TN,–	TN,TN,–
	Viral	TN,TN,–	TN,TN,–	FN,TN,–	FN,TN,–	FN,TN,TP	TP,FP,TP	FN,TN,–	FN,TN,–
Hybrid capture	Bacterial	TN,TN,–	TN,TN,–	TN,TN,–	TN,TN,–	TN,TN,TN	TN,TN,TN	TN,TN,–	TN,TN,–
	Viral	TN,TN,–	TN,TN,–	TP,TN,–	TP,FP,–	TP,TN,TP	TP,TN,TP	FN,TN,–	FN,TN,–

The data in each square represent (1) the spiked sample, (2) the negative control, and (3) the positive control. For example, TP,TN,TP indicates that the spiked sample is detected (true positive), the negative control is undetected (true negative), and the positive control is detected (true positive). Green shading, expected result; yellow shading, conflicting result; red shading, false positive result; dashed red outline, non-scenario-linked result.

that was used to detect SARS-CoV-2 and improved throughout the pandemic, allowing whole-genome modeling of geotemporal viral dispersion by variants in human populations throughout the world.²³

DISCUSSION

These results clearly show the difference between utilization of PCR for targeting known pathogens versus utilization of sequencing to characterize an unknown organism. Generally, if the target organism is known, the best guidance is the gold standard of PCR. PCR is cheap, timely, and reliable, and its easily interpretable results minimize false positives. However, a negative result may lead to more questions than answers, leaving the operator without a diagnostic call and yet still with a febrile patient with a likely infectious disease. In this case, sequencing with the hybrid enrichment protocol described in this article offers the best opportunity to detect a causative agent. In addition, using the protocol offers the best chance to obtain sequence-based information that could indicate whether the agent is a new strain or variant or, in the case of a microbe, whether there is any antimicrobial resistance, as well as any other countermeasure-relevant information present.

The information payoff gained from sequencing rather than PCR is apparent, and in many cases, even a positive PCR result could be important for confirmation. One intriguing option is direct sequencing of the amplicons from a PCR result. Through support and direction from the Defense Biological Product Assurance Office (DBPAO), APL has developed a methodology to do exactly this. An APL team modified biothreat-specific PCR primers to add library adapter sequences so that

the amplicon product could be directly inserted into the Oxford Nanopore sequencing protocol. The resulting approach allows a user to run a PCR assay for a biothreat agent and quickly confirm via sequencing the agent and its abundance.²⁴

Biothreat Detection in Cold Regions

Work is ongoing to package the hybrid detection technology into a handheld, field-portable sequencing-based viral detection capability. It was first demonstrated during the Ebola outbreak in West Africa just prior to the COVID-19 pandemic in 2019.²⁵ Commercial products offer handheld sequencers and informatics hardware. Computational power is limited, but future models of field-portable sequencing devices could overcome these limitations. These products also have the potential to be utilized in adverse environments, such as in subfreezing conditions. In February 2024, APL attended a DTRA-supported US Army Special Operations Command (SOCOM) demonstration of a handheld sequencer in arctic conditions at the Cold Regions Research and Engineering Laboratory (CRREL) permafrost tunnel facility in Fox, Alaska (Figure 3). During the 5 days of testing, temperatures ranged from 15°F to –25°F. During the first few runs of these exercises, operators had difficulty correctly loading the sequencer flow cells without adding disruptive air bubbles that confounded results. In addition, the cold weather dictated innovations such as using body heat to keep reagents from freezing before use. By the last 2 days, however, the soldiers were able to operate the sequencer and achieve the expected results nominally (data not shown). More information on the exercise is available in *CBNW Magazine*.²⁶ The exercise illustrated that the technology could be used in



Figure 3. Field demonstration of field-forward sequencing for biothreat detection. This demonstration took place at the February 2024 Arctic Edge exercise facilitated by the US Northern Command at the CRREL permafrost tunnel facility in Fox, Alaska. During the exercise, US Army Special Operations Command demonstrated use of a handheld sequencer developed by DEVCOM CBC through the F-FAST program.

a training scenario in cold environments with several modest adaptations.

CONCLUSION

Robust, deployable diagnostics are an important component of a military unit's medical surveillance and biothreat detection capability. A central question in field-forward, molecular diagnostics and detection is when to use qPCR versus when to use sequencing, particularly in a far-forward environment and in wide-ranging environmental conditions. The work described here illustrates that for suspected (i.e., known) pathogens, qPCR is still superior to sequencing in terms of cost, complexity, and time to answer. For novel outbreaks, or orthologous confirmation of a new outbreak, agnostic and pathogen-enrichment sequencing has significant utility. In addition, the field demonstration by DEVCOM CBC and SOCOM in the extreme cold and the ability to deploy sequencing to remote locations also offers important advantages for molecular detection of biothreats in austere environments. As costs decrease and ease of use increases, the utility of sequencing should continue to increase.

ACKNOWLEDGMENTS: Distribution Statement A—Approved for public release; distribution is unlimited.

REFERENCES

- ¹S. Yang and R. E. Rothman, "PCR-based diagnostics for infectious diseases: uses, limitations, and future applications in acute-care settings," *Lancet Infect. Dis.*, vol. 4, no. 6, pp. 337–348, 2004, [https://doi.org/10.1016/S1473-3099\(04\)01044-8](https://doi.org/10.1016/S1473-3099(04)01044-8).
- ²H. R. Boehringer and B. J. O'Farrell, "Lateral flow assays in infectious disease diagnosis," *Clin. Chem.*, vol. 68, no. 1, pp. 52–58, 2022, <https://doi.org/10.1093/clinchem/hvab194>.
- ³C. E. Bradburne, "Personalizing environmental health for the military—Striving for precision," in *Total Exposure Health: An Introduction*, K. A. Phillips, D. P. Yamamoto, and L. Racz, Eds., 1st ed., Boca Raton, FL: CRC Press, 2020, <https://doi.org/10.1201/9780429263286>.
- ⁴C. Bradburne, D. Graham, H. M. Kingston, R. Brenner, M. Pamuku, and L. Carruth, "Overview of 'omics technologies for military occupational health surveillance and medicine," *Mil. Med.*, vol. 180, suppl. 10, pp. 34–48, 2015, <https://doi.org/10.7205/MILMED-D-15-00050>.
- ⁵K. A. Wetterstrand, "DNA sequencing costs: Data," National Human Genome Research Institute Genome Sequencing Program, <https://www.genome.gov/about-genomics/fact-sheets/DNA-Sequencing-Costs-Data>.
- ⁶F. Luh and Y. Yen, "FDA guidance for next generation sequencing-based testing: Balancing regulation and innovation in precision medicine," *npj Genom. Med.*, vol. 3, art. 28, 2018, <https://doi.org/10.1038/s41525-018-0067-2>.
- ⁷"Infectious disease next generation sequencing based diagnostic devices: Microbial Identification and detection of antimicrobial resistance and virulence markers — Draft guidance for industry and Food and Drug Administration staff," US Food and Drug Administration, May 13, 2016, <https://public4.pagefreezer.com/content/FDA/16-12-2022T08:12/https://www.fda.gov/media/98093/download>.
- ⁸D. H. Song, W.-K. Kim, S. H. Gu, D. Lee, J.-A. Kim, et al., "Sequence-independent, single-primer amplification next-generation sequencing of Hantaan virus cell culture-based isolates," *Amer. J. Trop. Med. Hyg.*, vol. 96, no. 2, pp. 389–394, 2017, <https://doi.org/10.4269/ajtmh.16-0683>.

- ⁹ J. Quick, N. D. Grubaugh, S. T. Pullan, I. M. Claro, A. D. Smith, et al., "Multiplex PCR method for MinION and Illumina sequencing of Zika and other virus genomes directly from clinical samples," *Nat. Protoc.*, vol. 12, pp. 1261–1276, 2017, <https://doi.org/10.1038/nprot.2017.066>.
- ¹⁰ A. W. Lambisia, K. S. Mohammed, T. O. Makori, L. Ndwiga, M. W. Mburu, et al., "Optimization of the SARS-CoV-2 ARTIC network V4 primers and whole genome sequencing protocol," *Front. Med.*, vol. 9, art. 836728, 2022, <https://doi.org/10.3389/fmed.2022.836728>.
- ¹¹ Centers for Disease Control and Prevention Office of Readiness and Response, "Division of Regulatory Science and Compliance: What is a select agent?," <https://www.cdc.gov/ort/dsat/what-is-select-agents.htm> (last reviewed October 2, 2023).
- ¹² C. A. Rossi, M. Ulrich, S. Norris, D. S. Reed, L. M. Pitt, and E. K. Leffel, "Identification of a surrogate marker for infection in the African Green monkey model of inhalation anthrax," *Infect. Immun.*, vol. 76, no. 12, pp. 5790–5801, 2008, <https://doi.org/10.1128/IAI.00520-08>.
- ¹³ M. Terajima, J. D. Hendershot III, H. Kariwa, F. T. Koster, B. Hjelle, et al., "High levels of viremia in patients with the Hantavirus pulmonary syndrome," *J. Infect. Dis.*, vol. 180, no. 6, pp. 2030–2034, 1999, <https://doi.org/10.1086/315153>.
- ¹⁴ M. Evander, I. Eriksson, L. Pettersson, P. Juto, C. Ahlm, et al., "Puumala hantavirus viremia diagnosed by real-time reverse transcriptase PCR using samples from patients with hemorrhagic fever and renal syndrome," *J. Clin. Microbiol.*, vol. 45, no. 8, pp. 2491–2497, 2007, <https://doi.org/10.1128/jcm.01902-06>.
- ¹⁵ D. C. Sellon and M. T. Long, *Equine Infectious Diseases*, 2nd ed., St. Louis, MO: Elsevier, 2014.
- ¹⁶ S. Vilcarromero, P. V. Aguilar, E. S. Halsey, A. Laguna-Torres, H. Razuri, et al., "Venezuelan equine encephalitis and 2 human deaths, Peru," *Emerg. Infect. Dis.*, vol. 16, no. 3, pp. 553–556, 2010, <https://doi.org/10.3201/eid1603.090970>.
- ¹⁷ E. Quiroz, P. V. Aguilar, J. Cisneros, R. B. Tesh, S. C. Weaver, "Venezuelan equine encephalitis in Panama: Fatal endemic disease and genetic diversity of etiologic viral strains," *PLoS Negl. Trop. Dis.*, vol. 3, no. 6, art. e472, 2009, <https://doi.org/10.1371/journal.pntd.0000472>.
- ¹⁸ S. C. Weaver, R. Salas, R. Rico-Hesse, G. V. Ludwig, M. S. Oberste, J. Boshell, et al., "Re-emergence of epidemic Venezuelan equine encephalomyelitis in South America," *Lancet*, vol. 348, no. 9025, pp. 436–440, 1996, [https://doi.org/10.1016/S0140-6736\(96\)02275-1](https://doi.org/10.1016/S0140-6736(96)02275-1).
- ¹⁹ K. H. Rubins, L. E. Hensley, P. B. Jahrling, A. R. Whitney, T. W. Geisbert, et al., "The host response to smallpox: Analysis of the gene expression program in peripheral blood cells in a nonhuman primate model," *Proc. Natl. Acad. Sci.*, vol. 101, no. 42, pp. 15190–15195, 2004, <https://doi.org/10.1073/pnas.0405759101>.
- ²⁰ E. M. Mucker, A. J. Goff, J. D. Shamblin, D. W. Grosenbach, I. K. Damon, et al., "Efficacy of tecovirimat (ST-246) in nonhuman primates infected with variola virus (smallpox)," *Antimicrob. Agents Chemother.*, vol. 57, no. 12, 2013, pp. 6246–6253, <https://doi.org/10.1128/aac.00977-13>.
- ²¹ R. E. Barnewall, D. A. Fisher, A. B. Robertson, P. A. Vales, K. A. Knostman, and J. E. Bigger, "Inhalational monkeypox virus infection in cynomolgus macaques," *Front. Cell. Infect. Microbiol.*, vol. 2, art. 117, 2012, <https://doi.org/10.3389/fcimb.2012.00117>.
- ²² US Army 11th Airborne Division website, <https://11thairbornedivision.army.mil> (accessed Mar 1, 2024).
- ²³ J. Merlet, J. Lagergren, V. M. Vergara, M. Cashman, C. Bradburne, et al., "Data-driven whole-genome clustering to detect geospatial, temporal, and functional trends in SARS-CoV-2 evolution," in *PASC '23: Proc. Platform for Adv. Sci. Comput. Conf.*, June 2023, art. 26, pp. 1–7, <https://doi.org/10.1145/3592979.3593425>.
- ²⁴ R. Player, K. Verratti, A. Staab, C. Bradburne, S. Grady, et al., "Comparison of the performance of an amplicon sequencing assay based on Oxford Nanopore technology to real-time PCR assays for detecting bacterial biodefense pathogens," *BMC Genom.*, vol. 21, art. 166, 2020, <https://doi.org/10.1186/s12864-020-6557-5>.
- ²⁵ E. Kinganda-Lusamaki, A. Black, D. B. Mukadi, J. Hadfield, P. Mbal-Kingebeni, et al., "Integration of genomic sequencing into the response to the Ebola virus outbreak in Nord Kivu, Democratic Republic of the Congo," *Nat. Med.*, vol. 27, pp. 710–716, 2021, <https://doi.org/10.1038/s41591-021-01302-z>.
- ²⁶ J. P. Lee, "Polar pathogens," *CBNW Magazine*, Sep. 15, 2024, <http://nct-cbnw.com/polar-pathogens/>.

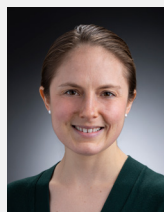


Christopher E. Bradburne, Asymmetric Operations Sector, Johns Hopkins University Applied Physics Laboratory, Laurel, MD

Christopher E. Bradburne is a biologist in APL's Asymmetric Operations Sector. He has a BS in biology and a BS in biochemistry from Virginia Polytechnic Institute and State University (Virginia Tech), an MS in biochemistry from Clemson University, and a PhD in bioscience from George Mason University. He has experience in genomics, personalized medicine, biodefense and infectious disease, nanotechnology, and astrobiology projects. His genomics and personalized medicine experience includes managing clinical utility studies collecting and using personal genomic information for preventative and precision care, as well as applying sequencing technologies to clinical diagnostics, environmental genomic surveillance, and national security applications. His email address is chris.bradburne@jhuapl.edu.



Robert A. Player is a bioinformatician. He previously worked in the Sequencing and Computational Biology Section in APL's Asymmetric Operations Sector. His email address is player.bioinfo@gmail.com.



Sarah L. Grady, Asymmetric Operations Sector, Johns Hopkins University Applied Physics Laboratory, Laurel, MD

Sarah L. Grady is a biologist in APL's Asymmetric Operations Sector. She has a BS in biology from St. Mary's College of Maryland and an MS and a PhD in molecular biology from Princeton University. She has over 12 years of experience in a wide variety of virological, molecular, and microbiology techniques with an emphasis in classical molecular biology/microbiology, virology, synthetic biology, field-forward polymerase chain reaction (PCR) sensors, and -omics technologies (RNA-seq, ribosome profiling, metabolomics, proteomics, etc.). Her email address is sarah.grady@jhuapl.edu.



Ellen R. Forsyth, Asymmetric Operations Sector, Johns Hopkins University Applied Physics Laboratory, Laurel, MD

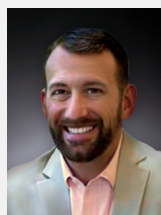
Ellen R. Forsyth is a molecular biologist in APL's Asymmetric Operations Sector. She has a BS in biology and a BS in chemistry from Pennsylvania State University and an MS in biotechnology from American University. She is pursuing a post-master's certificate in sequence analysis and genomics from Johns Hopkins University. She has an extensive background in next-generation sequencing

(NGS) and sample preparation and experience in polymerase chain reaction (PCR), clustered regularly interspaced short palindromic repeats (CRISPR), nucleic acid extractions, and other molecular techniques. She is also interested in high-containment sequencing and advanced molecular detection methods. Her email address is ellen.forsyth@jhuapl.edu.



Kathleen J. Verratti, Asymmetric Operations Sector, Johns Hopkins University Applied Physics Laboratory, Laurel, MD

Kathleen J. Verratti is a molecular biologist in APL's Asymmetric Operations Sector. She has a BS in psychology from Catholic University of America. She has an extensive background in genomics and next-generation sequencing technologies, and her focus has been working with and developing the latest next-generation sequencing technology to solve hard problems. She is the APL project manager for a Defense Biological Product Assurance Office (DBPAO)-funded project focused on applying sequencing technologies to biothreat detection assays. Her email address is kathleen.verratti@jhuapl.edu.



Jeffrey B. Bacon, Asymmetric Operations Sector, Johns Hopkins University Applied Physics Laboratory, Laurel, MD

Jeffrey B. Bacon is a science and technology intelligence professional in APL's Asymmetric Operations Sector. He holds a B.S. in environmental science from Norwich University; master's degrees in biology (Norwich University), biotechnology (Air Force Institute of Technology), and engineering management (Missouri University of Science and Technology); and a PhD in international relations (Tufts University). Jeff is an expert in counterproliferation and biosecurity and has served at the highest levels, including leadership roles in the Department of Defense's response planning and policy implementation during the early phases of the COVID-19 pandemic. In addition to his extensive operational experience, he is also an associate professor and graduate educator at the National Intelligence University. His email address is jeff.bacon@jhuapl.edu.



Wearables-Based Disease Surveillance: SIGMA+ Human Sentinel Networks Concept of Operations

Ivan Stanish, Jane E. Valentine, Damon C. Duquaine, Robert A. Stoll, Ray H. Mariner, and Dorsey R. Woodson

ABSTRACT

The Defense Advanced Research Projects Agency SIGMA+ program developed a persistent, real-time, early warning and detection system for the full spectrum of chemical, biological, radiological, nuclear, and explosive weapon of mass destruction threats at the city to region scale. In support of this program, and leveraging technical expertise in modeling and simulation, applied mathematics, and epidemiology, the Johns Hopkins University Applied Physics Laboratory (APL) characterized and quantified the impact a wearables-based human sentinel network would have on the ability to provide advanced detection of a naturally occurring or intentional biothreat event. Modeling results demonstrate that instrumenting as few as 5% of the population could advance detection of seasonal influenza by 5–14 days and an anthrax attack by ~1 day as compared with traditional public health surveillance. Early detection and geolocation of individuals exposed to biological threats enables timelier and more effective biothreat countermeasures and mitigation strategies.

PROGRAM BACKGROUND AND INTRODUCTION

The Defense Advanced Research Projects Agency (DARPA) SIGMA+ program developed a persistent, real-time, early warning and detection system for the full spectrum of chemical, biological, radiological, nuclear, and explosive (CBRNE) weapon of mass destruction threats at the city to region scale.¹ For biological threats, SIGMA+ developed novel methods of environmental and human-based sensing for improved real-time detection of naturally occurring or human-made biothreat events. Relative to the current state of the art, this effort aimed to provide days-earlier detection and geolocation of biological threats, enabling more effective countermeasures and mitigation strategies. DARPA tasked APL

to develop a concept of operations (CONOPS) framework centered on an integrated two-tier, human sentinel network (HSN) to enhance current disease surveillance.

APL leveraged previous computational modeling and analysis, engaged stakeholders via formal tabletop exercises (TTXs) and targeted discussions, and conducted additional research and fact-finding in support of preliminary CONOPS development. This research identified key materiel and nonmateriel considerations and risks related to implementation of the proposed HSN, including additional materiel development needs, regulatory compliance issues, participant recruitment and engagement strategies, and data management topics.

APL proposed several operational business models, with varying cost estimates and, in some cases, differing non-materiel considerations and risks. This work, in conjunction with the technological development described above, indicates that instantiation of an HSN program is feasible and would provide value to the public health community, the emergency response community, and individual participants.

PURPOSE AND SCOPE

Presented here is a CONOPS framework centered on an integrated two-tier HSN concept to enhance the current state of public health disease surveillance. The HSN concept is composed of wearable physiological monitors (hereafter, “wearable sensors”) (tier 1) distributed among a fraction of the adult population. Algorithms processing an individual’s physiological data would generate alerts in the event of a possible biological exposure; following a tier 1 alert, some individuals would be prompted to seek confirmatory testing for one or more pathogens (tier 2). Both the wearable alerts and test results would be reported in real time to a secure cloud-based platform via a dedicated application. The platform would aggregate the information and disseminate it to public health authorities and critical incident response entities.

The SIGMA+ program demonstrated multiple proofs of concept of system components, including:

- High-accuracy presymptomatic/asymptomatic illness alerting via wearable sensors and alerting algorithms in an influenza-challenge cohort study²
- Communications platforms and information management systems to support collection, storage, distribution, and analysis of HSN data
- User interfaces and visualization platforms both for individual HSN participants and for end users and consumers of population-level or group-level data

These components have been integrated into a pilot wearable network instance with stakeholders from Marion County, Indiana. Key considerations related to implementation of an HSN, such as materiel and nonmateriel factors, regulatory compliance, participant recruitment and engagement, data management, and operational business models, are also presented briefly.

METHODOLOGY

The analysis approach of this study consisted of three primary activities to inform HSN concept of employment/CONOPS development.

1. **Modeling.** An agent-based model of seasonal influenza and a custom-built probabilistic model for an intentional anthrax release were developed to assess the potential impact an HSN could have on accelerating the timeline of detecting a public health emergency. Each modeled disease characteristics, public health practices, tier 1 and tier 2 phenomena, and individual dynamics to simulate disease outbreaks and HSN detection in a given population. Results showed that if 5% to 25% of the population were instrumented within the proposed HSN, it could advance detection of seasonal influenza by 5–14 days and anthrax by ~1 day as compared with traditional public health surveillance.
2. **Scientific partnership.** This activity involved collaborative work with several SIGMA+ organizations:
 - Sandia National Laboratories: development of an integrated environmental-HSN CONOPS
 - RTI International: detection algorithm development and physiological wearable studies
 - Two Six Technologies: consultation on data storage and processing at scale
 - Massachusetts Institute of Technology Lincoln Laboratory: knowledge sharing on related physiological wearable studies and TTX planning
3. **End user/stakeholder engagements.** In coordination with the partners above, APL conducted TTXs and focus groups to elicit feedback on the utility of an HSN to support decision-making and incident response in the face of a public health emergency. Notional use cases, critical infrastructure and data elements, and gaps in planning and risks to operation were chief topic areas. The group engaged US government parties at the national, state, and local levels.

PROPOSED HSN CONOPS

System Concept Overview

The US public health surveillance system is a multi-layer (local, state, and national), heterogeneous network of private, public, and military entities. Surveillance may be active, passive, or syndromic. Traditional detection of outbreaks and public health emergencies is slowed by delays in diagnostic testing and reporting^{3,4} and is inadequate at estimating the magnitude of these events.^{5,6}

The SIGMA+ program developed a scalable network of sensors and intelligence analytics for the advanced surveillance and detection of CBRNE threats. For biological threats, the proposed system consists of environmental near-real-time aerosol biological sensors monitoring the atmosphere for pathogens (preferably in

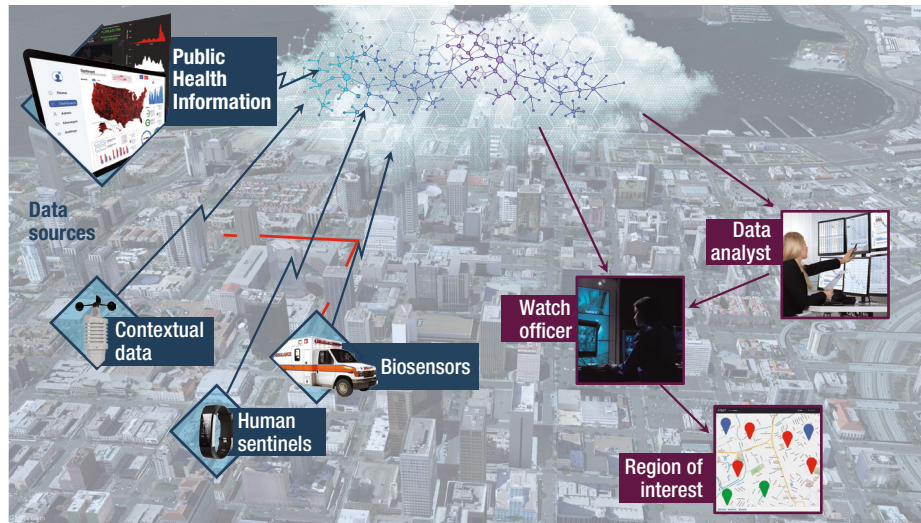


Figure 1. The envisioned HSN program. Sensor and relevant contextual data are uploaded, aggregated, and analyzed for display and to support decision-making.

mobile configurations), an HSN of individuals volunteering to share wearable sensor data (e.g., from smartwatches), and a cloud-based platform that aggregates and analyzes data from the environmental sensors, wearable sensors, and public health sources (Figure 1).

Integrating these novel data sources with existing ones (e.g., syndromic surveillance⁷) into a single platform will provide an opportunity for improved detection of emerging or crisis public health events through the fusion and analysis of all accessible data, providing comprehensive situational awareness to the public health and law enforcement response.

HSN Structure and Functionality

The purpose of the HSN is to significantly improve the speed and fidelity of surveillance of outbreaks and exposures to harmful biological agents. The network would consist of individuals outfitted with wearable sensors (tier 1) to monitor physiological markers, such as heart rate, heart rate variability, peripheral oxygen saturation (SpO_2), temperature, sleep quality, and activity levels. Algorithms, currently in the prototype phase, embedded within a smartphone application analyze changes in these markers to detect pre- and asymptomatic illness at the individual level.

HSN Data Flow and Technical Stack

Currently, wearable sensor data are insufficient to establish the cause of an infection. Therefore, deviations from baseline markers would trigger an alert to prompt the wearer to seek diagnostic testing at locations such as sentinel pharmacies or provider offices (tier 2). The alert, along with non-Personally Identifiable Information/Protected Health Information metadata from the wearable device, such as demographics, algorithm parameters triggered, and location, would

be sent to the cloud-based platform, integrated with the other public health data streams, and analyzed in near real time (Figure 2 and Figure 3).

The strength of the HSN concept is its ability to monitor the health of a population and push real-time alerts to relevant stakeholders. In aggregate, these alerts could serve as early warning mechanisms, prompting a more expedient response than is traditional and subsequently mitigating the impact of the emergency (Figure 4). Further, the detection of pre- and asymptomatic illness provides critical data on the magnitude of the event that would otherwise be missed because some individuals never seek medical care and others may not know they have been impacted.

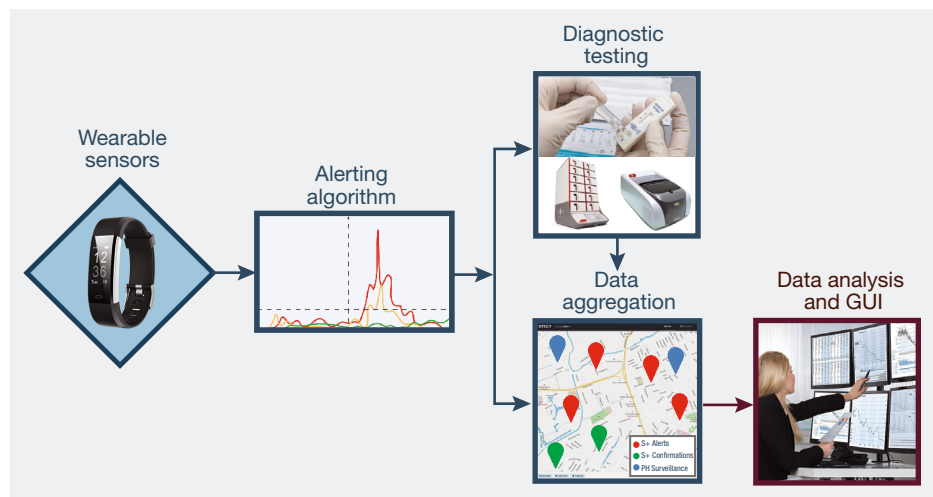


Figure 2. HSN data flow. Deviations from baseline markers would trigger an alert to prompt the wearer of the sensor to seek diagnostic testing. The alert, along with metadata from the wearable device, would be sent to the cloud-based platform, integrated with the other public health data streams, and analyzed in near real time.

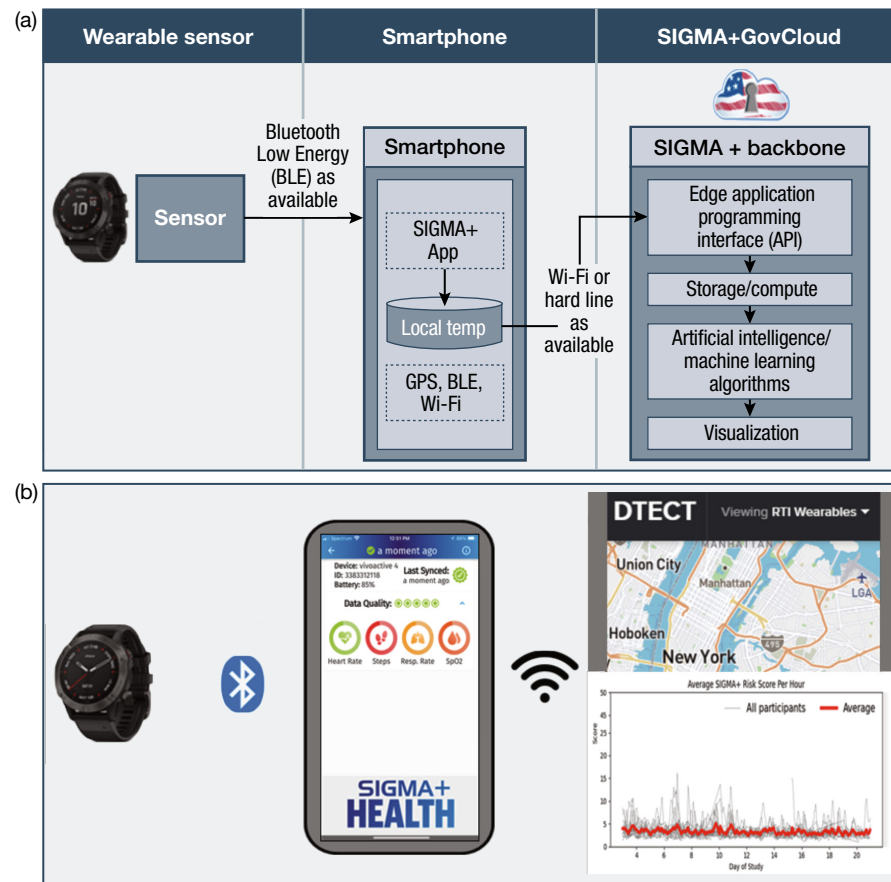


Figure 3. The wearable sensing and alerting architecture. Diagram of (a) the HSN subsystem, for collection, transmission, aggregation, and display of wearable data, and (b) its prototypical components for data collection (a commercial off-the-shelf fitness watch), data transmission (Bluetooth) to an auxiliary device (smartphone), local data analysis and transmission to HSN GovCloud for processing health risk scores and pushing alerts, and visualization (using Two Six Technologies' proprietary "DTECT" platform). (Figure courtesy of RTI International)

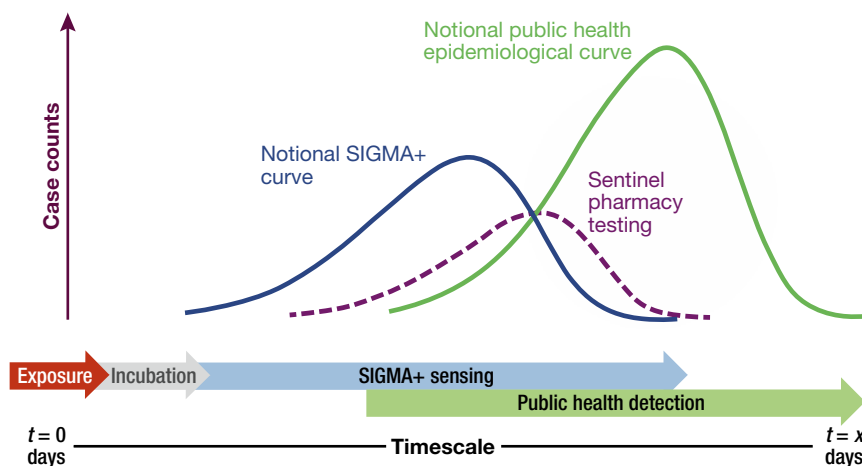


Figure 4. Notional epidemiological curves of disease incidence. Shown are incidence curves captured by means of traditional public health surveillance (green) and the two-tier HSN composed of wearable presymptomatic alerting (blue curve; tier 1), followed by presumptive identification through sentinel pharmacy testing (purple curve; tier 2).

HSN Use Case

The following is a use case for the HSN functioning as the sole SIGMA+ adjunct to public health entities.

Within a period of a few weeks in early summer, public health entities monitoring the HSN in a major US city notice an unseasonable and significant increase in wearable sensor-based alerts for respiratory illness. Local providers and hospitals are not yet reporting increases in visits or hospitalizations for respiratory illness, and syndromic surveillance is not indicating increases in over-the-counter cold and flu medication. Alerts begin to show clustering in more densely populated neighborhoods.

Public health entities issue an alert to local providers and hospitals to be vigilant for respiratory illnesses and to test suspected cases for viruses such as influenza and respiratory syncytial virus (RSV). People receiving alerts begin reporting to providers for evaluation and testing, and testing is negative for common respiratory pathogens. Isolate samples are sent to state public health laboratories for testing, and results are inconclusive. Isolates are sent to the Centers for Disease Control and Prevention, and public health entities begin case investigation interviews with affected persons to determine potential exposures and timelines, monitor symptoms, and characterize interaction networks.

Deployment of an HSN affords the following benefits:

- Even without positive diagnoses, the HSN can provide early warning of unusual disease activity to public health entities, permitting prompt and proactive investigation (including coordination with

local care providers and hospital systems). This, in turn, enables earlier and more accurate determination of the seriousness of the situation.

- Temporal and geographic data in combination with testing results may be modeled to estimate asymptomatic infection rates, attack rates, and areas at high risk of spread. These data can help refine assessments of the outbreak's significance. Further, these data can be used for more targeted epidemiological investigations, interventions, and testing strategies and to inform the use of nonpharmaceutical interventions such as wearing masks and limiting social gatherings.
- Enabling officials to investigate, mobilize resources, and intervene more quickly will reduce the spread of the virus and subsequently decrease morbidity and mortality associated with infection.
- During the early stages of the COVID-19 pandemic, after the virus was circulating in the United States, but before positive case identifications had begun in most cities, an HSN could have provided early indications of spread in specific regions, nuanced understanding of asymptomatic rates and disease severity, and information about transmission characteristics. This information could have supported government responses to the public health emergency and helped mitigate the impact of COVID-19.

HSN Stakeholder Landscape

Stakeholders in a notional HSN fall into three categories: participants, data providers, and end users. Participants include individuals outfitted with wearable sensors that actively transmit data to the HSN. This group may include members of the general public, first responders, and medical personnel. Data providers are nonparticipant entities that provide relevant contextual and surveillance-related data to the HSN. These entities may include hospitals, laboratories, syndromic surveillance networks, and environmental sensors. End users include those individuals who actively monitor and leverage data and analyses generated by the HSN to make decisions in the interest of public health. End users may include people in various levels of government public health, first responders, and members of law enforcement.

Nonmateriel Considerations

Several nonmateriel factors must be considered and addressed to ensure successful HSN system design and operational deployment. These factors include participant considerations, regulations, and data protection and management.

Adequate system performance relies on a sufficient number of participating adults in the population. Approaches to achieve the required participation threshold may include government support through device donations, subsidies, or incentivization; private or philanthropic organizations, insurance providers, or wearable sensor manufacture support; and citizen science or “bring-your-own-device” participation models. Further, factors such as lifestyle, privacy beliefs, or unfamiliarity with or distrust of commercial technology may preclude certain individuals from willingly participating.

The enabling technology of the HSN is the wearable physiological sensor, which can monitor physiological attributes, track location, and communicate the collected data about the wearer. Wearable sensors may be subject to compliance with a variety of regulations (e.g., the Health Insurance Portability and Accountability Act, or HIPAA). Thorough analysis of each regulation and collaboration with relevant agencies will be required.

The protection of personal information must be the highest priority. Transparent disclosure of the types of data, how they are used, and methods for safeguarding data must be clearly communicated to would-be participants. Safeguards at the highest level of government standards must be in place to protect against inadvertent or intentional release or access. The minimum amount of data must be collected to meet system performance thresholds, and data must be anonymized as much as possible.

Feedback on the CONOPS

A significant contributor to CONOPS development was feedback solicited during focus groups and TTXs. During these events, the infrastructure and functionality of the HSN were presented, followed by targeted questions and open discussion. Feedback on the HSN fell into two categories, capability and implementation and utilization, and is summarized below.

HSN Capability

- A wearable-based, two-tier HSN is conceptually well received and would add value to emergency and public health response.
- To be effective, high-fidelity data, such as GPS tracking/back-tracking and display of the triggering physiological parameters, should be displayed for cases requiring investigation.
- When possible, data should be integrated with biosensor, agent-specific data to support response.
- The HSN provides data and situational awareness, demonstrating more utility to support broader public health response than first responders.

HSN Implementation and Utilization

- Trust in the system is critical and may be low initially while it is unproven to individual users.
- Context is important: data from disparate sources must be aggregated and presented together to provide comprehensive situational awareness.
- Jurisdictional responsibility for data monitoring and action must be determined in advance.

SUMMARY AND IMPLEMENTATION CONSIDERATIONS

Based on computational modeling and analysis, stakeholder engagements, pilot HSN studies, and CONOPS/concept of employment analysis, an HSN network is both technologically and practically feasible and would provide value to public health authorities and other decision-makers, the emergency response community, and individual participants in the network. Wearable sensors with the required features, alerting algorithms, communications networks, analysis infrastructure (including algorithms), and user interfaces are all either demonstrated or achievable with current technology. Resolution of nonmateriel concerns, including meeting regulatory requirements, is likewise viable. Any implementation of an HSN will require close collaboration with stakeholders and end users to account for locally specific factors and will require cross-agency partnerships and development of a business model ensuring sufficient public participation.

Continued development of the HSN capabilities will require interfacing with existing public health systems to test and ultimately verify, through well-defined metrics, the HSN's ability to enhance disease surveillance. Thus, a transition partner (or partners) will likely need to conduct advanced development activities, evaluate the HSN capabilities as part of an initial operational test, conduct a pilot study of the proposed technology, and address and document full-system life-cycle challenges before deployment.

An HSN pushes the boundaries of traditional biosurveillance by providing real-time early warning updates to public health and law enforcement professionals. Information provided by the HSN will provide targeted and expedient situational awareness and subsequent decision support to mitigate the impacts of the emergency in question.

ACKNOWLEDGMENTS: The authors acknowledge valuable contributions from the following APL colleagues: Rebecca Eager, Ariel Greenberg, James Howard, Alison O'Hare, Alex Proescher, Christina Pikas, Travis Lim, and Joseph Warfield. This article leverages insights of the following SIGMA+ collaborators: Ann Hammer and Alexis Joiner of Sandia National Laboratories; Dorota Temple and David Dausch of RTI International; Kajal Claypool and Kevin Tangen of Massachusetts Institute of Technology Lincoln Laboratory; and John Magnus and John Hungerford of Two Six Technologies. This material is based on work supported by the Defense Advanced Research Projects Agency (DARPA) under Contract No. HR0011-22-D-0001. The views, opinions, and/or findings expressed are those of the author(s) and should not be interpreted as representing the official views or policies of the Department of Defense or the US government. Distribution Statement A: Approved for public release, distribution is unlimited.

REFERENCES

- ¹DARPA, "Broad Agency Announcement: SIGMA+ Sensors," DARPA/DSO, HR001118S0035, Apr. 5, 2018.
- ²D. S. Temple, M. Hegarty-Craver, R. D. Furberg, E. A. Preble, E. Bergstrom, et al., "Wearable sensor-based detection of influenza in presymptomatic and asymptomatic individuals," *J. Infect. Dis.*, vol. 227, no. 7, pp. 864–872, 2023, <https://doi.org/10.1093/infdis/jiac262>.
- ³CDC, "Flu Season," <https://www.cdc.gov/flu/about/season/> (last reviewed Sep. 20, 2022).
- ⁴CDC, "U.S. Influenza Surveillance: Purpose and Methods," <https://www.cdc.gov/flu/weekly/overview.htm> (last reviewed Oct. 13, 2023).
- ⁵C. L. Gibbons, M. J. J. Mangen, D. Plass, A. H. Havelaar, R. J. Brooke, et al., "Measuring underreporting and under-ascertainment in infectious disease datasets: A comparison of methods," *BMC Public Health*, vol. 14, no. 1, pp. 1–17, 2014, <https://doi.org/10.1186/1471-2458-14-147>.
- ⁶C. M. Zipfel, V. Colizza, and S. Bansal, "Health inequities in influenza transmission and surveillance," *PLOS Computat. Biol.*, vol. 17, no. 3, art. e1008642, 2021, <https://doi.org/10.1371/journal.pcbi.1008642>.
- ⁷CDC National Syndromic Surveillance Program (NSSP), "What Is Syndromic Surveillance?" <https://www.cdc.gov/nssp/overview.html> (last reviewed Sep. 20, 2023).



Ivan Stanish, Asymmetric Operations Sector, Johns Hopkins University Applied Physics Laboratory, Laurel, MD

Ivan Stanish is a project manager in APL's Asymmetric Operations Sector. He has a BS in chemical engineering with a bioengineering option and a PhD in chemical engineering with a minor in inorganic

chemistry, both from the University of California, Los Angeles. He has 24+ years of technical, project/program management, and systems engineering experience that encompasses research, development, and acquisition efforts focused on the detection and defeat of chemical, biological, radiological, nuclear, and explosive threats. He has coauthored 15 publications, has contributed to multiple scientific conference proceedings, and holds two patents. His email address is ivan.stanish@jhuapl.edu.



Jane E. Valentine, Asymmetric Operations Sector, Johns Hopkins University Applied Physics Laboratory, Laurel, MD

Jane E. Valentine is a data scientist, biomedical engineer, and project manager in APL's Asymmetric Operations Sector. She has a BS in mathematics and French and a PhD in biomedical engineering, both from Carnegie Mellon University. Her work focuses on using data to understand complex situations and processes and to support better decision-making. Notable projects include epidemiological and disease surveillance modeling and analysis, machine learning on health data, quantitative metrics (and associated dashboards) development for complex systems and processes, and decision support tool development. Her email address is jane.valentine@jhuapl.edu.



Damon C. Duquaine, Asymmetric Operations Sector, Johns Hopkins University Applied Physics Laboratory, Laurel, MD

Damon C. Duquaine is a public health epidemiologist, project manager, and supervisor in APL's Asymmetric Operations Sector. He has a BS in biology and an MPH, both from the University of Michigan. His work focuses on population health, infectious disease, data analytics, hospital quality improvement, modeling and simulation, and patient safety experience. His email address is damon.duquaine@jhuapl.edu.



Robert A. Stoll, Asymmetric Operations Sector, Johns Hopkins University Applied Physics Laboratory, Laurel, MD

Robert A. Stoll is a project manager in APL's Asymmetric Operations Sector. He has a BS in mathematics and physics from Millersville University, an MBA from

Johns Hopkins University, an MS in optics from the University of Rochester, and a PhD in engineering management from George Washington University. He has diverse technical and managerial expertise in systems engineering, program and project management, staff development, mathematical modeling, test and evaluation, and chem-biodefense. His email address is robert.stoll@jhuapl.edu.



Ray H. Mariner, Asymmetric Operations Sector, Johns Hopkins University Applied Physics Laboratory, Laurel, MD

Ray H. Mariner is an assistant program manager in APL's Asymmetric Operations Sector. He has a BS in chemistry from Loyola College (now Loyola University Maryland) and an MS in homeland security management from the University of Maryland University College (now the University of Maryland Global Campus). He has 25+ years of experience as an analytical chemist and data scientist, with areas of expertise including analytical chemistry, data science, semantic modeling, threat modeling, and threat prioritization. His email address is ray.mariner@jhuapl.edu.



Dorsey R. Woodson, Asymmetric Operations Sector, Johns Hopkins University Applied Physics Laboratory, Laurel, MD

Dorsey R. Woodson is a program manager in APL's Asymmetric Operations Sector. He has a BA in psychology from Syracuse University and an MA in human resources management from Webster University. He manages programs focused on technology development for counter-weapons of mass destruction situational awareness, with an emphasis on chemical, biological, radiological, and nuclear threats and related detection and defeat technologies. In this role, he directs the development and delivery of knowledge advantage and decision aid architectures, analytics, and tools. His email address is dorsey.woodson@jhuapl.edu.

APL Achievement Awards and Prizes: The Lab's Top Inventions, Technical Breakthroughs, and Staff Achievements for 2023 and 2024

APL Staff Writers

ABSTRACT

The Johns Hopkins University Applied Physics Laboratory (APL) is dedicated to delivering game-changing technical solutions to our nation's most critical challenges. In addition to making technical contributions, APL staff members advance enterprise services, participate in and expand a robust innovation ecosystem, and embody the organization's core values in their work. Every year the Laboratory honors staff members' accomplishments with an awards program. This article details the awards presented for achievements in 2023 and 2024.

INTRODUCTION

APL honored a total of nearly 360 staff members for their exceptional contributions in 2023 and 2024. Staff members received awards for outstanding work in areas such as publications, research and development, innovation, invention, and mission-driven programs. A new award debuted for 2023: The Courageous Achievement Award recognizes significant contributions to APL or the nation that exemplify courage, integrity, and leadership.

This article details the 2023 and 2024 awards and winning staff members. Although some of the honored efforts would not have been possible without external collaborators, the awards program is limited to current APL staff members, so only those contributors are named.

PUBLICATION AWARDS

The publication awards, first presented in 1986, are the genesis of APL's annual Achievement Awards program. Administered by the *Johns Hopkins APL Technical Digest* editorial board, these awards encourage and celebrate scholarship through publication in the professional

literature. Departments and sectors may submit up to two nominations in each of the eight award categories. Judges consider nominated works' significance and clarity, emphasizing publications that significantly advance science, engineering, or APL's mission.

Author's First Paper in a Peer-Reviewed Journal or Proceedings

This award recognizes an early-career investigator who has published their first paper as lead author at APL. The award for a 2023 publication went to Gabriella Hunt for "High Emissive Contrast of Adaptive, Thin-Film, Tungsten-Doped VO₂ Composites."¹ This paper describes APL researchers' work to develop a highly efficient adaptive thermal management solution by utilizing novel phase-change material. The design parameters they explored and selected will enhance the performance of thermal management devices, ultimately reducing total energy consumption in homes and industries.

The 2024 award went to Carlos Braga for “A Coronal Mass Ejection Impacting Parker Solar Probe at 14 Solar Radii.”² This paper describes the novel analysis and unprecedented measurements Parker Solar Probe made while crossing through a solar transient within the solar corona. These findings clarify long-standing questions on coronal mass ejection structure with important implications for space weather analyses.

Outstanding Paper in the *Johns Hopkins APL Technical Digest* (The Walter G. Berl Award)

This award recognizes excellence in APL’s own technical journal, which has been published since 1961. The honor is named for Walter Berl, who was editor-in-chief of the *Digest* when the publication awards program was created and who oversaw the program for many years.

Winners for 2023 were Andrew Cheng, Ralph McNutt, and Harold Weaver for “Science Highlights from NASA’s New Horizons Mission.”³ The paper details science discoveries from New Horizons, the first mission to explore Pluto and the Kuiper Belt. The mission transformed our understanding of Pluto and its giant moon Charon from mere points of light into geologically complex worlds formed of exotic materials. It revealed the Kuiper Belt object Arrokoth to be a comet “contact binary” with an organic-rich surface.

There were two winning publications in 2024. The first was “A Multidimensional Cyber Threat Scenario Enumeration Model for Resilience Engineering” by Anurag Dwivedi.⁴ This article describes a threat scenario characterization and enumeration approach that does not rely on intelligence or threat databases and allows for tailored abstraction of threat scenarios to inform mitigation decisions and facilitate cybersecurity and resilience engineering. The second award was presented to Khamphone Inboun, S. John Lehtonen, Nicholas Nowicki, and Vanessa Rojas for “Microelectronics Packaging at APL: Delivering Custom Devices for Critical Missions.”⁵ This paper highlights APL’s advancements in microelectronics packaging, focusing on custom, high-reliability solutions for mission-critical applications. It details novel processes, such as laser cutting and hermetic sealing, and showcases contributions to key programs, such as NASA’s Double Asteroid Redirection Test (DART) and Dragonfly missions, emphasizing APL’s unique capabilities in prototyping and delivering specialized devices.

Outstanding Research Paper in an Externally Refereed Publication

This award recognizes research, including investigations in basic and applied science and engineering, published in a peer-reviewed journal. The 2023 award went to Elena Adams, Olivier Barnouin, Nancy Chabot, Michelle Chen, Andrew Cheng, Terik Daly, Carolyn Ernst, Zachary Fletcher, Mark Jensenius, and Andrew

Rivkin for “Successful Kinetic Impact into an Asteroid for Planetary Defence,” published in *Nature*.⁶ This paper describes the DART spacecraft’s autonomous kinetic impact into Dimorphos, a small moon of the near-Earth asteroid Didymos. Details include the timeline leading up to impact, the location and nature of the impact site, and the size and shape of Dimorphos. The impact event and the resulting change in Dimorphos’s orbit demonstrated that kinetic impactor technology is a viable technique to defend Earth if necessary.

The award for a 2024 publication went to another DART paper, this one by Ronald Ballouz, Olivier Barnouin, Nancy Chabot, Andrew Cheng, Terik Daly, Carolyn Ernst, Andrew Rivkin, and Angela Stickle and titled “The Geology and Evolution of the Near-Earth Binary Asteroid System (65803) Didymos.”⁷ This paper describes the physical properties of Didymos and its moon Dimorphos, which were analyzed using data collected during DART’s Dimorphos encounter and deflection demonstration. Didymos is mechanically weak, similar to other small rubble pile asteroids, and Dimorphos is even weaker, probably as a result of its formation from loose debris from Didymos.

Outstanding Development Paper in an Externally Refereed Publication

This award celebrates development efforts, including applications of science or engineering to the development of a system or a specific product or prototype, published in a peer-reviewed journal. The 2023 award went to Robert Armiger, Matthew Fifer, Priya Gajendiran, Meiyong Pelos, Courtney Moran, Harrison Nguyen, Luke Osborn, Jonathan Pierce, Richard Ung, Rama Venkatasubramanian, and Jared Wormley for “Evoking Natural Thermal Perceptions Using a Thin-Film Thermoelectric Device with High Cooling Power Density and Speed,” published in *Nature Biomedical Engineering*.⁸ The paper describes how APL researchers used novel thin-film thermoelectric devices, robotic systems, and targeted neurostimulation to enable amputees to intuitively perceive the temperature of objects they grasped with an advanced prosthesis. Evoking thermal sensations at biologically relevant timescales will help achieve advanced human–machine interfaces with enhanced realism and function.

Winners of the 2024 award were Debra Buczkowski, Katie Hancock, Yuki Itoh, Alexandra Matiella Novak, Frank Morgan, Scott Murchie, A. Hari Nair, Frank Seelos, Kim Seelos, and Christina Viviano for “The CRISM Investigation in Mars Orbit: Overview, History, and Delivered Data Products.”⁹ The APL-designed, -built, and -operated CRISM instrument and associated data have provided spectra that demonstrate the mineralogy of the surface of Mars. This paper details the wealth of data the CRISM instrument collected over the roughly 15 years that it operated.

Outstanding Professional Book

This award recognizes outstanding books written by APL staff members. The award for a 2023 book went to Edward Birrane, Sarah Heiner, and Kenneth McKeever for *Securing Delay-Tolerant Networks With BPsec*, published by John Wiley & Sons.¹⁰ This book examines how delay-tolerant networks can be secured when operating in environments that would otherwise break many of the common security approaches used on the terrestrial internet today. The text includes considerations and tutorials for deploying Bundled Protocol Security, or BPsec, in both regular and delay-tolerant networks.

There were no nominations in this category for 2024.

Outstanding Special Publication

This award recognizes publications and publication activities, such as book chapters, review papers, tutorials, and book or proceedings editorship, that are outside of the other publication award categories. The award for a 2023 special publication went to Robert Allen, Robert Decker, Russell Howard, Vamsee Jagarlamudi, James Kinnison, Nour Rawafi, Guillermo Stenborg, and Angelos Vourlidas for “Parker Solar Probe: Four Years of Discoveries at Solar Cycle Minimum,” published in *Space Science Reviews*.¹¹ This publication summarizes the scientific advances NASA’s Parker Solar Probe made mainly during the first four years of the mission.

The winner for a 2024 publication was Adrienn Luspai-Kuti, editor of the book *Triton and Pluto: The Long Lost Twins of Active Worlds*.¹² Neptune’s moon Triton and the dwarf planet Pluto are near-twins with similar but distinct histories. This book, which Luspai-Kuti coedited with a former APL staff member, captures the current state of knowledge of these two worlds and is an important reference on Kuiper belt objects and ice giant planets.

Outstanding Conference Publication

This award emphasizes the value of participating in conferences to meet colleagues and establish professional contacts. The 2023 award went to Michelle Chen, Musad Haque, Stephen Jenkins, Mark Jensenius, Daniel O’Shaughnessy, Carolyn Sawyer, and Emil Superfin for “SMART Nav Guidance: Ensuring Asteroid Impact for the DART Mission,” published in the *Proceedings of the 45th Annual American Astronautical Society Guidance and Control Conference*.¹³ This paper describes the APL-developed Small-body Maneuvering Autonomous Real-Time Navigation, or SMART Nav, system that performed onboard, autonomous asteroid detection, targeting, and guidance during DART’s four-hour terminal phase, enabling successful intercept.

The winners for a 2024 conference publication were Samuel Audia, Benjamin Estacio, Rachel Hartig, Greta Kintzley, Matt Landes, and Aayush Sharma for “Hypervelocity Impact Properties of Polyimide Aerogels

for Space Debris Shielding and Capture,” published in *Proceedings of the 2024 IEEE Aerospace Conference*.¹⁴ This paper describes RAVIOLI (Removing Articles Via In-situ On-orbit Localized Impacts), a technology that leverages the properties of aerogels and Kevlar materials to protect against a wide range of small particle impacts in space. Research has validated RAVIOLI as a candidate for spacecraft shielding, and current work is extending its use to hypersonic reentry systems.

Lifetime Achievement Publication Award

This award honors an author’s career of achievement through a substantial body of publications that are significant in terms of peer recognition, prizes, citation frequency, or influence on the innovation ecosystem. For 2023, APL honored two staff members with this prestigious award: Barry Mauk,¹⁵ for his extensive and insightful writing on space missions spearheaded by APL, illuminating the complexities and triumphs of space exploration; and Donald G. Mitchell,¹⁶ for advancing our understanding of the solar system through his prolific contributions and significant research in planetary science and astrophysics.

For 2024, Brian Anderson,¹⁷ a space physicist and magnetic field measurement scientist, was recognized for his contributions to the geosciences community through participation in more than 300 scientific publications as either lead or contributing researcher.

R. W. HART PRIZES FOR EXCELLENCE IN INDEPENDENT RESEARCH AND DEVELOPMENT

The Hart Prizes—first presented in 1989 and named for former APL assistant director for research and exploratory development Robert W. Hart—recognize significant contributions that advance science and technology through independent research and development. Sectors and departments recommend candidates, and managing executives judge the nominations on their quality and importance to APL. Prizes are awarded in two categories: best research project and best development project.

Best Research Project

The 2023 award went to Brian Bittner, Scott Gibson, Michael Kepler, Zachary Kurtz, Varun Madabushi, Christopher Moran, Jason Reid, Lee Schloesser, and Nick Zielinski for “Advanced Perception and Control for Autonomous UUV Manipulation.”

The award for the best research project in 2024 went to Rachel Altmaier, Stav Elazar Mittelman, Diarny Fernandes, Konstantinos Gerasopoulos, Evan Jacque, Michael Jin, Richard Korneisel, Courtney McHale, Adam Simmonds, and Jason Tiffany for “FABRICS: Fiber Architecture Breakthroughs In Conversion and Storage.”¹⁸

Best Development Project

Winners for 2023 were Curt Albert, Scott Gibson, John Lindemon, Toni Salter, Andrew Skow, Paul Stankiewicz, and Vivek Viswanathan for “USV Perception and Autonomy Development and Demonstration.”

The 2024 honor went to Daniel Berman, Tom Curtis, Laura Dunphy, Rickey Egan, Libby Lewis, and Diego Luna for “Fung-AI: AI/ML-Driven Antifungal Discovery.”

Invention of the Year

The Invention of the Year Award was first presented in 2000 to encourage new technology and innovation at APL. To identify the top technology from the preceding year, an independent review panel judges invention disclosures. The judges, including technical and business consultants, technology transfer professionals, and intellectual property attorneys, assess inventions’ creativity, novelty, improvement to existing technology, commercial potential, and probable benefit to society.

Winners for their 2023 invention were Jarod Gagnon, Lisa Pogue, and Scott Shuler for “Method for Recycling Rare Earths from End-of-Life Electronics.”

The award for the best 2024 invention went to Alexander Beall and Harley Parkes for “Behavioral Alerting Sets for Control Systems (BAS/CS).”

Master Inventor Award

Lab management first presented the Master Inventor Award in 2007 to honor those staff members who have demonstrated a career of innovation with 10 or more patents based on APL intellectual property. To date, only 35 staff members have attained the honor. The two newest master inventors are Konstantinos Gerasopoulos and Robert Osiander.¹⁹ Among Gerasopoulos’ notable patents are an unbreakable, incombustible lithium-ion battery; battery- and solar-powered fibers; and a safe, high-energy-density battery anode. Osiander’s patents address a range of challenges and gaps, from biomedical innovations to novel materials to navigation tools.

Government Purpose Invention

The first Government Purpose Invention Award, recognizing an invention that meets a critical sponsor need, was presented in 2011. Selected by a team of technical leaders from across the Lab who are acquainted with APL’s technology transfer practices, finalist inventions are judged on their novelty and potential impact to the sponsor community.

The award for 2023 was presented to Timothy Allensworth, Jonathan Bierce, Raymond Lennon, Matthew Shanaman, Clara Smart, Christopher Stiles,

and Steven Storck for “Novel Additive Structures for Pressure Vessels.”

Winners for a 2024 invention were Chuck Forrest, Christopher Gardner, Christopher Gifford, Juliana Illingworth, Zachary Kurtz, Jonathan Ligo, Samim Manizade, Denise Nemenz, Hee Won Pak, and Adam Watkins for “Tactical Agile Model Refinement (AMR).”

Project Catalyst Awards

To position the organization to respond to increasingly complex national challenges and to capitalize on rapid technological advances, APL’s leaders have introduced several initiatives to encourage innovation.²⁰ One of these initiatives, Project Catalyst, offers staff members three funding opportunities for bold, high-risk, transformational ideas that will ensure our nation’s preeminence in the 21st century. Staff members submit ideas in response to challenges posted during several cycles throughout the year. Peers and leaders vote on the submissions, and finalists receive funding to develop their ideas. Awards recognize excellent work funded through Project Catalyst.

Ignition Grant Prize for Innovation

The inaugural Project Catalyst award, the Ignition Grant Prize, was presented for the first time in 2013 for the Ignition Grant project judged to be most creative and to have the greatest potential impact.

The winners of the 2023 prize were Xiomara Calderón-Colón, Spencer Langevin, and Michael D. Sherburne for “Strain Sensing Nanomaterial-Based Paint (SSNaP) for Naval Applications.”

For a 2024 project, Xiomara Calderón-Colón, Christine Chung, Savannah Est-Witte, Corrine Fuller, and Sarah Ton were recognized for “Lab Veins: Vasculature Model for Cell Growth.”

Combustion Grant Prize for Innovation

The Combustion Grant Prize, first presented in 2017, recognizes high-risk, high-impact technical ideas.

The award for 2023 went to Denise Hoover, Nicholas Pavlopoulos, and Nathan Rafisiman for “N2A: Nitrogen-to-Ammonia for Sustainable Energy.”

Daniel Berman, Amanda Ernlund, and Libby Lewis won for their 2024 project “MutaGAN: Boosting Seasonal Vaccines with Deep Learning Farther.”

Propulsion Grant Prize for Innovation

And, finally, presented for the first time in 2018, the Propulsion Grant Prize honors ideas that were selected for their third year of Propulsion Grant funding.

The first 2023 prize went to Ben Baker, Bryan Bates, Daniel Binion, Richard Maltagliati, and Andrew Raab for “Poseidon’s Net Raid Neutralizer.” The second was

presented to Ian Bird, Molly Gallagher, Sarah Grady, Mika Helfers, and Jessica Resnick for “Immunity Twin: Developing Parallel Biological and Computational Immunological Model Systems.” And the third 2023 prize went to Matthew Bailey, Walter Kelso, Ryan Seery, Daniel Shaefer, and Dajie Zhang for “Omega Prime – Reconfigurable Equipment Section.”

For 2024, the first prize went to Jeffrey Garstecki, John Hamilton, Stephen Mitchell, Olukayode Okusaga, and Sam Reynolds for “Neural Networked Clock Ensemble for Coherent Sensing.” Rylie Bull, Dawn Graninger, Max Harrow, Sabrina Pellegrini, and Devin Protzko for were awarded a 2024 prize for “LOCUST: Lots Of Cubesats Used to Survey a Target.” And Nick Andrejow, Sean Bailey, Michael Herman, Brice Pridgen, and Bryan Rex won for “Deep Diving Tuna — Targeting Demersal Objects.”

MISSION ACCOMPLISHMENT AWARDS

The Outstanding Mission Accomplishment Awards, first presented in 2014, recognize major achievements in mission-oriented programs and projects. Awards are given in two categories: a current challenge and an emerging challenge. For both types, a review team of managers and executives from APL’s sectors and mission areas solicits nominations for technical accomplishments in sponsored programs during the previous year. A program has to have achieved a significant milestone within the previous fiscal year to be eligible. The panel judges entries on technical excellence and potential impact.

Outstanding Mission Accomplishment for a Current Challenge

The 2023 award went to core team members Timothy Allensworth, TJ Coleman, Matthew DeHart, Douglas Haefeli, Justin Jones, Dillon Kasmer, Andrew Miller, David Orr, Thomas Sherman, and Tony Zampardo for “Anguilla.”

Two awards were presented for 2024 challenges. The first went to Simmie Berman, Carl Engelbrecht, Stuart Hill, Taejoo Lee, Adrienn Luspai-Kuti, Thomas Magner, Joseph Niewola, Sofia Stachel, Zibi Turtle, and Kyle Weber for “NASA’s Europa Clipper Mission.” The second was presented to E. David Beksinski, Brad Couto, Emily Gotowka, Matthew Kazanas, Armen Melikian, Eric Reidelbach, Josey Stevens, and Eric Uthoff for “Real-World Cell for Middle East Defensive Operations.”

Outstanding Mission Accomplishment for an Emerging Challenge

The 2023 award was presented to core team members Teck Choo, Chuong Dang, Mo DeVillier, Barry Fridling, Mick Marana, Trystan May, Dante Sanaei, Jack Santori,

Joshua Sloane, and Benjamin Waida for “Electromagnetic Maneuver Warfare Capabilities for Zumwalt.”

The 2024 award went to Daniel Araya, Dennis Berridge, Cameron Butler, Parth Kathrotiya, Rubbel Kumar, Prasad Kutty, Gregory McKiernan, John Melcher, Bradley Wheaton, and Thomas Wolf for “Boundary Layer Transition (BOLT-1B) Flight Experiment.”²¹

ALVIN R. EATON AWARD

The Alvin R. Eaton, or A – R – E, Award has been presented annually since 2001 but was not presented publicly during the awards ceremony until 2016. It honors staff members who have spent much of their careers leading remarkable achievements that we cannot talk about openly. Awardees are selected by APL’s director and assistant director for programs. The award is named for Al Eaton, who worked at APL for more than 65 years and, among other achievements, helped establish APL’s highly sensitive program structure. The A – R – E Award was first presented to Eaton himself.

The 2023 award went to Russell Popkin for delivering technical analysis and revolutionary system capabilities for service and joint sponsors.

The 2024 honor was presented to Robert Reichert for his extraordinary contributions to homeland defense.

ENTERPRISE ACCOMPLISHMENT AWARD

The Enterprise Accomplishment Award, first presented in 2015, recognizes the enterprise accomplishment with the greatest impact on APL’s operations and culture of innovation. Winners are selected by a joint panel of APL’s operations executives and managing executives.

Winners for a 2023 accomplishment were David Caselbury, David Harper, Kristine Harshaw, Scott Kim, Jillian Kingwood, Julia Mooney, Sylvie Porter, Gregory Schilsson, and Briana Vecchio-Pagán for “Slack Enterprise Launch and Adoption.”

The 2024 award went to Kenny Carter, Claire DeSmit, Janeen Kawabata, Lee Lachman, Christen McBeth, and Michelle Shirey for “Campus Enterprise Wayfinding Initiative.”

DIRECTOR’S AWARD FOR SPECIAL ACHIEVEMENTS

Sometimes a major accomplishment is outside the usual award categories. The Director’s Award for Special Achievements recognizes such accomplishments. This award was first presented in 2017.

The 2023 award went to Garret Bonnema, Michael S. Brown, Benjamin Henty, Sara Margala, Katherine Newell, Xochitl Oliveros, Vincent Pagán, Daniel Tebben, Chad Weiler, and Christine Zgrabik for “TAMERLANE.”

Two awards were presented for 2024. The first went to Matthew Cross, Kelly DeLawder, Radmil Elks, Chad Orbe, and Gregory Stabler for “GroundHog Day.” The second award was presented to Kharl Bocala, Jonathan Graf, Peter Green, Andy Im, Randy Maurizio, William McCollom, Jerry Richard, Eric Schuler, Mac Sparks, and Rose Trepkowski for “AMDS Special Study Team.”

THE “BOLDIES”

In early 2018, APL management asked a team of technical leaders and contributors for recommendations to increase APL’s boldness. This group, Team Bold, proposed instituting two formal awards to celebrate boldness.

Bumblebee Award

The first award, the Bumblebee Award, recognizes improbable designs that had remarkable results, much like APL’s historic Bumblebee program, whose name was inspired by a quote attributed to aviation pioneer Igor Sikorsky: “According to recognized aerotechnical tests the bumblebee cannot fly because of the shape and weight of his body in relation to the total wing areas. BUT, the bumblebee doesn’t know this, so he goes ahead and flies anyway.”

Winners for 2023 were Brad Bazow, Mary Daffron, Daniel Eby, Samuel Gonzalez, Andrew Lennon, Kyle Lowery, Salahudin Nimer, Vincent Pagán, Michael Pekala, and Steven Storck for “Debunking Current Military Specifications for Additive Manufactured (AM) Part Qualification.”

The 2024 award recognized Andrew DiPrinzio, Brandon Filo, Manav Gandhi, Tyler Golden, Rachel Hartig, Garrett Krol, John O’Neill, William Shaw, Zachary Sweep, and Paul Venginickal for “SOUL TRAIN.”

Noble Prize

The second award in this category, the Noble Prize, celebrates work that was not fully successful but yielded valuable lessons. Its name is a play on Nobel Prize and noble failure.

The award for 2023 was presented to Hannah Collins, Zachary Kiick, Steven Knowlden, Brian Koronkiewicz, Allison Moyer, and Scott Shuler for “OLD BAE: Operable Ligands for Decontaminating Befouled Aquatic Environments.”

For 2024, Jenny Boothby, Avi Bregman, William Fahy, Collin McClain, Nicholas Pavlopoulos, Nathan Rafisiman, Elizabeth Robinson, Clare Sabata, and Alexander Yuan were recognized for “Green Concrete: Handling CO₂ Nature’s Way.”

LIGHT THE FUSE AWARD

The Light the FUSE Award was first presented during the 2021 ceremony. This award recognizes significant contributions that promote a positive culture at the Laboratory, increasing APL’s potential for innovation.

The award for 2023 was presented to David Díaz Márquez, Teresa Johnson, Hannah Kowpak, Ronald Ostrenga, Robin Qualls, Krista Rand, and Katie Zaback for “APL Accessibility Map Project.”

The 2024 award went to Greyson Brothers, Paul Hage, David Helmer, Sage Jessee, Willa Mannering, Griffin Milsap, Harrison Nguyen, Martin Veloso, Kerstin Vignard, and Robert Wilson for “Human–Machine Teaming Testbed.”

ANALYTICAL ACHIEVEMENT AWARD

The Analytical Achievement Award was first presented during the 2022 ceremony. It recognizes the most insightful analytic work that resulted in a critical contribution to a government decision-maker or program.

Two teams were recognized in 2023: Dylan Carter, Bill Lee, Chris Najmi, Tahzib Safwat, John Schmidt, and Naruhisa Takashima for applying analysis to inform the establishment of a partnership between the United States and Japan; and Stephanie Allen, Xander Dawson, Jim Farrell III, Eric Gerdes, Jason Miller, Joshua Mueller, Jared Ott, Kevin Peters, and Andrew Ridenour for leading an effort to develop system-of-system requirements for the US Navy and US Air Force.

The 2024 award went to Richard Arnold, Dennis Evans, Matthew Lytwyn, and Mitch Nikolich for critical analysis of a novel adversary threat.

COURAGEOUS ACHIEVEMENT AWARD

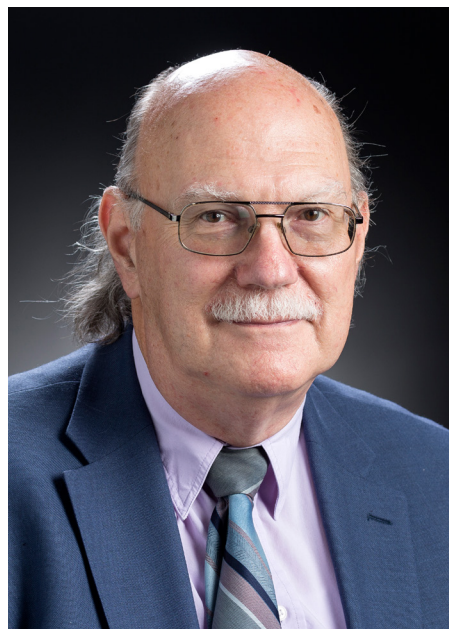
The Courageous Achievement Award was established in 2023 to recognize significant contributions to APL or the nation that exemplify courage, integrity, and leadership in how staff members engage with colleagues and serve the Laboratory or its sponsors. Winners are selected by the director, assistant directors, and chief of staff.

Two awards were presented for 2023. The first award went to Tyler Boehmer, David Frankford, Yuriy Noyvert, Katrina Roarty, Antonio Trujillo Parra, and Kyle Weber for “Identification and Mitigation of Foreign-Sourced Printed Circuit Boards.” And the second award went to Sara McGarity for “Courage to Report Discrepancies.”

The 2024 award went to Matt Cilli, Charles Crossett, Michael Hartigan, Christopher MacGahan, Royce Marsingill, Samantha Marsingill, George Pyryt, Douglas Roldan, Wes Rudy, and Sharon Singer-Barnard for “Strategic Systems Programs Trident II D5LE2 Life Extension Program.”

REFERENCES

- ¹G. M. Hunt, J. A. Miragliotta, J. Ginn, A. P. Warren, and D. B. Shrekenhamer, "High emissive contrast of adaptive, thin-film, tungsten doped VO₂ composites," *Appl. Phys. Lett.*, vol. 123, no. 7, art. 071103, 2023, <https://doi.org/10.1063/5.0164936>.
- ²C. R. Braga, V. Krishna Jagarlamudi, A. Vourlidis, G. Stenborg, and T. Nieves-Chinchilla, "A coronal mass ejection impacting Parker Solar Probe at 14 solar radii," *Astrophys. J.*, vol. 965, art. 185, 2024, <https://doi.org/10.3847/1538-4357/ad2b4e>.
- ³H. A. Weaver, S. A. Stern, L. A. Young, J. R. Spencer, C. B. Olkin, A. F. Cheng, and R. L. McNutt Jr., "Science highlights from NASA's New Horizons mission," *Johns Hopkins APL Tech. Dig.*, vol. 37, no. 1, pp. 73–92, 2023, <https://secwww.jhuapl.edu/techdigest/Content/techdigest/pdf/V37-N01/37-01-Weaver.pdf>.
- ⁴A. Dwivedi, "A multidimensional cyber threat scenario enumeration model for resilience engineering," *Johns Hopkins APL Tech. Dig.*, vol. 37, no. 2, pp. 139–149, 2024, <https://www.jhuapl.edu/sites/default/files/2024-09/37-02-Dwivedi.pdf>.
- ⁵V. O. Rojas, S. J. Lehtonen, N. M. Nowicki, and K. Inboun, "Microelectronics packaging at APL: Delivering custom devices for critical missions," *Johns Hopkins APL Tech. Dig.*, vol. 37, no. 3, pp. 219–227, 2024, <https://www.jhuapl.edu/sites/default/files/2024-09/37-03-Rojas.pdf>.
- ⁶R. T. Daly, C. M. Ernst, O. S. Barnouin, N. L. Chabot, A. S. Rivkin, et al., "Successful kinetic impact into an asteroid for planetary defence," *Nature*, vol. 616, pp. 443–447, 2023, <https://doi.org/10.1038/s41586-023-05810-5>.
- ⁷O. Barnouin, R.-L. Ballouz, S. Marchi, J.-B. Vincent, H. Agrusa, Y. Zhang, et al., "The Geology and evolution of the near-earth binary asteroid system (65803) Didymos," *Nature Commun.*, vol. 15, art. 6202, 2024, <https://doi.org/10.1038/s41467-024-50146-x>.
- ⁸L. E. Osborn, R. Venkatasubramanian, M. Himmtann, C. W. Moran, J. M. Pierce, et al., "Evoking natural thermal perceptions using a thin-film thermoelectric device with high cooling power density and speed," *Nature Biomed. Eng.*, pp. 1–14, 2023, <https://doi.org/10.1038/s41551-023-01070-w>.
- ⁹F. P. Seelos, K. D. Seelos, S. L. Murchie, M. A. Matiella Novak, C. D. Hash, M. F. Morgan, et al., "The CRISM investigation in Mars orbit: Overview, history, and delivered data products," *Icarus*, vol. 419, art. 115612, 2024, <https://doi.org/10.1016/j.icarus.2023.115612>.
- ¹⁰E. J. Birrane III, S. Heiner, and K. McKeever, *Securing Delay-Tolerant Networks with BPsec*, Wiley, 2023.
- ¹¹N. E. Raouafi, L. Matteini, J. Squire, S. T. Badman, M. Velli, et al., "Parker Solar Probe: Four Years of discoveries at solar cycle minimum," *Space Sci. Rev.*, vol. 219, art. 8, 2023, <https://doi.org/10.1007/s11214-023-00952-4>.
- ¹²A. Luspai-Kuti and K. Mandt, eds. *Triton and Pluto: The Long Lost Twins of Active Worlds*. Bristol, UK: Institute of Physics (IOP) Publishing, 2024.
- ¹³M. A. Jensenius, M. Chen, P. Ericksen, M. Haque, S. Jenkins, et al., "SMART Nav guidance: Ensuring asteroid impact for the DART mission," in *Proc. 2023 AAS GNC Conf.*, Feb. 6, 2023.
- ¹⁴A. R. Sharma, G. K. Kintzley, R. K. Hartig, S. Audia, M. Landes, and B. Estacio, "Hypervelocity impact properties of polyimide aerogels for space debris shielding and capture" in *Proc. 2024 IEEE Aerosp. Conf.*, pp. 1–8, 2024, <https://doi.org/10.1109/AERO58975.2024.10521073>.
- ¹⁵Barry Mauk, bio, Johns Hopkins University Applied Physics Laboratory, <https://www.jhuapl.edu/about/people/barry-mauk>.
- ¹⁶Donald Mitchell, bio, Johns Hopkins University Applied Physics Laboratory, <https://www.jhuapl.edu/about/people/donald-mitchell>.
- ¹⁷Brian Anderson, bio, Johns Hopkins University Applied Physics Laboratory, <https://www.jhuapl.edu/about/people/brian-anderson>.
- ¹⁸APL, "Breakthrough process creates next generation of powered wearable fibers," press release, May 22, 2024, <https://www.jhuapl.edu/news/news-releases/240522-fiber-power>.
- ¹⁹A. Sigler, "Johns Hopkins APL celebrates master inventors as beacons of innovation," press release, May 28, 2025, <https://www.jhuapl.edu/news/news-releases/250528-master-inventors-gerasopoulos-osiander>.
- ²⁰A. E. Kedia and J. A. Krill, "Inspiring innovation and creativity at APL," *Johns Hopkins APL Tech. Dig.*, vol. 35, no. 4, pp. 363–379, 2021, <https://www.jhuapl.edu/Content/techdigest/pdf/V35-N04/35-04-Kedia.pdf>.
- ²¹APL, "U.S. Air Force, Johns Hopkins APL hypersonic experiment soars and collects vital data," press release, Sep. 5, 2024, <https://www.jhuapl.edu/news/news-releases/240905-apl-bolt-launch-collects-data>.



Harry K. Charles Jr. (1944–2025)

Dr. Harry K. Charles Jr., an APL Master Inventor, former department head, and deeply respected expert in electrical engineering and microelectronics, died on May 8, 2025, at the age of 80.

After earning his doctorate in electrical engineering at Johns Hopkins University in 1972, Harry began his career at APL in 1973 as a senior engineer in microelectronics. As an expert in the development and packaging of miniaturized electronic, electro-optical, and electro-mechanical devices, he created systems for use in a wide variety of challenging environments, including in space and underwater, and for an equally broad range of applications, including avionics and biomedicine.

Harry was recognized internationally for his work in interconnection, wire-bond testing, thin- and thick-film circuitry, multi-chip modules, and ultrathin and flexible laminate packaging technology. He published more than 200 technical papers on his work. His outstanding record of 17 issued patents and more than 50 invention disclosures was recognized with an APL Master Inventor Award in 2016. Harry was a member of APL's Principal Professional Staff and received an APL Lifetime Achievement Publication Award in 2012. He was also a Life Fellow of the International Microelectronics and Packaging Society. The citation for this honor expressed appreciation for Harry's community leadership in the field of electronics packaging technology.

Harry served in many leadership roles at APL, including section, group, and branch supervisor positions; a chief engineer position; and head of the Technology

Services Department. From 2013 to the time of his retirement in 2024, he served as the editor in chief of the *Johns Hopkins APL Technical Digest*.

As a firm believer in lifelong learning, Harry was a dedicated educator. He served as the group supervisor of the APL Education Center from 2013 to 2024. In this position, he managed the Johns Hopkins University Whiting School of Engineering (WSE) master's degree program, Engineering for Professionals (EP). This program now serves more than 7,000 students across the world. He also served as chair of EP's Applied Physics Program and as the associate dean for non-residential graduate programs at the Johns Hopkins Whiting School of Engineering. In addition to his contributions to EP, Harry led the APL Strategic Education Program, which continues to grow and thrive.

Harry was more than just a manager when it came to education. He developed and taught a dozen courses in electrical engineering and applied physics for EP. These courses include:

- Introduction to Electronics and the Solid State, I
- Introduction to Electronics and the Solid State, II
- Introduction to Electronic Packaging
- Semiconductor Device Physics
- Introduction to Electronic Materials
- VLSI Technology and Applications
- Microelectronics Topics

- Solar Energy Technology and Applications
- Material Science
- Alternate Energy
- Solid State Physics
- Nanoelectronics

Enrollments in Harry's courses over the years exceeded 3,000. From 2008 to 2012, Harry taught classes in the Electrical Engineering Department at the United States Naval Academy and held the position of Office of Naval Research Distinguished Chair in Science and Technology. He developed and taught two new courses for electrical engineering majors and served as a mentor for Trident Scholars as well.

When the Doctor of Engineering Program was established at Johns Hopkins University, the pilot program was carried out at APL. Harry served as central coordinator for the program in its early years, even after the pilot program was completed. Once the program was well established, Harry turned the leadership over to a dedicated program director.

Harry was a nationally recognized expert on US postal stamps, and he had an extensive collection of rare stamps. He published many articles for postal journals and regularly attended national and international stamp conferences where he spoke and displayed items from his collection.

At the time of his retirement in 2024, many APL staff members had fond memories of working with Harry.

Allen Keeney, a chief engineer, noted, "When I started at the Lab 26 years ago, Harry was the department head, but he continued to be very involved with the work, which I admired and respected. He also made time to mentor a lowly new grad throughout his early years at the Lab and encouraged me to pursue both technical excellence and my management degree. I am extremely grateful to Harry for his time and efforts."

Mike Boyle, a group supervisor, recalled a very succinct quote from Harry's time as head of the Technology Services Department: "Remember, I have n+1 votes!"

Howard Feldmesser, a principal staff engineer, noted another classic quote from Harry: "It takes a big man to make a small circuit!"

Chris Ratto, a group supervisor, recalled, "I had the pleasure of serving on the committee led by Harry to review APL-Whiting School research assistantships. He was always a pleasure to work with and was dedicated to supporting graduate students whose research could have national impact. As you might imagine, we had quite a few 'out there' applicants with some pretty wild ideas. Harry usually reacted to these with equal parts dry humor and genuine curiosity, which made our hot wash discussions something I always looked forward to. He will be missed."


Hayley Beach, a program coordinator and e-learning technical specialist who worked with Harry in the Office of Education, expressed the thoughts of many in her words: "Harry inspired countless young professionals through his extensive experience and impressive academic background. As a mentor and supervisor, the greatest lesson he shared with me was to never stop learning—a message that continues to guide me. Harry fiercely believed in the power of education as he encouraged others to embrace challenges, pursue advanced degrees, and seize opportunities to grow. His legacy as a lifelong learner and educator will live on."

APL Director Dr. Ralph Semmel knew Harry well and respected him deeply. Ralph's reflections capture the feelings that many of us had for Harry: "Harry was a wonderful colleague, sought-after mentor, and selfless leader. At various times throughout my career at APL, I turned to Harry for sage advice. He cared deeply about the Lab and our staff, and he served as a model for all of us. He held a variety of positions ranging from research scientist to department head, and in his final role at the Lab, he helped us significantly strengthen ties with the university through his stellar leadership of the APL Education Office. We will miss him dearly."

Harry was preceded in passing by his wife of more than 50 years, Virginia Wall Charles. He is survived by his loving daughter, Heather Kay Charles, and two grandsons, Blake and Weston.

Harry's dedication to APL as a premier national research and engineering institution set a high standard of excellence, and everyone who knew and worked with Harry will remember him for his outstanding technical achievements and for exemplifying the APL core value of unquestionable integrity throughout his life.

Harry's family plans to establish a memorial engineering scholarship in his name. To inquire about contributing to this scholarship fund or to share additional thoughts and favorite memories of your time with Harry, email rememberingdrharrykcharlesjr@gmail.com.



APL designs and
builds operational
chemical detectors.



JOHNS HOPKINS
APPLIED PHYSICS LABORATORY

<https://www.jhuapl.edu/technical-digest>